

# Brain Microelectrode Array Systems

by

Timothy Andrew Fofonoff

B.S., Engineering Physics (2000)

B.S., Computer Science (2000)

University of Saskatchewan

SUBMITTED TO THE DEPARTMENT OF MECHANICAL ENGINEERING IN  
PARTIAL FULFILLMENT OF THE REQUIREMENTS FOR THE DEGREE OF

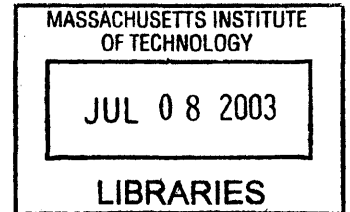
MASTER OF SCIENCE IN MECHANICAL ENGINEERING

AT THE

MASSACHUSETTS INSTITUTE OF TECHNOLOGY

FEBRUARY 2003

© 2003 Massachusetts Institute of Technology  
All rights reserved



Signature of Author:.....  
Department of Mechanical Engineering  
January 17, 2003

Certified by:.....  
Ian W. Hunter  
Hatsopoulos Professor of Mechanical Engineering and Professor of BioEngineering  
Dissertation Supervisor

Accepted by:.....  
Ain A. Somn  
Professor of Mechanical Engineering  
Chairman, Department Committee on Graduate Students

**BARKER**



# **Brain Microelectrode Array Systems**

by

TIMOTHY ANDREW FOFONOFF

Submitted to the Department of Mechanical Engineering  
on January 17, 2003 in Partial Fulfillment of the Requirements for  
the Degree of Master of Science in Mechanical Engineering

## **Abstract**

New methods for manufacturing microelectrode array assemblies, passive devices designed for intracortically recording brain activity in nonhuman primates, were developed and explored. Wire electrical discharge machining (EDM), chemical etching, micromilling, parylene deposition, and laser ablation were some of the processes employed to create distinctive microstructures with fine features and high aspect ratios. These microstructures, constructed from a variety of metals and polymers, were assembled to form the mechanical front end of a brain-machine interface (BMI).

The developed techniques were used to produce microelectrode array assemblies for the Telemetric Electrode Array System (TEAS), a surgically implantable wireless device to be used for motor cortex studies in nonhuman primates. Two prototypes of the TEAS microelectrode array assemblies were implanted in animals in order to validate the design and the manufacturing processes. Neural activity was successfully recorded. Future work is required in order to refine and further automate the processes. Similar devices could one day develop into neural prostheses for clinical use by outputting motor intent captured from brain activity in paralyzed patients.

Thesis Supervisor: Ian W. Hunter

Title: Hatsopoulos Professor of Mechanical Engineering and Professor of BioEngineering

# Acknowledgments

I would first like to thank Sylvain Martel, my mentor and good friend, for initiating and driving the TEAS project, and for inviting me to take part. I also give many thanks to Professor Ian Hunter for giving me the opportunity to work in the exciting MIT BioInstrumentation lab.

I would like to acknowledge the other members of the TEAS team, Johann Burgert and Jan Malásek for all their help and collaboration; Bobby Dyer and Colette Wiseman for their initial design and fabrication testing; Marie-Maude de Denus Baillangeon for helping me build the first prototype; and Thor Bjarnason, Martin Labrecque, and Fedor Danilenko for their contributions.

I would like to thank our neuroscience collaborators, Nicho Hatsopoulos, John Donoghue, Matthew Fellows, and Misha Serruya at Brown University for their input and for the opportunity to participate in the brain surgery that was performed there. And, I would like to especially thank Nicho, Naoum Issa, and Atul Mallik at the University of Chicago, for making the later surgeries in Chicago possible.

I thank Bobby Dyer, Bryan Crane, and Peter Madden for teaching me how to machine and for always being willing to help me with mechanical engineering problems. I also thank the others in and around the lab, Ariel Herrmann, Patrick Anquetil, Robert David, Laura Proctor, Grant Kristofek, Rachel Zimet, Nate Vandesteeg, Mike Garcia-Webb, Andrew Taberner, Cathy Hogan, Lynette Jones, James Tangorra, Mealani Nakamura, Kate Melvin, John Madden, Wilson Chan, Aimee Angel, Michal Berris, Rachel Peters, Keng Hui Lim, Steve Buerger, and James Celestino, for helping to make this such a great place to work.

I also wish to thank all those close to me, some nearby and many now far away, who have been there for me and with me over the years, and who have supported me when I've needed them most. Thank you guys!

And, most of all, I'd like to thank my parents, Dan and Ann Fofonoff, for all their loving support and understanding.

# Table of Contents

Abstract .....	3
Acknowledgments.....	4
List of Figures .....	8
List of Tables .....	12
Chapter 1: Introduction.....	13
1.1 Brain-Machine Interfaces.....	13
1.2 Intracortical Recording .....	14
1.3 The Telemetric Electrode Array System (TEAS).....	15
Chapter 2: Brain Electrode Systems .....	18
2.1 The Brain .....	18
2.2 The Action Potential .....	19
2.3 Extracellular Recording .....	20
2.4 Wire Electrodes.....	21
2.5 Microelectrode Arrays .....	22
2.5.1 The Utah Arrays.....	23
2.5.2 The Michigan Arrays .....	24
Chapter 3: Design Considerations .....	26
3.1 Modularity.....	26
3.2 Size and Shape .....	26
3.3 Material Properties.....	28
3.3.1 Electrode Materials .....	28
3.3.2 Insulating Materials .....	29
3.3.3 Biocompatibility .....	29
3.3.4 Strength Considerations .....	30
3.3.5 Volume Considerations.....	33
3.4 Recording Considerations.....	34
3.4.1 Electrode Surface Metals .....	34
3.4.2 Impedance Values.....	35
3.4.3 Grounding and Reference Paths.....	37

3.5	Device Implantation.....	37
Chapter 4:	Design and Fabrication .....	39
4.1	The TEAS Array Design.....	39
4.2	Wire Electrical Discharge Machining.....	42
4.3	Fabrication Process Overview .....	45
4.4	Microelectrode Array Fabrication.....	48
4.4.1	Planning and Generating a Cutting Path.....	50
4.4.2	Clamping Considerations.....	52
4.4.3	Machining Time Estimates .....	57
4.4.4	Electrode Materials .....	58
4.4.5	Chemical Etching.....	59
4.4.6	Electroplating.....	62
4.4.7	Other Fabricated Microelectrode Arrays .....	63
4.5	Insulating Substrate Fabrication .....	68
4.5.1	Substrate Alternatives .....	68
4.5.2	The TEAS Insulating Substrate .....	69
4.5.3	Other Manufacturing Methods.....	71
4.6	Electrical Insulation .....	71
4.6.1	Parylene Deposition.....	72
4.6.2	Insulation Removal .....	75
4.6.3	Laser Ablation.....	76
4.7	Connector Cable Fabrication .....	79
4.7.1	The TEAS Connector Cable .....	79
4.7.2	Other Connector Designs.....	81
4.8	Assembly and Encapsulation .....	81
4.8.1	Securing the Insulating Substrate.....	82
4.8.2	An Alternative Design .....	83
4.8.3	Electrical Connection.....	84
4.8.4	Final Coatings .....	86
Chapter 5:	Results.....	87
5.1	Electrode Characterization.....	87

5.2	Implantation of the Prototypes.....	93
5.2.1	Implantation into a Monkey.....	93
5.2.2	Implantation into Mice.....	98
5.3	Mechanical Results .....	101
5.4	Neural Recording Results .....	103
Chapter 6:	Conclusion .....	106
Chapter 7:	Future Work.....	108
References.....		110

# List of Figures

Figure 1-1. Images of a monkey skull showing the approximate areas available for the telemetric electrode array system (TEAS) [8,11]. (Photos: Jan Malášek)..... 17

Figure 2-1. Diagram of the brain. (Illustration: The Society for Neuroscience [13])..... 18

Figure 2-2. Diagram showing the shape of a typical intracellular action potential. .... 20

Figure 2-3. Plot of neural spikes intracortically recorded from the motor cortex of a monkey [8,11]. (Graph: Jan Malášek) ..... 21

Figure 2-4. Image of the “Utah Array” (left) and connection options for an 11-electrode assembly (upper right) and a 74-electrode assembly (lower right) manufactured for use in chronic recording. (Photos: Bionic Technologies, LLC [24], and Cyberkinetics, Inc. [25]) ..... 23

Figure 2-5. Images of microelectrode arrays that were manufactured using silicon micromachining. (Photos: University of Michigan, Ann Arbor [22]) ..... 25

Figure 3-1. Drawing of an electrode subjected to an axial load upon insertion. .... 30

Figure 3-2. Drawing of an electrode subjected to a transverse force..... 32

Figure 4-1. Image of the first prototype of the TEAS mechanical front end. (Photo: Robert Dyer)..... 40

Figure 4-2. Schematic of the TEAS mechanical front end showing the major components. .... 41

Figure 4-3. Image the Charmilles Technologies wire electrical discharge machine (wire EDM)..... 43

Figure 4-4. Drawing showing the wire EDM process. After the initial roughing cut, several skim passes are normally performed in order to obtain the desired surface finish. .... 44

Figure 4-5. Image of an assembled TEAS microelectrode array assembly [11]. ..... 45

Figure 4-6. Schematic showing the steps in the microelectrode array assembly fabrication process..... 47

Figure 4-7. Image of a microelectrode array still connected to its base. The array was machined from a 9.5 mm diameter titanium rod. The electrodes are 1.7 mm in length and are spaced 508  $\mu\text{m}$  apart..... 48



Figure 4-8. Schematic showing the dimensions of the TEAS microelectrode array. ....	49
Figure 4-9. Drawing of a typical cutting path used when wire electrical discharge machining a microelectrode array. The wire starts at the crosshairs and loops in the direction of the arrow. ....	52
Figure 4-10. Image of a workpiece clamped and suspended in the tank of the wire EDM machine. The rotation of the workpiece that is done after the first cut is complete is shown by the arrow. ....	53
Figure 4-11. Image of several clamps used in the fabrication of microelectrode arrays by wire EDM. ....	54
Figure 4-12. Image of a microelectrode array clamped in order to prevent damage from occurring when it is separated from the rod. When the wire cuts through the rod, the clamp will hold the array in place. ....	55
Figure 4-13. Image of a microelectrode array held in place with a specially-designed fixture just before being removed from its base by wire EDM. ....	56
Figure 4-14. Magnified images of the microelectrode array, epoxied into the insulating substrate, just before being removed from its base by wire EDM. ....	57
Figure 4-15. SEM images of a titanium microelectrode array before (left) [8,11] and after (right) it has undergone the chemical etching process. ....	60
Figure 4-16. SEM Image of a titanium microelectrode array with a human hair. ....	61
Figure 4-17. SEM images of titanium alloy microelectrode arrays before (left) and after (right) they have been chemically etched and electroplated with gold. ....	62
Figure 4-18. Image of a microelectrode array with electrode lengths exceeding 5 mm...	63
Figure 4-19. SEM image of a microelectrode array that was machined to contain electrodes of varying lengths [10]. ....	64
Figure 4-20. SEM Image of an 1141-electrode titanium alloy array that was machined in a honeycomb pattern. ....	65
Figure 4-21. SEM images of hexagonal microelectrodes after they have been electroplated with gold. ....	66
Figure 4-22. Image of a fixture used when making honeycomb-patterned arrays. The fixture is capable of rotating the array 60 degrees with minimal misalignment and was manufactured from stainless steel by wire EDM. ....	66

Figure 4-23. Image of forty-nine 100-electrode arrays that were electrical discharge machined in parallel from a 100 mm diameter disk of titanium alloy..... 67

Figure 4-24. Magnified images of the 100-electrode arrays that were machined in parallel. The elevated sections are 5 mm square and the arrays' inter-electrode spacing is 500  $\mu\text{m}$ . ..... 67

Figure 4-25. Image of a microelectrode array epoxied into a polyimide substrate and held with forceps..... 70

Figure 4-26. Schematic showing the parylene coating process. .... 73

Figure 4-27. Image of the TEAS microelectrode array assembly fixed in place for the parylene deposition process. .... 75

Figure 4-28. SEM images of a parylene-coated assembly, consisting of platinum-coated electrodes epoxied into a polyimide substrate, after the electrode tips have undergone laser ablation. .... 77

Figure 4-29. SEM image of a parylene-coated electrode that has had its tip laser ablated. .... 78

Figure 4-30. Image of the components of the TEAS prototype connector cable. They include a flexible PCB and an 80-pin connector [8,11]. (Photo: Jan Malášek)..... 80

Figure 4-31. Image of a TEAS microelectrode array held in a fixture while the insulating substrate is epoxied to the electrodes..... 82

Figure 4-32. Image of a honeycomb-shaped tungsten carbide 1027-electrode array with a glass substrate mounted over the microelectrodes. The inter-electrode spacing is 250  $\mu\text{m}$ . .... 83

Figure 4-33. Images showing the shorter supports used to position the substrate while it is secured. .... 84

Figure 4-34. Images of an array assembly held in a soldering fixture (left) and of the solder junctions that join the electrodes to the connector cable (right). .... 84

Figure 5-1. Image of a typical plot from the impedance analyzer. The TEAS microelectrode array was immersed in 0.9 % saline and a platinum reference electrode was used. (Photo: Ariel Herrmann)..... 89

Figure 5-2. Graph showing the effect on the measured electrode impedance values from changing the number of laser pulses used when ablating parylene from the electrode tips..... 91

Figure 5-3. Graph showing the effect of changing the number of laser pulses used on the resulting electrode impedances. .... 92

Figure 5-4. Images of the percutaneous connectors (left) and the printed circuit board adapter made to connect the TEAS mechanical front end to the data acquisition system. (Photos: Robert Dyer) ..... 94

Figure 5-5. Image of the monkey’s skull and an exposed portion of its brain prior to the implantation. .... 95

Figure 5-6. Image of the TEAS microelectrode array assembly cemented into place prior to insertion. .... 96

Figure 5-7. Image of the microelectrode array moments before insertion with a pneumatic insertion tool [11]. (Photo: Jan Malášek)..... 97

Figure 5-8. Image of the final acrylic encapsulating layer being applied [11]. (Photo: Jan Malášek)..... 98

Figure 5-9. Images of the microelectrode array assembly mounted onto a micromanipulator for implantation. .... 99

Figure 5-10. Image of a microelectrode array above the mouse brain before implantation. .... 100

Figure 5-11. Image of the surgeons attempting to deform the connector cable to the shape of the brain [11]. (Photo: Jan Malášek)..... 102

Figure 5-12. Plots of four neural spikes recorded from the cortex of a mouse..... 104

Figure 5-13. Plots of four neural spikes that were recorded from the brain of a mouse using the TEAS microelectrode array assembly. .... 105

All images, drawings, and schematics are by Timothy Fofonoff unless stated otherwise.

# List of Tables

Table 3-1. Material Properties of Some Possible Electrode Materials [26,27,28,29]. ..... 28

Table 4-1: Example wire EDM cutting durations for a titanium alloy microelectrode array  
cut from a 10 mm diameter rod..... 57

Table 4-2. Target Fluence Levels for General Classes of Materials [43]..... 76

# Chapter 1: Introduction

Recent advances in neurophysiology and neuroscience in general are driving the prospects of the brain-machine interface (BMI). Alongside these advances are those in the areas of microfabrication and the development of microelectromechanical systems (MEMS). Neuroscience has quickly become an area where such systems are common. Implants in mammals serve as scientific tools and may soon develop into medical devices for human application [1,2,3,4].

Some brain-related devices are already in medical use. Deep brain stimulator implants, such as are used in therapy to relieve the effects of Parkinson's disease, are currently implanted and inject signals into the brains of patients in order to influence brain activity. Auditory prostheses, which stimulate the periphery auditory nervous system in order to restore some sense of hearing, are currently approved for human use and have been implanted in thousands of deaf patients of all ages [1].

Certain neuroscience studies have centered on establishing a link between the brain and the outside world. In particular, the cerebral cortex is an area where a lot of this work has focused. It is widely accepted that this area provides the easiest access to motor intent and sensory perception [2], and it is this region where potential future devices for restoring lost neurological functions associated with degenerative muscular diseases, stroke, or spinal cord injury would be interfaced.

## 1.1 Brain-Machine Interfaces

Progress towards creating brain-machine interfaces (BMIs) for use in humans is quickly accelerating [2]. The potential quality of life improvements that would be possible by developing an input BMI such as visual prosthesis that would allow a blind patient to see, or an output BMI that would allow a paralyzed patient to move, are immense. Even simpler devices that would allow a patient to move a cursor on a screen, or to possibly move a robotic arm, would make a significant impact. Although devices that do both output and input, allowing the user to additionally regain some position

feedback and possibly even some sense of touch, are a number of years away, simpler unidirectional devices will be emerging in the near future.

In addition to grouping BMIs by whether they input or output signals to the cortex, BMIs can be categorized into indirect BMIs and direct BMIs. An indirect BMI measures signals from outside the cortex. Several indirect BMIs use electroencephalogram (EEG) electrodes to noninvasively record electrical signals. Scalp recordings detect the synchronized activity of large numbers of neurons [5]. These signals are known as field potentials. Individuals have been trained to modulate these signals, which occur on the scale of a few seconds. The quality of EEG recordings can be improved by placing the electrodes beneath the skull and above the dura mater, the layer of tissue that covers the brain. Indirect BMIs can provide an interface for paralyzed victims, but it normally requires several seconds for a single action to be taken [2]. This is due to the inherent length of the signals and the indirect manner in which one modifies them. The use of such a BMI requires one's full attention. It is not possible for the BMI to record one's intended action or movement. For more resolution, one must use a direct BMI, which, in nonhuman primates, has been shown to predict intended movement by capturing the action potentials of many individual neurons from within the cortex [4].

## **1.2 Intracortical Recording**

Direct BMIs are intracortical devices intended to record groups of individual neural signals, or spikes. These intracortical recording devices tend to be quite complex, both electrically and mechanically. Because the neural signals are normally 1 ms to 2 ms in duration and are about 100  $\mu$ V in peak-to-peak, significant electronics are required in order to amplify, digitize, and possibly record the signals. If a prosthesis were to be controlled, a real-time processor would also be needed in order to sort the signals from noise and to interpret the captured information in a reasonable amount of time.

Although not yet ready for use in humans, intracortical recording devices are routinely used to conduct neuroscience research in monkeys. Mechanically, the devices must gather signals from a number of recording sites, typically arranged in a grid pattern. This structure is often referred to as a microelectrode array, and the larger mechanical

front end is often referred to as a microelectrode array assembly. Miniaturization is required in order to reduce the trauma that occurs upon insertion of the array into the brain and to ensure that the assembly can fit inside the limited volume available.

If a device is to be implanted long-term, biocompatibility becomes a primary concern. The electronics of the system can reside either inside or outside the body. From a medical point of view, it is highly desirable to have the entire device implanted, with no elements penetrating through the skin. If the electronics are placed outside, which is the current norm, the percutaneous connector where the signals leave the head via cables requires special attention because it promotes an increased chance of infection at that location. From an electrical point of view, the use of cables has sometimes been problematic with recording performed in monkeys [6]. The cable's length increases the likelihood that electrical interference will be observed; artifacts are created when the cable is moved; and the monkeys sometimes have a tendency to abuse the cable. It was the desire to circumvent the problems encountered with the current cabled systems that lead to the development of the Telemetric Electrode Array System (TEAS).

### **1.3 The Telemetric Electrode Array System (TEAS)**

The goal of the Telemetric Electrode Array System (TEAS) [7,8,9,10,11,6] was to create new hardware and to fabricate prototypes of the mechanical and electrical components of a wireless, brain-controlled prosthetic device. Designed for motor cortex studies in *Macaca mulatta* monkeys, the TEAS amplifies and digitizes action potentials and uses peak detection to extract the information-carrying features of the microvolt neural signals. The gathered information is then outputted through the skin by a wireless communication system. These functions are all performed by electronic systems that are implanted into the body, with no wires leaving the body. Because the neural signals are digitized in the body, there is less signal attenuation due to the shortening of the interconnecting wires, and the signal integrity is improved by the elimination of noise and artifacts previously caused by the movement of the connector cable [9]. An aim of the project was to eliminate the need for percutaneous connectors and cables. In addition to reducing the probability of infection by removing the connector site, freedom of

movement would be gained by the removal of the tethers that are presently required during recording. For a human subject, this would represent an appreciable quality of life improvement.

The TEAS places inside the body only the functionality absolutely necessary to record and transfer the desired signal timings and waveforms. By allowing the device to be reprogrammable and modular, software and functionality can be upgraded easily and without additional surgery or further risk to the subject. Much of the required computation is done outside of the body, where power and heating requirements are far less restrictive.

There are several components to the TEAS design: the mechanical front end, consisting of a microelectrode array assembly that is inserted into the brain in order to record neural activity; the analog electronics section, responsible for filtering, conditioning, and amplifying the recorded signals; the digital section that digitizes and buffers the amplified signals; the wireless unit that sends chosen information to an off-board computer; and the power section, comprised of batteries and a recharging unit. With the exception of the power section, which is situated in the abdomen of the monkey, where there is more room, the other components are designed to be implanted on the head of the animal. Figure 1-1 shows an image with highlighted areas reserved for the microelectrode array and the electronics section. Note that although the microelectrode array is implanted into the brain, the electronics are placed between the skull and the skin of the animal.



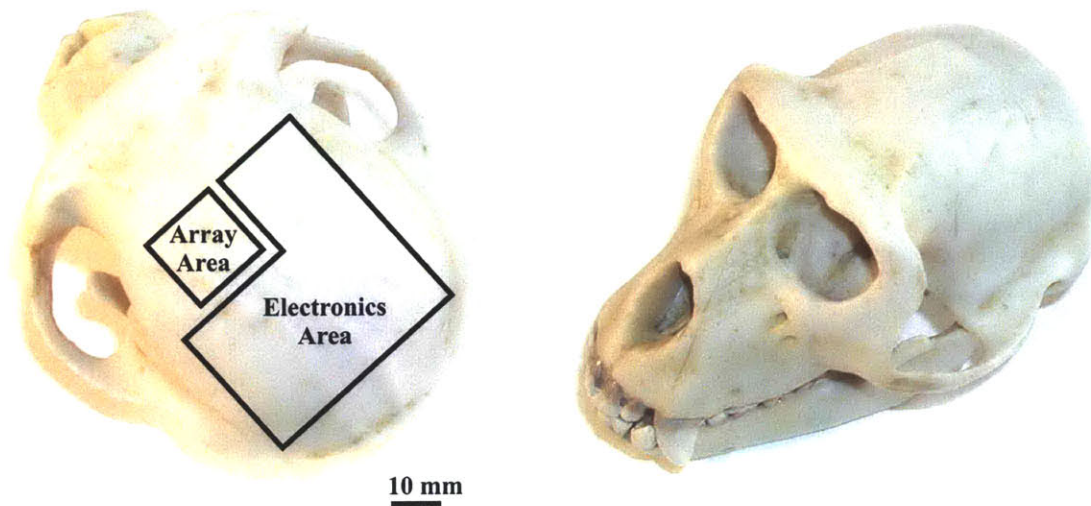


**Figure 1-1. Images of a monkey skull showing the approximate areas available for the telemetric electrode array system (TEAS) [8,11]. (Photos: Jan Malášek)**

The TEAS design incorporates commercial off the shelf (COTS) components whenever possible in order to decrease development time and complexity. A Bluetooth-based radio link is used to transfer the information in real time, and recharging of lithium polymer batteries through skin allows the system to be completely implanted. Although the COTS parts are state of the art and optimized for low-power operation and performance [7,8], the design of custom chips might result in significant space savings.

For the TEAS, the use of computer-controlled manufacturing techniques was also emphasized in an attempt to reduce development, revision, and fabrication time. An effort was made to keep as many design steps as possible under the control of the TEAS team members. This was especially true in the development of the mechanical front end. All machining, whether by wire electrical discharge machining (EDM), by micro mill, or by excimer laser, and all encapsulating, whether by soldering, by electroplating, by epoxying, or by depositing parylene, were done in the laboratory.

# Chapter 2: Brain Electrode Systems

## 2.1 The Brain

A diagram of the brain is shown in Figure 2-1. The primary motor cortex (M1) is the area of interest for the telemetric electrode array system (TEAS) project. The TEAS device was designed to aid in the study of the interactions among groups of neurons and the information they convey about motor behavior [12].

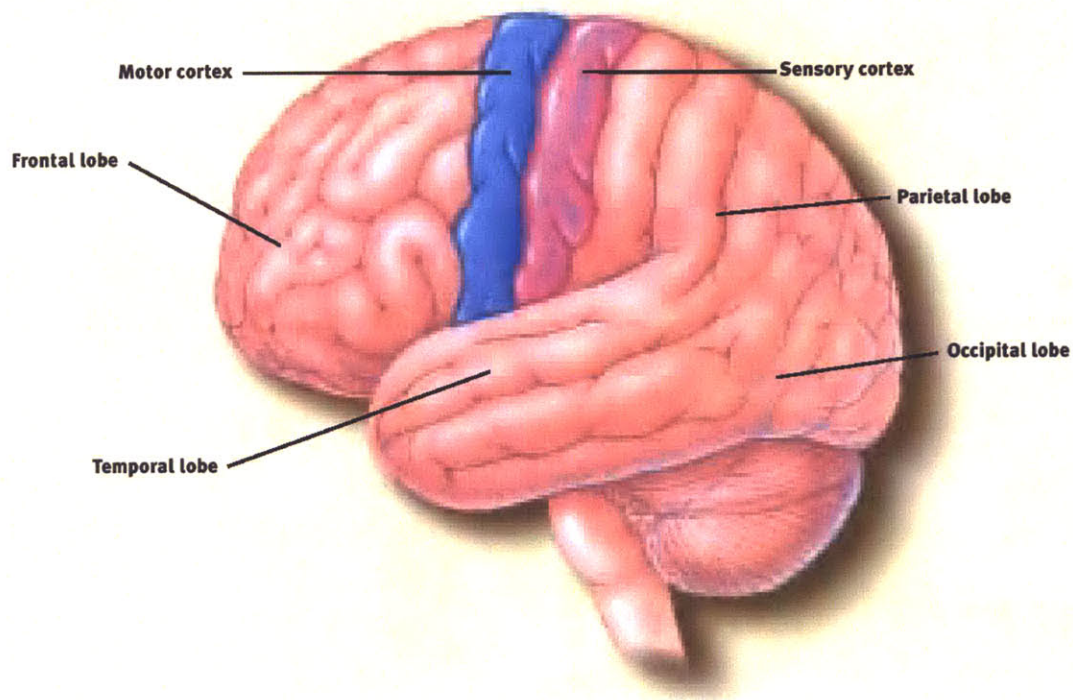


**Figure 2-1. Diagram of the brain. (Illustration: The Society for Neuroscience [13])**

The neurons in the motor cortex have cell bodies that typically vary between  $20\ \mu\text{m}$  and  $40\ \mu\text{m}$  in size [5] and are spaced  $40\ \mu\text{m}$  to  $60\ \mu\text{m}$  apart [14]. The thin tube-like structures that extend from the neurons, called neurites, can extend for over  $100\ \mu\text{m}$ , however. These branch-like neurites can be divided into types: the dendrites, which function as the antennae of the neurons, and the axons, which serve to relay information through synapses at their ends.

Upon receiving input signals from other parts of the brain, the neurons in M1 have been found to relay those signals through synaptic transmission from one neuron to another, progressing through the central nervous system (CNS) in order to drive a group of muscles toward a desired goal. Bursts of neuronal activity, observed as neural spikes that occur in quick succession are observed immediately before and during movement [15]. It is believed that this brain activity encodes the force and direction of voluntary movement. In patients that have become paralyzed, it is often the case that though one cannot move a limb, for example, typical M1 activity still occurs. The signals are interrupted somewhere along the path from the M1 region to the destined muscle group. It is the activity in the M1 region, in the form of individual neural spikes or action potentials, which is the focus of the TEAS.

## **2.2 The Action Potential**

At rest, the inside of a neuronal cell body is at a potential difference of about -65 mV with respect to the surrounding extracellular fluid and tissue [15]. This potential difference between the interior and exterior of the cell is maintained by the expenditure of metabolic energy by the cell and results in an ionic gradient across the membrane of the cell. The cell membrane serves as a semipermeable barrier which allows certain substance and ions to flow in and out of the cell. When a neuron responds to a stimulus, the membrane potential depolarizes, reverse polarizes, and repolarizes by means of a rapid ion exchange [16]. This rapid change of the potential across the membrane potential is known as an action potential. A typical neuronal action potential is about 100 mV in amplitude and lasts about 2 ms. Figure 2-2 shows a diagram of a typical action potential, also known as a neural spike.

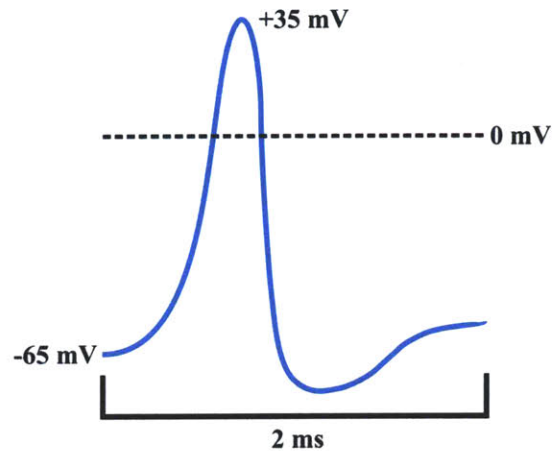


**Figure 2-2. Diagram showing the shape of a typical intracellular action potential.**

The voltage potentials of the signal presented in Figure 2-2 are those typically present inside the cell body, when measured with respect to the reference potential of the intercellular medium that surrounds the neuron. This waveform is similar to what one would expect from an intracellular recording in which an electrode is made to penetrate through the cell wall of a neuron. When electrodes are placed into cortex, however, they do not typically penetrate the neurons and therefore are used to make extracellular recordings.

### **2.3 Extracellular Recording**

Since the fluids and tissues that surround neurons are electrically conducting, current flows in the environment surrounding the neuron when it undergoes the depolarizing-repolarizing effect of the action potential [16]. When electrodes are placed into the cortex of the brain in order to record neural spikes, the electrodes typically measure voltage fluctuations that occur outside of the cell bodies. The observed waveforms are on the same time scale as the intracellular action potentials, but are much lower in amplitude; extracellular recordings normally yield peak-to-peak amplitudes of up to 100  $\mu\text{V}$ . Figure 2-3 shows neural spikes that were intracortically recorded from a monkey using a tethered data acquisition system [8,11].

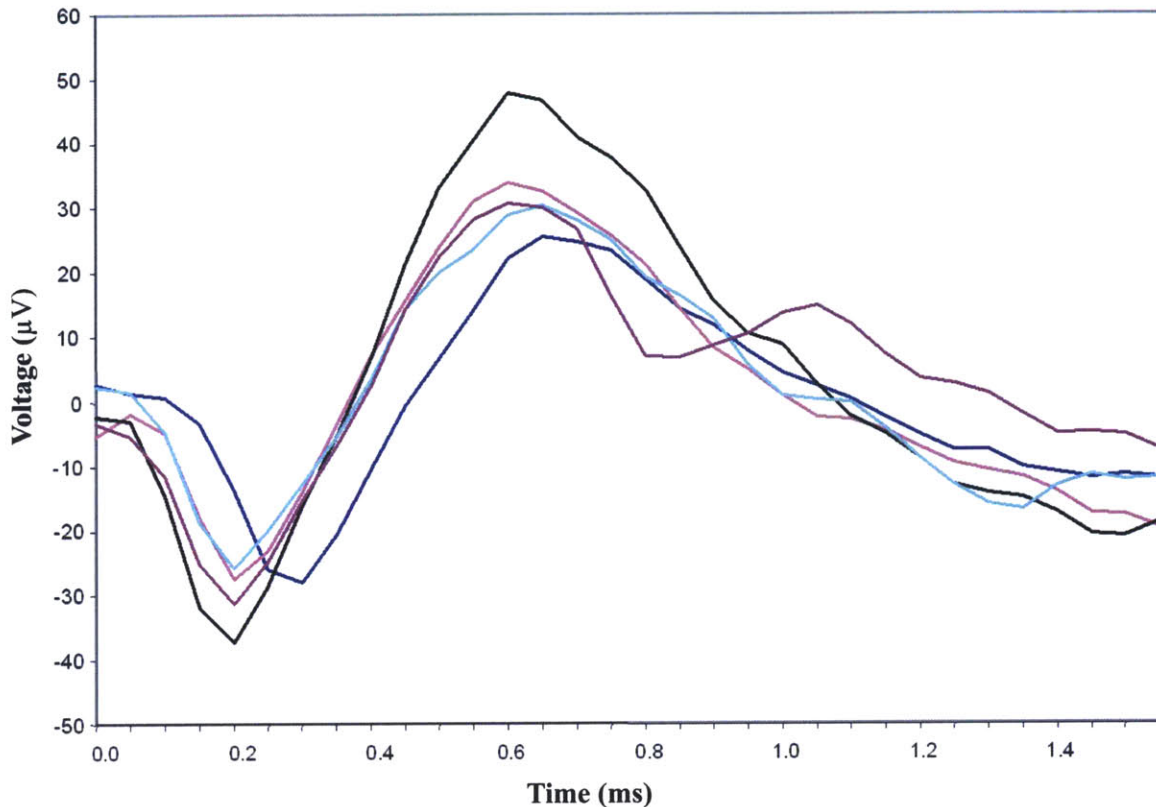


**Figure 2-3.** Plot of neural spikes intracortically recorded from the motor cortex of a monkey [8,11]. (Graph: Jan Maláček)

## 2.4 Wire Electrodes

One of the first and simplest techniques employed for the extracellular recording of neural spikes was the use of individual wire electrodes [17,1]. These electrodes are most easily created by simply cutting an insulated wire so that a cross-sectional surface is created at the end of the wire, although some sharpened tips have been obtained using etching techniques [17]. The exposed surface areas serve as the recording sites and the back ends of the wires are connected directly to a data acquisition system. Wires composed of platinum, stainless steel, or tungsten, for example, with diameters ranging from 13  $\mu\text{m}$  to more than 80  $\mu\text{m}$ , have been used to make chronic recordings of neural activity. Common materials used for insulation include silicon nitride, polyimide, Teflon [18], and parylene. When smaller-diameter microwires are used, larger-diameter probes can be used to reinforce the wires while they are being implanted. One or more microwires can be temporarily attached to a 150  $\mu\text{m}$  diameter tungsten needle, for

example, using sucrose, dextrose, or a wax. The needle reinforces the microwires while they are inserted, and then is withdrawn after the binding agent dissolves in the body.

Both for scientific study and in the development of neural prostheses, there has been a desire for more electrodes to be used concurrently. As the number of signals recorded simultaneously was progressively increased, the use of individually inserted wire electrodes became increasingly difficult. It was this challenge that led to the development of the microelectrode array.

## **2.5 Microelectrode Arrays**

Microelectrode arrays allow one to capture neural signals from a collection of recording sites with a known spatial distribution. A state of the art microelectrode array typically consists of a flat substrate out of which extend 25 to 100 parallel 1 mm long probes, or electrodes, which typically have diameters of about 80  $\mu\text{m}$  and are evenly spaced at about 500  $\mu\text{m}$ . The region of interest when making intracortical recordings is typically at a depth of about 1 mm below the surface of the brain, and some exposed, conductive part of each of these electrodes is used for the recording neural signals at this depth. The size of the recording site is carefully chosen in order to obtain a desirable electrical impedance value. Individual electrical paths must be made for each of the recorded signals to reach the front-end electronics with as little signal degradation as possible. These signal paths must be electrically isolated from each other and the entire array assembly must be insulated from all other brain activity.

The recording sites must be structurally supported during implantation. An assembly structure is required to connect the microelectrode array to additional cabling or to implanted electronics. When chronic recordings are made, a percutaneous connector is typically used as the exit point from the body. Biocompatibility is also especially important in long-term implants.

Many microelectrode array designs have been created over the past few years using a variety of techniques [1,2,17,19]. Few of these techniques however, involve batch process, computer aided design (CAD), computer numerical control (CNC), or automation of any kind. They generally lack the precision and repeatability required to

produce multitudes of arrays with virtually identical characteristics. Typically, the fabrication of a single microelectrode array requires many hours of manual labor. Some automation and repeatability has been achieved, however. Two successful silicon-based approaches are a single-component design developed at the University of Utah [20,21] and a contrasting assembly technique undertaken at the University of Michigan [22,23].

### 2.5.1 The Utah Arrays

The microelectrode structures developed more than ten years ago at the University of Utah, commonly referred to now as “Utah Arrays” [20,21], consist of up to 100 pointed silicon electrodes projecting from a silicon substrate. The electrodes are isolated from one another by non-conducting glass and are typically 0.5 mm, 1.0 mm, or 1.5 mm in length with electrically-exposed tip regions of about 40  $\mu\text{m}$ , when measured along the electrodes from their tips. These exposed areas correspond to electrode impedance values in the range of 50 k $\Omega$  to 100 k $\Omega$ , when measured in 0.9 % saline with a reference electrode. The current form of this array is commercially available as the Bionic [24] array and is manufactured by Cyberkinetics, Inc. [25]. Figure 2-4 shows an image of the Bionic array and two connection options available for performing chronic recordings.

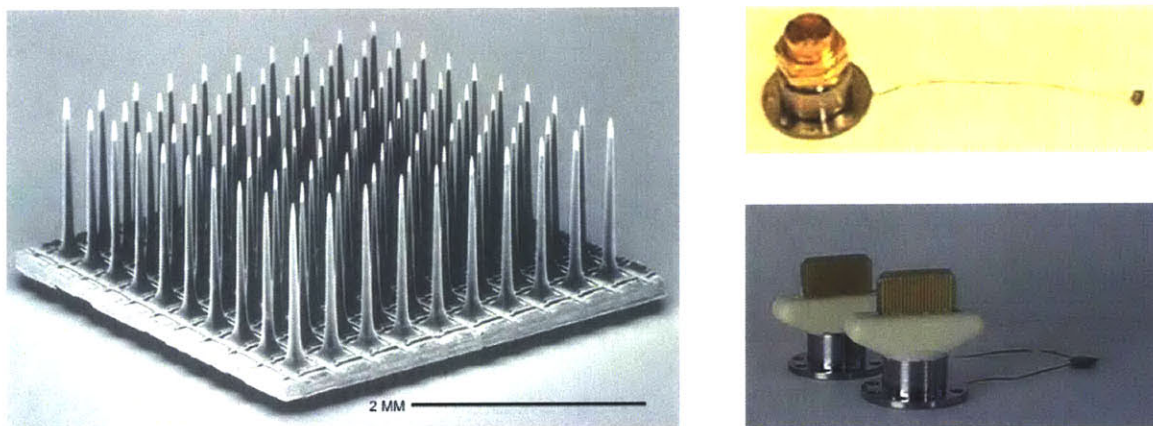


**Figure 2-4. Image of the “Utah Array” (left) and connection options for an 11-electrode assembly (upper right) and a 74-electrode assembly (lower right) manufactured for use in chronic recording. (Photos: Bionic Technologies, LLC [24], and Cyberkinetics, Inc. [25])**

The percutaneous connectors shown in Figure 2-4 (upper right) and (lower right) are secured on the outside of the animal’s skull, and provide connectivity with 11 and 74 electrodes, respectively. Thin connector cables, consisting of several insulated individual

wires, link the connector to the microelectrode array, which is implanted into the brain beneath the dura mater.

This design and its manufacturing processes do have drawbacks. Foremost among them are the lack of flexibility in making minor alterations to the design and the number of manual processes used in constructing the devices. The processes used in creating these devices are not computer numerically controlled (CNC), and the precision and repeatability of the characteristics of these arrays are only achieved through the diligence of practiced, highly-skilled technicians. The addition of features to these arrays, the modification of array configuration, and the use of alternate electrode materials are limited with this approach.

Bionic microelectrode arrays are widely regarded as having highly-desirable recording characteristics. They have been successfully implanted in many animals and historically deliver good recordings.

### **2.5.2 The Michigan Arrays**

Microelectrode arrays recently manufactured at the University of Michigan, Ann Arbor, have been successfully fabricated using a silicon-wafer-based approach that combines silicon micromachining with complementary metal oxide semiconductor (CMOS) fabrication processes [22,23]. Reactive ion etching (RIE), the evaporating of metals onto surfaces, and the application of photoresists are all extensively used in the creation of these complex array structures. The fabrication of these microelectrode arrays requires many steps, but benefits from using a number of CNC processes. Additionally, CMOS circuitry, such as preamplifiers, buffers, and multiplexers, has been successfully integrated into the array structures. Examples of these array structures are shown in Figure 2-5.



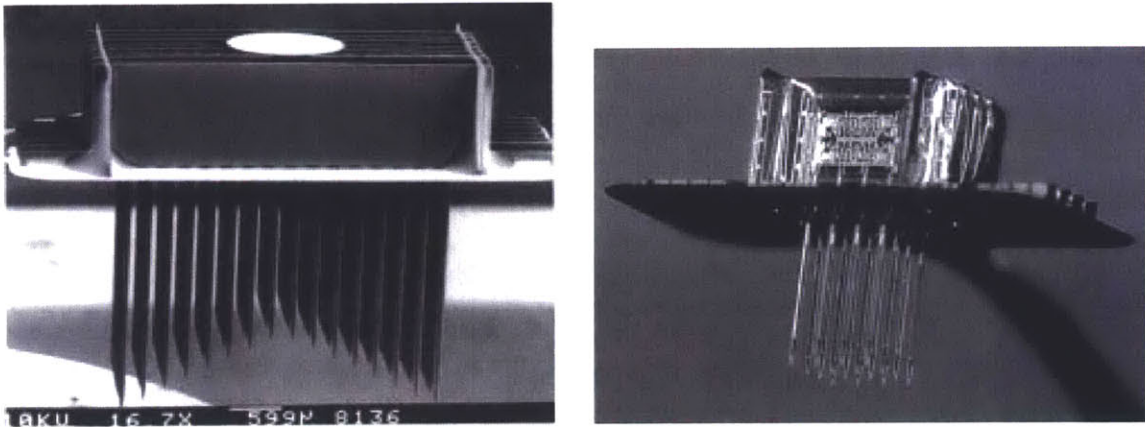


**Figure 2-5. Images of microelectrode arrays that were manufactured using silicon micromachining. (Photos: University of Michigan, Ann Arbor [22])**

Although this approach represents a significant evolutionary step in the development of microelectrode arrays, it is not clear whether the integration of electronics with the microelectrode array structure itself is worth the loss in modularity and the overall increase in the complexity of the device and its fabrication. Though bringing the electrical front end as close to the array as possible is certainly advantageous, it might add flexibility and reduce complexity to create the CMOS circuitry as a separate module that can be attached to a mechanical front end chosen to suit a particular application. This would increase the versatility of the device and could also allow one to create electrodes from materials other than silicon.

Although these arrays have been widely used in recording field potentials, their ability to isolate neural signals from large populations of individual neurons has been limited [17].

## Chapter 3: Design Considerations

There are many aspects to the design of microelectrode array assemblies. Several considerations must be weighed and the design details should be carefully chosen to match the intended application. The requirements for the TEAS device were largely determined by collaborating with neuroscientists who had a working knowledge of what had performed well in the past and of the type of environment in which the device would eventually reside. It was decided that an eight-by-eight array of 1 mm long electrodes with an inter-electrode spacing of about 500  $\mu\text{m}$  was suitable for the first prototypes. These dimensions have been proven to work in practice and are very similar to those of the Bionic [24] arrays, commercially available from Cyberkinetics, Inc. [25], and they were seen as a good starting point.

### 3.1 Modularity

Using a configuration similar to one that is commercially available was seen as a way to increase the modularity of the design. A Bionic [24] array could be used in the place of the TEAS microelectrode array assembly in order to test the electronics if the need arose. And, conversely, the TEAS microelectrode array assembly could be connected to an existing data acquisition system in order to compare its characteristics and performance with those of the Bionic array.

Modularity is also highly desirable because it allows the TEAS to be more easily modified or tuned to suit specific applications. One can potentially use the same electronics modules with different arrays, or the array can be connected in a tethered configuration for acute experiments. This could also potentially allow portions of the system to be reused or replaced in subsequent implantations.

### 3.2 Size and Shape

What shape is best for microelectrodes is an issue often debated by neuroscientists. Sharp pointed tips are generally considered best, though blunt electrodes have been used extensively in the past [19]. The degree of taper given to the electrodes

and the shape of the electrode cross-section are additional variables that must be selected. Some argue that microelectrodes with round cross-sections are best. Others believe that electrodes with square cross-sections may more easily penetrate the brain. This could possibly reduce problems associated with the dimpling of the brain that is observed upon insertion of the device and the amount of trauma that is caused to the animal. It is thought, however, that the most pronounced contributing factors in the amount of trauma caused upon insertion of a microelectrode array are how the device is inserted and the volume that is occupied by the device in the brain [1]. By decreasing the cross-sectional areas of the electrodes, without reducing their length, one decreases the volume that the electrodes occupy in the brain. Ideally, the size of the electrode cross-sections should be determined based on the strength of the materials used in their manufacturing. There is a tradeoff, however, between the cross-sectional area of the electrodes and their strengths.

The overall structure of the mechanical front end can also take several forms. The electrodes must somehow be held in place at the chosen inter-electrode spacing, and electrical connectivity must be made between the electrodes and the front-end electronics. Recording sites with appropriate surface areas must be created and the remaining electrode structure must be insulated.

If the microelectrode array is to be used in acute experiments only, then the overall structure need not be as miniature, and it becomes advantageous to build bigger, more manageable connectors into the array.

### 3.3 Material Properties

#### 3.3.1 Electrode Materials

Table 3-1 gives elastic moduli and strength characteristics for several materials that could be used in the fabrication of microelectrodes. It should be noted that many of the values in Table 3-1 can vary significantly depending on how the material was prepared by the supplier. The table does give values suitable for a rough comparison, however.

**Table 3-1. Material Properties of Some Possible Electrode Materials [26,27,28,29].**

<b>Material</b>	<b>Elastic Modulus (GPa)</b>	<b>Strength (MPa)</b>
Stainless Steel, ANSI Type 316L, Annealed	207	Tensile Yield: 205 Ultimate Tensile: 515
Titanium Alloy, Ti90-Al6-V4, Annealed	110	Tensile Yield: 880 Compressive Yield: 970 Ultimate Tensile: 950
Titanium (100 %)	116	Tensile Yield: 140 Ultimate Tensile: 220
Tungsten Carbide Cemented in 10 % Cobalt	680	Compressive Yield: 6250
Gold (100 %)	80	Ultimate Tensile: 120
Platinum (99.95 %)	171	Ultimate Tensile: 140
Iridium (100 %), Annealed	524	Ultimate Tensile: 1000
Silicon (100 %)	112	Compressive Yield: 120

### **3.3.2 Insulating Materials**

Several alternatives exist for the materials used for insulating the array electrodes. These choices include silicon nitride, polyimide, Teflon [18], and parylene. Silicon nitride has historically been the most widely used material [17], but parylene is now generally perceived to deliver the best performance due to its inertness in the body and its being impervious to almost all substances. Additionally, its ability to be deposited in a uniform, pinhole-free conformal coating is very advantageous.

### **3.3.3 Biocompatibility**

Biocompatibility is an important concern when chronic recording is to be done using microelectrode arrays. All of the materials involved in the fabrication of the assembly should be carefully chosen in order to minimize any harmful reactions in the body. If possible, this should include even the fully-encapsulated materials in order to protect against the unlikely event of the encapsulation being worn away. As BMIs are developed for clinical use, biocompatibility issues will become even more important.

When a microelectrode array system is designed and constructed to be used acutely, biocompatibility considerations can be altered accordingly. Using a microelectrode array assembly built for taking chronic recordings in an acute experiment would likely put unnecessary constraints on the design. For example, one is normally less concerned with biocompatibility issues if the device will not be left for a long time in the animal, and even less so if the animal is to be sacrificed immediately following the experiment. This is not to say that the materials should be chosen arbitrarily, but stronger, less biocompatible materials could be used in the underlying, encapsulated components of the device. Also, less costly approaches can be taken. This may be especially true in the design of the connection between the array and the data acquisition system. Acute experiments are normally performed with the cranium open, which allows for the possibility of using larger, simpler connectors in place of the specially-designed, more costly connectors typically used for chronic recordings.

### 3.3.4 Strength Considerations

If a large enough axial load is incident on the array's microelectrodes upon insertion into the brain, for example, the electrodes are at risk of undergoing buckling and collapse. Buckling occurs when lateral bending is observed [30]. Under an increasing axial load, the lateral deflection of the electrode will increase as well, until the electrode undergoes inelastic yielding, or in the case of a brittle material, until the electrode fractures. An array of microelectrodes can be modeled as a collection of ideal elastic columns fixed in a substrate at one end and free at the other. Upon insertion, an electrode is subjected to an axial Euler load as shown in Figure 3-1.

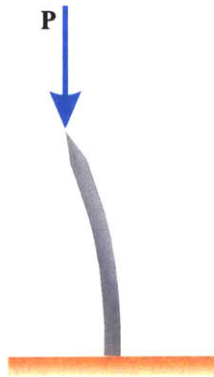


Figure 3-1. Drawing of an electrode subjected to an axial load upon insertion.

The critical load for an ideal elastic column that undergoes Euler buckling is given by

$$P_{cr} = \frac{\pi^2 EI}{L_e^2}, \quad (3-1)$$

where  $P_{cr}$  is the critical load,  $E$  is the elastic modulus of the material,  $I$  is the moment of inertia of the column, and  $L_e$  is the effective length of the column [30]. For a column fixed at the base and free at the top, the column deflects in a mode where the effective length is twice the length of the column. The effective length is therefore

$$L_e = 2L, \quad (3-2)$$

where  $L$  is the length of the electrode. Substituting Equation (3-2) into Equation (3-1) gives

$$P_{cr} = \frac{\pi^2 EI}{4L^2}. \quad (3-3)$$

The moment of inertia for an electrode with a square cross-section is given by

$$I = \frac{w^4}{12}, \quad (3-4)$$

where  $w$  is the width of the electrode.

From Equations (3-3) and (3-4), one observes that the critical load,  $P_{cr}$ , depends only on the dimensions of the electrode and the elastic modulus of the material from which the electrode is made. For an electrode of given dimensions, the critical load is proportional to the elastic modulus value. When the axial load is less than  $P_{cr}$ , the electrode remains stable and will return to its rest position after the load is removed. If the load is larger than  $P_{cr}$ , the electrode becomes unstable and the structure buckles.

Using the data from Table 3-1 and the above equations, one observes that silicon, titanium, and titanium alloy can all bear similar axial loads. Stainless steel 316L can bear about 85 % more axial load than silicon, however, and tungsten carbide can bear over 600 % more.

From Equations (3-3) and (3-4), one also observes that the critical axial load is proportional to the inverse of the square of the electrode's length and directly proportional to the electrode's width, raised to the fourth power. Put another way, if one doubles the length of an electrode, the axial load that it can bear is decreased by a factor of four, and if one decreases the width of an electrode by a factor of two, the axial load that the electrode can bear is decreased by a factor of sixteen. Again using the data from Table 3-1, one can calculate that by using tungsten carbide in the place of silicon or titanium, one can reduce the electrode widths by over 35 %, while still being able to bear similar axial loads.

When one refers to one array being stronger than another, one is often referring to the susceptibility of the arrays to damage while being positioned during the implantation procedure or while they are being connected to additional hardware. The maximum stress will occur in an electrode, for a given force, when the force is applied transversely at the electrode tip, as shown in Figure 3-2. This represents the least amount of force required in order to damage the electrode.

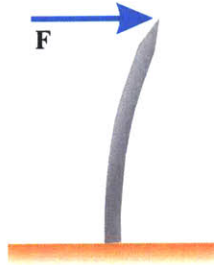


**Figure 3-2. Drawing of an electrode subjected to a transverse force.**

Because the electrode can be considered a long slender beam, and because the shear stresses are much smaller than the bending stresses due to the geometry, the maximum stress [31] is given by

$$\sigma_{\max} = \frac{Mc}{I}, \quad (3-5)$$

where  $M$  is the maximum bending moment,  $c$  is the distance from the neutral axis of the deflection to the edge of the electrode, and  $I$  is the moment of inertia of the column.

The maximum stress in the electrode occurs at the section with the greatest bending moment, which in this case is at the electrode's base. By balancing the moments on the electrode and substituting, Equation (3-5) becomes

$$\sigma_{\max} = \frac{FLc}{I}, \quad (3-6)$$

where  $F$  is the transverse force and  $L$  is the length of the electrode. From Equation (3-6), one observes that the maximum stress is proportional to the transverse force that is applied to the electrode, as well as to the electrode's length. In order to ensure that electrodes will not collapse, all forces that are applied to the electrodes for whatever



reason should be kept at levels which ensure that the maximum resulting stresses remain significantly below the yield strength of the electrode material.

An important consideration when choosing a base material for a microelectrode array is whether it is desirable for the electrodes to be brittle or to be ductile. Electrodes made of silicon or tungsten carbide will tend to break off if exposed to high forces, while electrodes constructed from stainless steel or titanium will tend to bend. One should consider whether it is more advantageous to have an electrode break off or to have it bend and collapse when subjected to high loads. In fabrication and assembly, electrodes can be bent back into position. This can increase the yield of the manufacturing processes by reducing the likelihood of irreversible damage. Also, one may want to reduce the possibility of dislocated, detached electrodes retained in the brain. There is a tradeoff, however, as the use of a cemented composite like tungsten carbide introduces a considerable increase of strength to the electrodes, allowing them to bear greater loads.

### **3.3.5 Volume Considerations**

In order for a neuroprosthesis to provide fine motor control, it is necessary to produce recording sites distributed at a high spatial density. By increasing the number of recording sites over a given area, one increases the likelihood of capturing the necessary neural signals. Unfortunately, in doing so, one tends also to increase the volume that is occupied by the array electrodes in the brain. Trauma to the brain is related to the volume of neural tissue that is displaced. It is therefore desirable to maximize the number of recording sites per volume of neural tissue displaced, the RS/NTD ratio [1].

Several approaches can be taken when manufacturing microelectrode arrays in order to increase the density of the recording sites. One approach is to simply decrease the inter-electrode spacing of the array. Without simultaneously decreasing the electrode widths and therefore increasing the RS/STD ratio, however, an increased volume of neural tissue will be displaced. By using stronger materials, one can reduce the electrode widths and increase the RS/NTD ratio without compromising electrode strength. This can potentially be used to avoid the increase in the volume of brain that would otherwise be displaced.

Another approach that can be taken is to alter the array pattern or configuration. Electrode arrays are typically manufactured in square or rectangular configurations. The use of alternative configurations is possible, however. For example, microelectrode arrays with hexagonal configurations resembling the shape of a honeycomb, with the electrodes equally spaced from their six closest neighboring electrodes, could be manufactured. This configuration increases the electrode spatial density of the array by over 15 % for a given inter-electrode spacing when compared with the common square configuration. Arrays with this configuration are displayed in Chapter 4.

Yet another approach that can be taken is to distribute the recording sites over a range of depths. This can be accomplished by fabricating arrays of electrodes with varying lengths, as demonstrated in Chapter 4. In addition, one could also potentially fabricate microelectrode arrays with more than one recording site on each electrode. The recording sites could, for example, be distributed over a range of depths along each electrode. Although this represents a challenging fabrication problem, it would dramatically increase the RS/NTD ratio, provided that the recording sites could be added to the electrodes without substantially increasing the electrode dimensions.

### **3.4 Recording Considerations**

Whenever recording of bioelectric events is performed, one must pay special attention to the impedance values involved. These include the impedances of the analog front-end electronics, of the microelectrodes and the connecting wire, and of the junctions between the metal electrodes and the fluid of the brain. Carefully selecting these impedance values is especially important when making intercellular recordings in the cortex due to the small signals involved.

#### **3.4.1 Electrode Surface Metals**

When a metallic electrode is introduced into a biological environment or an aqueous solution, some of the metal ions will typically enter into solution and some the ions in the solution will typically combine with the electrode [19]. The net result of this reaction is that a charge potential appears at the electrode-electrolyte interface. This

charge potential at the electrode-electrolyte interface impedes to some degree the electrode's ability to pass charge and introduces capacitive effects. The resulting ionic distribution has been found to substantially affect an electrode's properties. It has been found that platinum, and more specifically a form of porous platinum known as platinum black, delivers very favorable electrode-electrolyte impedances. It is for this reason, and due to its excellent biocompatibility, that platinum is seen as the metal encapsulant of choice when fabricating microelectrode arrays.

### 3.4.2 Impedance Values

Because of the nature of the electrode-electrolyte interface at the recording sites, electrode impedance can be represented by an equivalent series combination of resistance and capacitance [19]. In microelectrodes, both resistance and capacitance typically vary approximately inversely with the square root of frequency. Additionally, the reactance,  $X$ , of an electrode, which can be represented by

$$X = \frac{1}{2\pi f C}, \quad (3-7)$$

where  $f$  is the frequency and  $C$  is the series capacitance, is typically approximately equal to the electrode's resistance [19].

An electrode's series capacitance,  $C$ , is known to vary with the surface area,  $a$ , of its recording site according to

$$C = \frac{K a}{f^\alpha}, \quad (3-8)$$

where  $K$  is a constant that depends on the nature of the metal-electrolyte junction and  $\alpha$  is a constant that describes the rate at which the capacitance decreases with increasing frequency. Typical values for the constants  $K$  and  $\alpha$  are 1.608 F/m<sup>2</sup> and 0.525 for stainless steel and 117.59 F/m<sup>2</sup> and 0.211 for platinum black, when measured in 0.9 % saline [19]. As can be seen from these  $K$  values, electrolytically-preparing the electrode, for example by the deposition of platinum black, can have a dramatic effect on the series

capacitance and impedance of the electrode. Roughened surfaces, increased electrolyte concentrations, and increased temperatures have all additionally been found to increase the values of the series-equivalent capacitance [19].

The constant  $\alpha$  is typically about 0.5 and is related to the phase angle,  $\phi$ , by

$$\phi = \frac{\pi}{2}(1 - \alpha). \quad (3-9)$$

The phase angle,  $\phi$ , whose tangent is the ratio of reactance to resistance, is typically therefore about 45 degrees and is fairly constant over the most relevant frequency range of 100 Hz to 10 kHz [17]. The electrode impedance,  $Z$ , for the series-equivalent resistance,  $R$ , and reactance,  $X$ , is given by

$$Z = \sqrt{R^2 + X^2}. \quad (3-10)$$

By assuming  $R = X$ , and by substituting Equations 3-7 and 3-8 into Equation 3-10, the impedance becomes

$$Z = \sqrt{2}X = \frac{1}{\sqrt{2\pi f^{(1-\alpha)}Ka}}. \quad (3-11)$$

A suitable range for the electrode impedances is believed to be 50 k $\Omega$  to 150 k $\Omega$  at 1 kHz when measured using a reference electrode after immersing the array in 0.9 % saline [17]. This range of values is consistent with those experimentally measured on a Bionic [24] microelectrode array system known to give satisfactory results. Using values of 0.366 and 49.5 F/m<sup>2</sup> for constants  $\alpha$  and  $K$ , corresponding to a medium platinum black finish, an electrode recording site area of 570  $\mu\text{m}^2$  is required in order to produce an impedance of 100 k $\Omega$  at 1 kHz. Assuming a hemispherical electrode tip with a 10  $\mu\text{m}$  radius, which is a fair approximation, this surface area leads to a recording site diameter of about 20  $\mu\text{m}$  when viewed from above the electrode tip.

Tradeoffs are involved when selecting the electrode impedances. One is the tradeoff between good signal recording and the likelihood of recording any signal at all. If one selects a lower impedance value for an electrode, one will increase the likelihood

of recording from a nearby neuron. But at the same time, one increases the likelihood of recording from more than one neuron, and one will likely also record an increased amount of noise. The neural spike could potentially get washed out. If one were to select a higher impedance value, the quality of the potential neural recording is increased. However, with a higher impedance value, the recording site would have to be closer to the neuron in order to register a signal at all.

The impedance should additionally be kept well below the input impedance of the front-end electronics in order to minimize loading errors and other potential problems. The impedance values chosen for the electrodes must be compatible with the input impedances of the first-stage operational amplifiers (op-amps) of the analog front end. If the input impedance of the analog front end is too low, significant loading errors can occur. Charging of the electrodes can result from the bias currents of the op-amps, creating undesirable DC offset errors, if no bias return path is provided.

Creating electrodes with chosen impedance values is not a simple task. Whatever method is used to produce exposed surface areas on the electrode tips will require considerable calibration. In addition to the area that is exposed, the resulting impedance will be a function of the surface metal, including its porosity and its uniformity.

### **3.4.3 Grounding and Reference Paths**

A ground or reference electrode is required in order to make the recordings. A low-impedance return path is preferred in order to ensure that the observed signal is derived from the intended electrode and is not a result of the presence of noise on the reference electrode. An insulated wire, with a 1 mm to 2 mm recording site is normally used for this lower-impedance electrode. Other options for this reference path include the use of a microelectrode on the array with a recording site of increased area and the use of several electrodes connected in parallel.

## **3.5 Device Implantation**

How a microelectrode array will be implanted is an important consideration for its design. Insertion of the array can be done using a variety of tools and at a variety of

speeds. For example, the array can be inserted slowly using a micromanipulator or an electric micrometer drive. Some dimpling of the brain is often observed when the array is inserted slowly, however. This effect becomes more pronounced as the density of the array is increased. It has been demonstrated that by generating a controlled impulse on that back side of the array, it can be propelled into the brain with minimal dimpling. The Bionic [24] pneumatic inserter, manufactured by Cyberkinetics, Inc. [25], is a device that has been designed to serve this purpose.

## Chapter 4: Design and Fabrication

A microelectrode array assembly consists of several components, all of which present fabrication challenges. When designing a device at this scale, one must at once consider how each component will be built and how all of the components will be assembled. Often, special tools and fixtures must be constructed in order to aid in handling and in order to ensure the proper alignment of the components.

Microelectrode array assemblies can take a large variety of forms, and there are numerous manufacturing technologies and methods that could be used in their fabrication. The methods that were developed in order to construct the TEAS mechanical front end and the other microelectrode arrays shown here were derived from expertise and technologies available at the Massachusetts Institute of Technology's BioInstrumentation Laboratory. Specifically, the use of wire electrical discharge machining (EDM), printed circuit board rapid-prototyping equipment, and parylene deposition equipment were instrumental in the creation of these arrays.

### 4.1 The TEAS Array Design

The first two prototypes of the mechanical front end fabricated for the TEAS project were designed to be implanted into the motor cortex of a *Macaca mulatta* monkey. The region of interest for the intended recording is at a depth of 1 mm below the surface of the brain. The design of the first prototypes is most similar to that of the Bionic [24] microelectrode array assemblies manufactured by Cyberkinetics, Inc. [25]. As highlighted in Section 2.5.1, this type of assembly, commonly known as the Utah array [20,21], is normally used for intracortical recording and consists of an evenly-spaced, square array of silicon electrodes that are normally made to penetrate about 1 mm below the surface of the brain. This type of array assembly has delivered satisfactory results and its specifications were seen as a good starting point for the TEAS design. Figure 4-1 shows an image of the first prototype of the TEAS mechanical front end. This microelectrode array assembly was implanted into the motor cortex of a monkey.

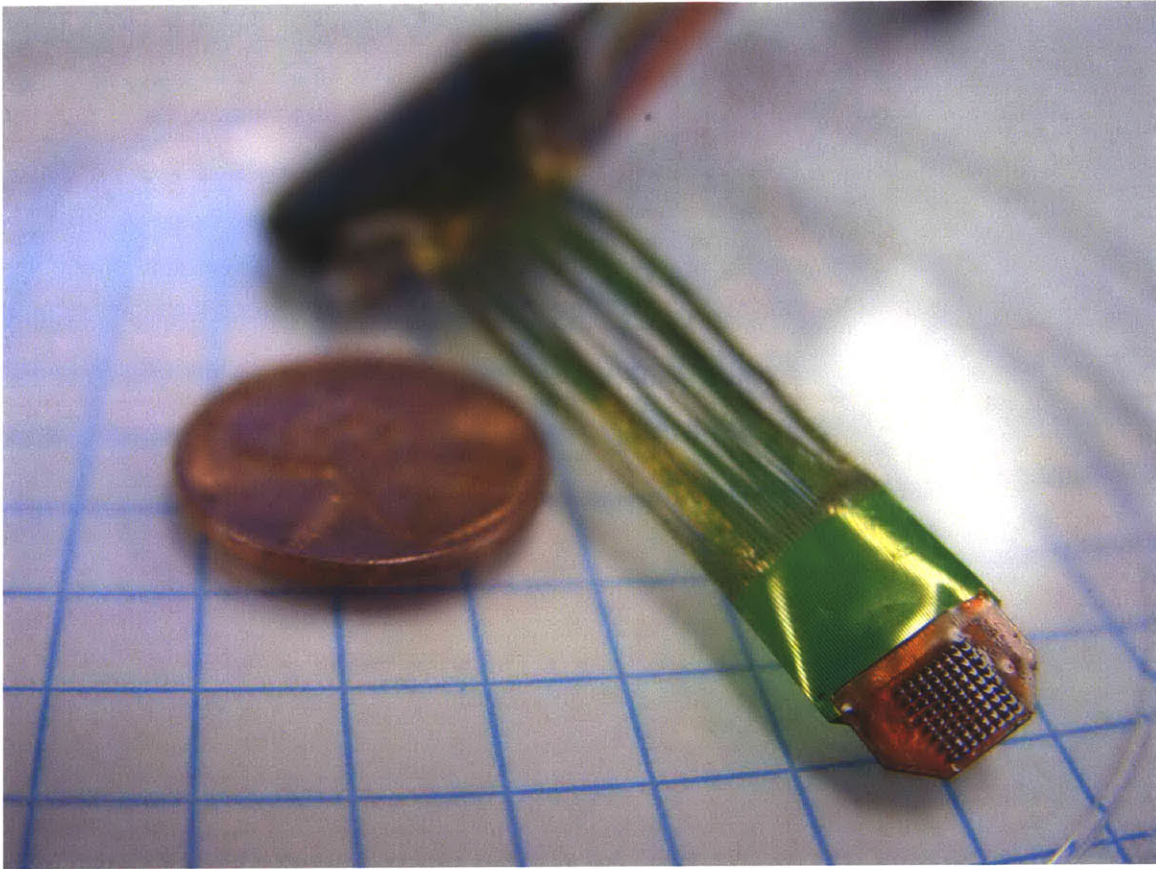


**Figure 4-1. Image of the first prototype of the TEAS mechanical front end. (Photo: Robert Dyer)**

Although the Utah arrays and the TEAS arrays are similar in shape and function, the methods involved in the manufacturing of these arrays differ significantly. The use of computer aided design (CAD) and computer numerically controlled (CNC) processes are fundamental to the methods developed for manufacturing the TEAS array assemblies. A goal of the TEAS mechanical assembly process is to use and develop fabrication methods that can be automated to greatest extent possible. By using CAD and CNC processes, minor changes to the specifications of the array assembly can be made relatively easily and with predictable results. For example, the shape, the dimensions, and the inter-electrode spacing of the array assembly can be changed through the use of CAD, and the impedance values at the electrode tips can be changed by altering the manufacturing parameters.

A square array of 64 electrodes with an inter-electrode spacing of 508  $\mu\text{m}$  was chosen for the configuration of the first prototypes of the TEAS mechanical front end.



The array is made up of square cross-section electrodes with widths of 80  $\mu\text{m}$  and lengths of 1 mm from electrode tip to the insulating substrate that supports the electrodes. The insulating substrate at the base of the electrodes is designed to extend past the electrodes. This increases the area resting on the surface of the brain, which helps to maintain the recording sites at the desired depth. Additionally, this extended area provides a surface that can be used in the handling and the assembly of the array structure. A decision was made to use flexible printed circuit board technology to make the first prototype connector cable. This technology is well developed and was thought to be a good fit for the cable requirements. The cable dimensions were chosen based on the relative locations of the implantation site on the cortex of the *Macaca mulatta* monkey and the location to which the electrical module would be secured. The components of the array assembly and their basic dimensions are shown in Figure 4-2. Note that a fine-pitch connector (not shown) at the base of the connector cable (upper-left) joins the TEAS mechanical front end to its electronic subsystems.

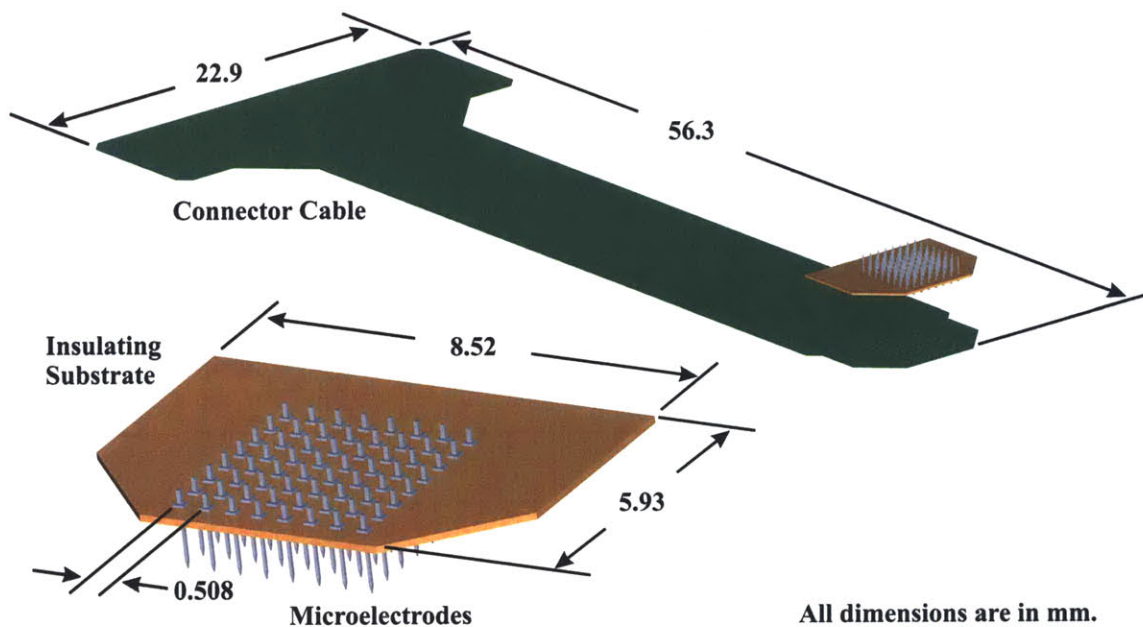


Figure 4-2. Schematic of the TEAS mechanical front end showing the major components.

## 4.2 Wire Electrical Discharge Machining

Electrical discharge machining, often referred to as EDM, makes use of the erosive effects of an electrical discharge to remove material from the workpiece [32,33]. It is a forceless process in which there is no contact between the workpiece and the machining electrode. Sparks are generated several thousand times a second between an electrode and the workpiece, which are separated by a dielectric fluid. The energy that results from the sparks is dissipated by the melting and vaporizing of the materials making up the workpiece and the electrode. This erosive process occurs at the  $\mu\text{m}$ -scale. At the beginning of each sparking cycle, which typically lasts on the order of  $10\ \mu\text{s}$ , current flows between the electrode and the workpiece over areas where the gap is smallest. The dielectric fluid is then transformed into a plasma of hydrogen and oxides filled with ionized or electrically charged particles. As current flows through the plasma, it quickly reaches a temperature on the order of 10,000 degrees C. The voltage soon reaches a threshold, normally on the order of 100 V to 200 V, and then momentarily drops, resulting in a dramatic loss in the plasma's energy. The electrical supply is cut off for the latter part of the machining duty cycle, at which time the plasma implodes due to a sudden drop in its temperature, creating a low-pressure pulse which draws in dielectric fluid and flushes away the removed material which has solidified into a collection of small spheres. The cycle then repeats. EDM, in general, occurs in a tightly-controlled environment and uses computer numerically controlled (CNC) stages in order to perform positioning with  $\mu\text{m}$ -precision. The two common types of EDM are sink or plunge EDM and wire EDM.

In wire EDM, the electrode is in the form of a wire that is continuously fed through and past the workpiece at a rate of about 150 mm/s. The wire is held at a constant tension by a control system using a complex collection of belts, sensors, and drives. The wire's position through the EDM tank is held in place by a pair of wire guides. The wire is never in contact with the workpiece, and because it is continuously fed through the system, it is always of known dimensions and has a consistent surface finish, which ensures the precision of the EDM cut. The spark gap, created by the sparks occurring between the wire and the workpiece, is continuously flushed with fluid in order

to cool the zone and remove debris. The dielectric fluid used in wire EDM is typically deionized water. The deionization is normally done using chemical distillation by an organic resin, and the fluid is continuously filtered and held at a temperature of 20 °C.

The wire electrical discharge machine, generally also referred to as a wire EDM, used to create many of the structures described in this document, is a Robofil 1020SI, manufactured by Charmilles Technologies AG [34]. An image of the machine is shown in Figure 4-3.

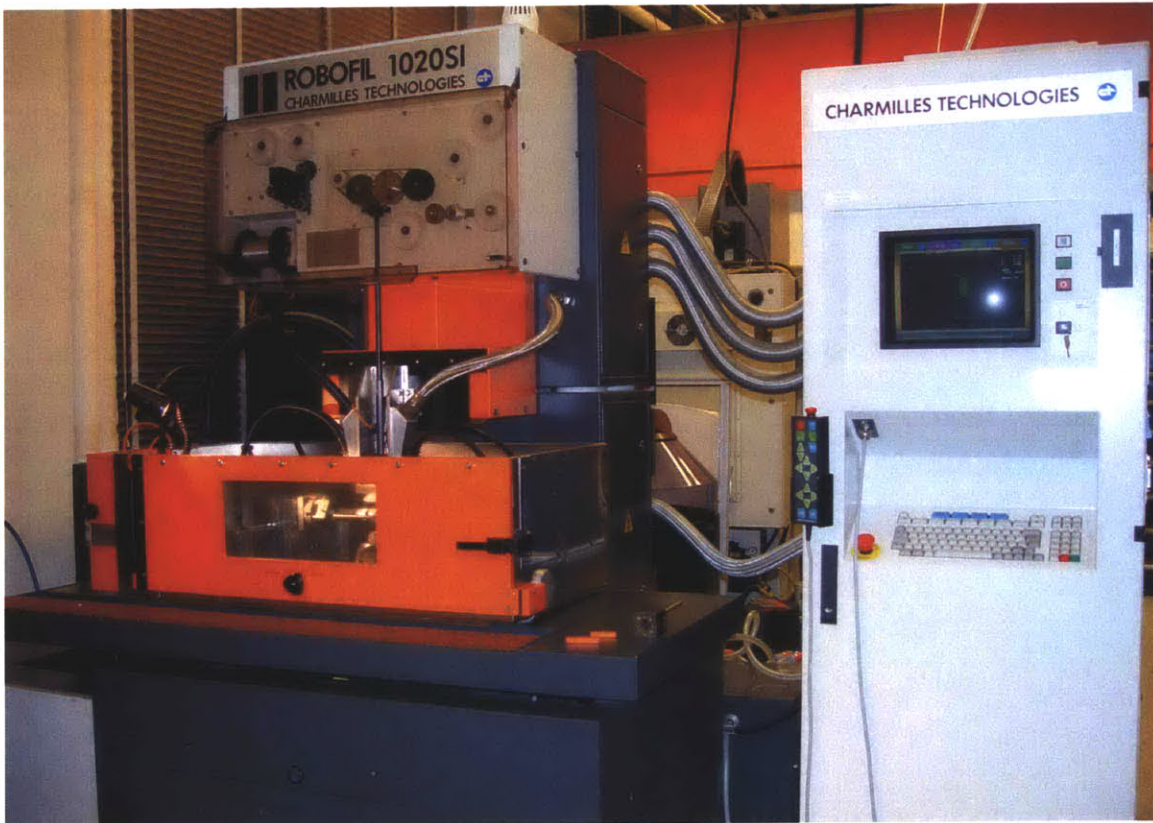


**Figure 4-3. Image the Charmilles Technologies wire electrical discharge machine (wire EDM).**

In wire EDM, several passes are normally performed in a repeated loop in order to produce the desired surface finish. The machining speed is servo controlled, with the cut advancing faster when the amount of material encountered decreases and slower when more material is present. The first cut, known as the roughing cut, proceeds through solid, uncut material, and it is the slowest due to the volume of material encountered. It is the highest-powered cut, however, and removes material at a higher rate than the subsequent cuts, or passes. The subsequent passes, also known as skimming

or finishing cuts, are performed at lower power levels. They are completed faster, however, because they follow a previously cut path. The finishing cuts are also performed at higher sparking frequencies, which produce finer surface finishes. Figure 4-4 shows a drawing of the wire EDM process. The roughing cut creates the initial path through the workpiece. The subsequent finishing passes remove less and less material, but they also give finer and finer surface finishes. Note that the initial cut must be substantially offset from the final part dimension. For each subsequent pass, the offset is then progressively reduced until the final finishing cut. The offsets are normally calculated by the machine software according to the number and power-levels of the passes that are selected. One must, however, specify on which side of the roughing cut the subsequent passes should be offset.

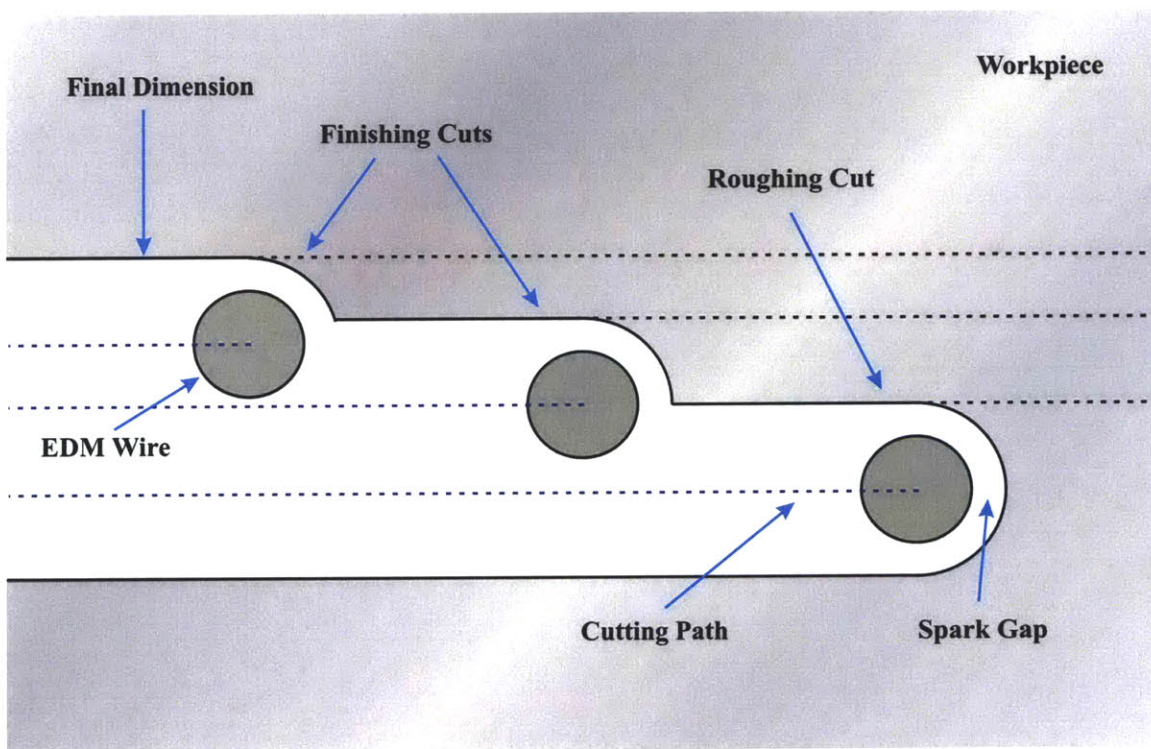


**Figure 4-4.** Drawing showing the wire EDM process. After the initial roughing cut, several skim passes are normally performed in order to obtain the desired surface finish.

Wire EDM is capable of delivering highly repeatable results. Structures with very high aspect ratios can be produced with this process due to its forceless nature. Because it is computer numerically controlled and is based on a computer aided design (CAD) process, design modifications are straightforward to implement and lead to predictable

results. More details on the use of wire EDM in the fabrication of microelectrode arrays are given in Section 4.4.

### 4.3 Fabrication Process Overview

The microelectrode array shown in Figure 4-5 was designed as a prototype for the mechanical front end of the TEAS system and was implanted into the motor cortex of a monkey. The assembly consists of several components: the array of microelectrodes, the insulating substrate, the connector cable, and the connector that attaches the assembly to the electrical front end. For the first implanted prototypes, additional adapter boards were constructed and used to connect the signal paths to the data acquisition system via percutaneous connectors.



Figure 4-5. Image of an assembled TEAS microelectrode array assembly [11].

The mechanical assembly process used for the fabrication of the first prototypes of the TEAS mechanical front end involves a number of steps. A schematic of the steps in the fabrication process a microelectrode array assembly is shown in Figure 4-6. Step 1 in the process is the manufacturing of the metal microelectrode array. The microelectrode array is wire Electrical Discharge Machined (wire EDM) from a solid piece of metal. Chemical etching is also used in order to further reduce the array feature sizes, thereby increasing the aspect ratio of the electrodes. Chemical etching also removes oxide from the surfaces of the electrodes, which aids in electroplating. The array is electroplated with a metal such as gold or platinum in order to improve the biocompatibility and the electrical characteristics at the junction between the electrode tips and the brain. In Step 2, an insulating polyimide substrate is manufactured using printed circuit board rapid-prototyping equipment. The substrate serves as the foundation of the array assembly. The substrate is machined with a hole pattern that matches the inter-electrode spacing of the array. In Step 3, the insulating substrate, with holes large enough to easily fit around the electrodes, is lowered over the electrodes until it rests on the ledges built into them. The holes are covered with a thin layer of epoxy before the substrate is lowered onto the array. Surface tension keeps the epoxy in the holes at the electrode ledges while the epoxy cures.

Because the electrodes are machined from a single piece of metal, they are initially connected to a solid metal electrode base. In Step 4, after the epoxy has cured, the array assembly is removed from the base by wire EDM. In Step 5, a connector cable is manufactured using flexible printed circuit board technology. The connector cable was designed to have through holes with a hole pattern that matches the inter-electrode spacing of the machined array. Electrical pads, made of gold, surround the through holes on the connector cable. In Step 6, with the help of a specially-designed fixture, the connector cable is lowered over the back ends of the electrodes which protrude from the insulating substrate. In Step 7, the back ends of the electrodes are soldered to the electrical pads on the connector cable. The solder joints are then covered with a layer of epoxy. In Step 8, the array assembly is coated with parylene in a vapor deposition process. Parylene is removed from the electrode tips using laser ablation. In Step 9, the array assembly is prepared for implantation and connected to the front-end electronics.

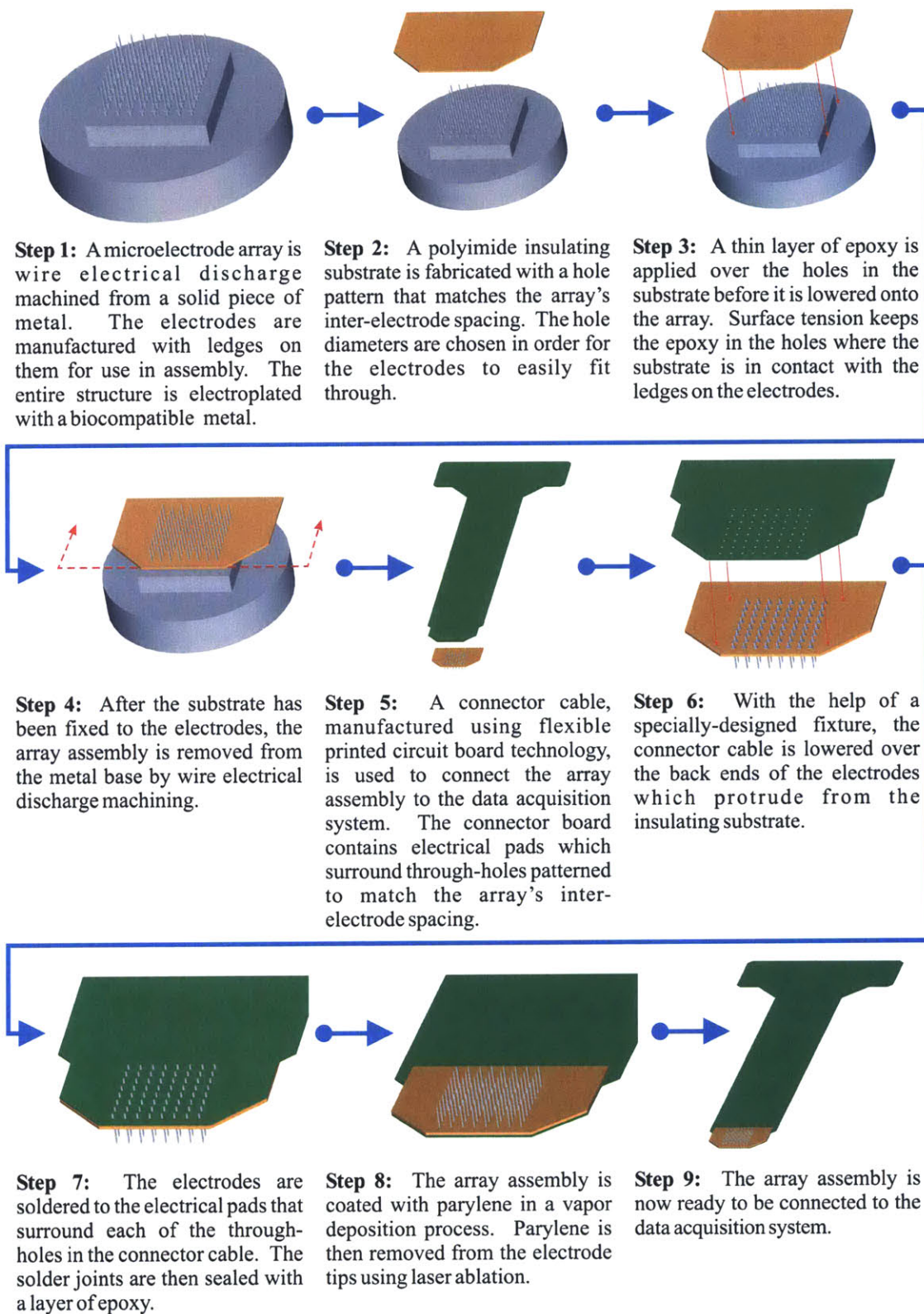
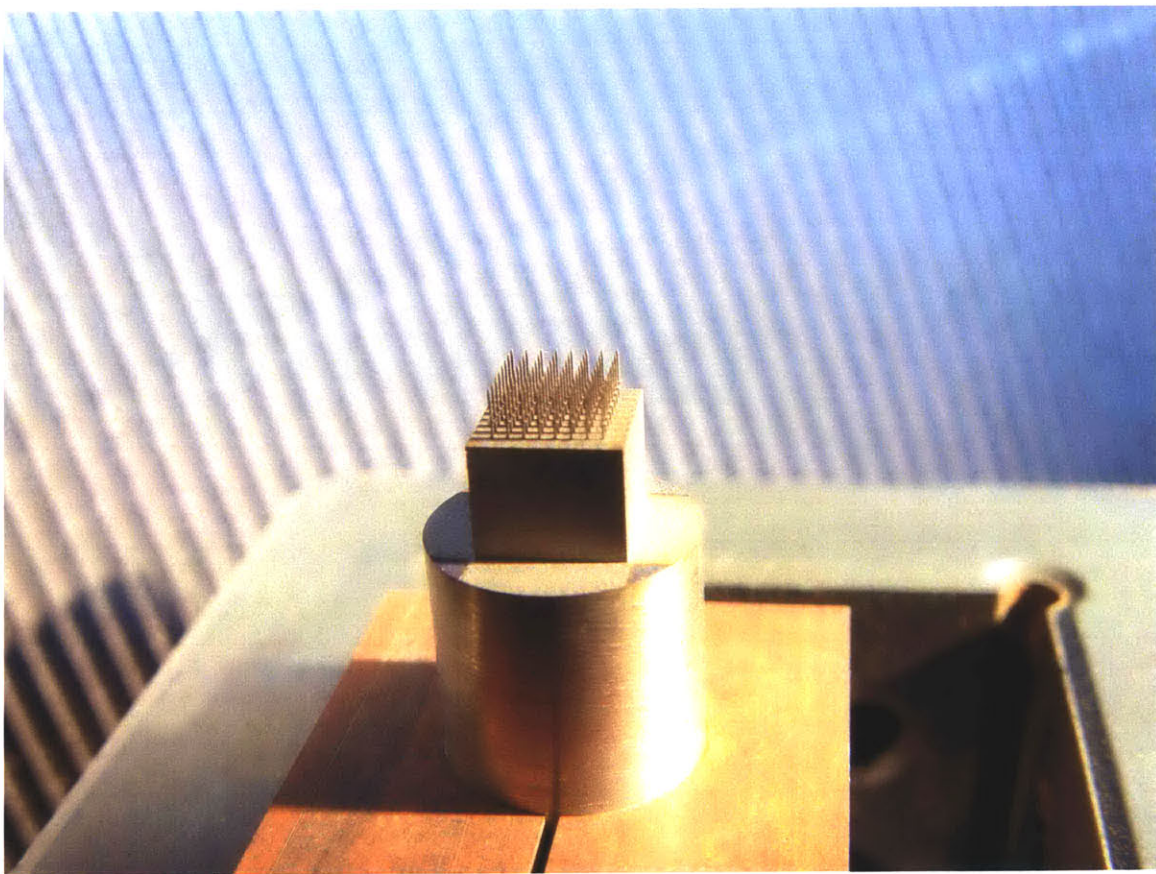


Figure 4-6. Schematic showing the steps in the microelectrode array assembly fabrication process.

## 4.4 Microelectrode Array Fabrication

The microelectrode arrays are manufactured by wire electrical discharge machining (wire EDM) a solid piece of a conductive material. A Charmilles Technologies [34] Robofil 1020SI, running with a 100  $\mu\text{m}$  diameter wire, was used to produce the structures shown below. Solid titanium (99.6+ %) was used for the first prototype of the TEAS array assembly. Titanium-aluminum-vanadium alloy (Ti90-Al6-V4) was used for the second prototype. The forceless EDM process allows one to obtain aspect ratios and surface features suitable for assembly and insertion into brain. Because the design and manufacturing of the electrodes is done using a computer aided design (CAD) process and computer numerically controlled (CNC) machining, one can alter the shapes of the electrodes and the dimensions of the arrays with little difficulty. Figure 4-7 shows a microelectrode array that was machined from a 9.5 mm diameter titanium rod.



**Figure 4-7.** Image of a microelectrode array still connected to its base. The array was machined from a 9.5 mm diameter titanium rod. The electrodes are 1.7 mm in length and are spaced 508  $\mu\text{m}$  apart.



For the first prototypes of the TEAS array assemblies, the electrodes were designed to be 1 mm in length after being assembled through the insulating substrate. They were machined to 80  $\mu\text{m}$  by 80  $\mu\text{m}$ , square, and were spaced 508  $\mu\text{m}$  apart. The electrode tips were rounded at a radius of 10  $\mu\text{m}$  and angled out until they reached the full electrode width of 80  $\mu\text{m}$ , 15  $\mu\text{m}$  from the tips. The electrodes were initially machined to a length of 1.7 mm, with ledges part way along the electrodes that serve as platforms for securing an insulating substrate. The ledges were machined square, with overall widths of 200  $\mu\text{m}$  and thicknesses of 50  $\mu\text{m}$ . Figure 4-8 shows the dimensions of the TEAS microelectrode array.

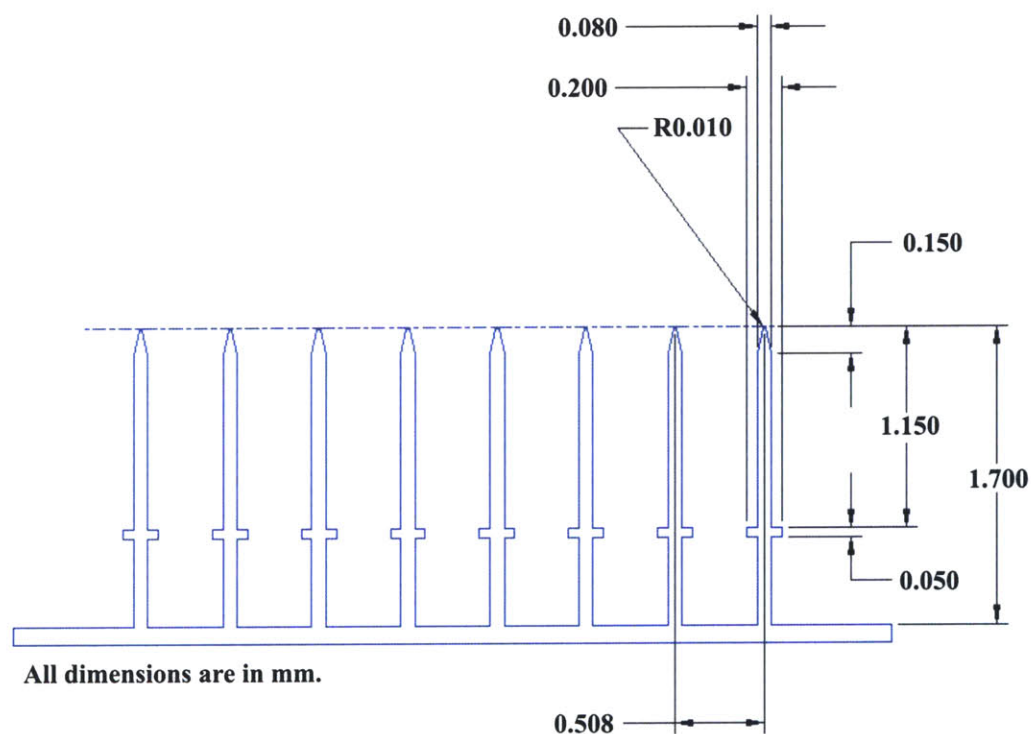


**Figure 4-8. Schematic showing the dimensions of the TEAS microelectrode array.**

Wire EDM readily produces electrodes with square cross-sections. If circular cross-sections were desired, an additional method would have to be used in order to round the edges of the electrodes. Chemical etching is a process that has been shown capable of rounding the edges of electrodes [19,30,21,21]. It was decided, however, that the electrodes would be left square and that effort would be better spent obtaining microelectrode arrays with uniform surface finishes. Additional effort would be spent

reducing the cross-sectional areas of the electrodes, an important parameter in the reduction of trauma experienced by the brain.

#### **4.4.1 Planning and Generating a Cutting Path**

A typical wire EDM cut is normally a result of three general steps. The steps are: the development of the three-dimensional design, the extraction of two-dimensional drawings from the three-dimensional design, and the development of cutting paths based on the drawings. Each of these three steps has a set of software tools associated with it.

The first step, the development of a three-dimensional design, is normally translated into a solid model using a computer aided design (CAD) software package such as Pro/ENGINEER [35], SolidWorks Office [36], or AutoCAD [37]. This process is helpful in visualizing how the machined part will fit into the overall design. When developing the solid model, one should consider how the workpiece is to be machined and how it will be held when the machining is performed. One should also consider how the part will eventually be removed from the workpiece and should account for it in the design. Also, in wire EDM, one is limited to line-of-sight cuts. That is, the wire is at all times a straight line while it moves through a workpiece. Additionally, though angled cuts are possible, it is easier to work with cuts that are perpendicular to the horizontal base of the EDM tank. This is especially true when using smaller-diameter EDM wire, such as the 100  $\mu\text{m}$  diameter wire used in creating the structures featured in this document. This normally translates in the solid model to planning two cuts that are perpendicular to one another.

Once the solid model has been developed, two-dimensional drawings of the cross-section of the object are created. In the case of the TEAS microelectrode arrays, the electrodes are machined with square cross-sections, and the arrays are symmetric. An identical cut is therefore performed twice, and only a single drawing needs to be generated. The drawings are normally exported in DXF format. For simpler designs, or when doing modifications, one can bypass the solid model step and simply create cross-section drawings.

From cross-section drawings, cutting paths are created. This is normally done using a computer aided manufacturing (CAM) software package such as ESPRIT [38] or FeatureCAM [39]. Using this software, one imports the previously generated drawings and creates ISO files which contain machine-specific G-Code. These files are then loaded into the wire EDM and interpreted by its software. Alternatively, both the ESPRIT and FeatureCAM software packages are also capable of creating solid models, which provides one with even more options in the generation of the cutting paths and the G-Code. As CAD modeling software packages and CNC interfaces continue develop, this process will undoubtedly become simpler and more efficient, with an even greater range of options available to the user.

The cutting path for wire EDM is normally planned so that it starts at a point some known distance away from the workpiece. The wire EDM is capable of accurately offsetting the wire from the workpiece, which allows one to move the workpiece to the planned starting position relative to the EDM wire. When the cutting cycle begins, the workpiece is moved up to the EDM wire until machining begins, and it continues uninterrupted along the cutting path through the workpiece. The path is normally in the form of a complete loop, which allows for the multiple passes that normally constitute a wire EDM cut. Care must be taken to plan a path that results in waste material falling clear of the workpiece. A drawing of a cutting path used for manufacturing microelectrode arrays is shown in Figure 4-9. The path is as would be seen from above when operating the machine. One important consideration that is included with the G-Code is on which side of the cutting path the EDM wire should be offset. It is important for the wire to be offset away from the part that is being machined so that subsequent passes result in finer and finer surface finishes on the part. For the cutting path shown in Figure 4-9, the wire is offset to the right.

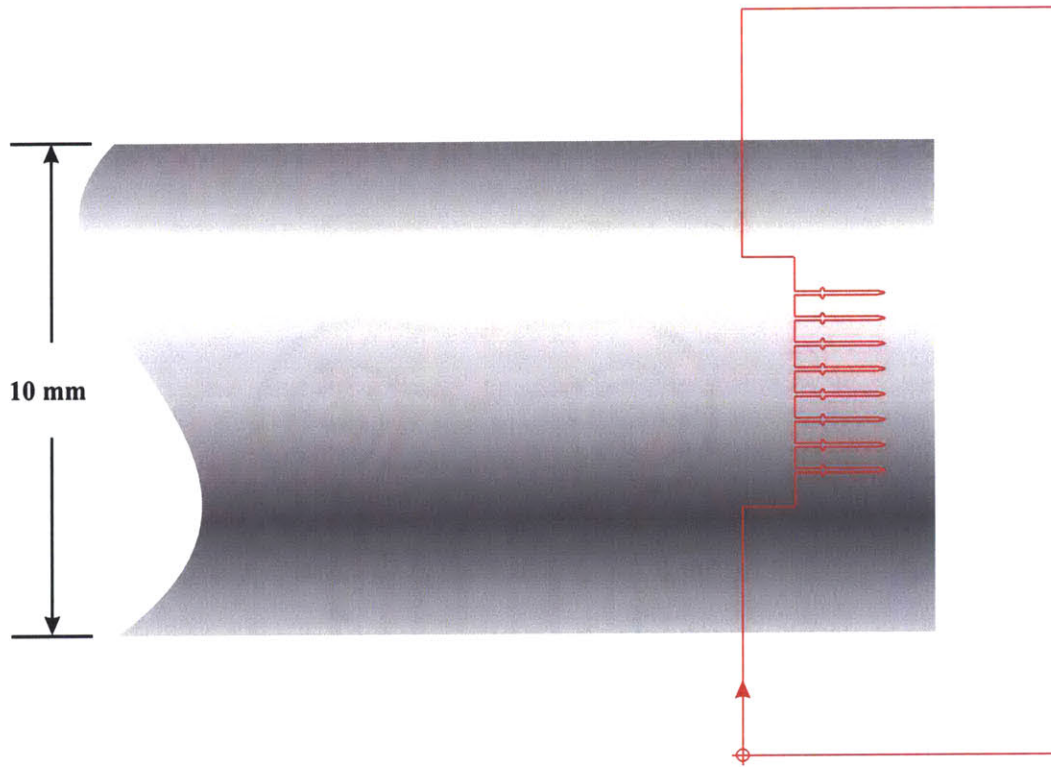


**Figure 4-9. Drawing of a typical cutting path used when wire electrical discharge machining a microelectrode array. The wire starts at the crosshairs and loops in the direction of the arrow.**

#### **4.4.2 Clamping Considerations**

When microelectrode arrays are machined by wire EDM, a piece of bulk material, normally a bar or a rod, is clamped at one end, and then held horizontal and perpendicular to the cutting wire, as shown in Figure 4-10. The microelectrode array results from performing an intricate cut through one plane, rotating the workpiece ninety degrees with respect to the EDM wire, and then repeating the cut. System 3R [40] fixtures are used to align the workpiece in the EDM tank. The use of the 3R-651.7E-S reference element on the 3R-602.21 chuck adapter allows one to rotate the workpiece in ninety-degree increments with minimal misalignment.

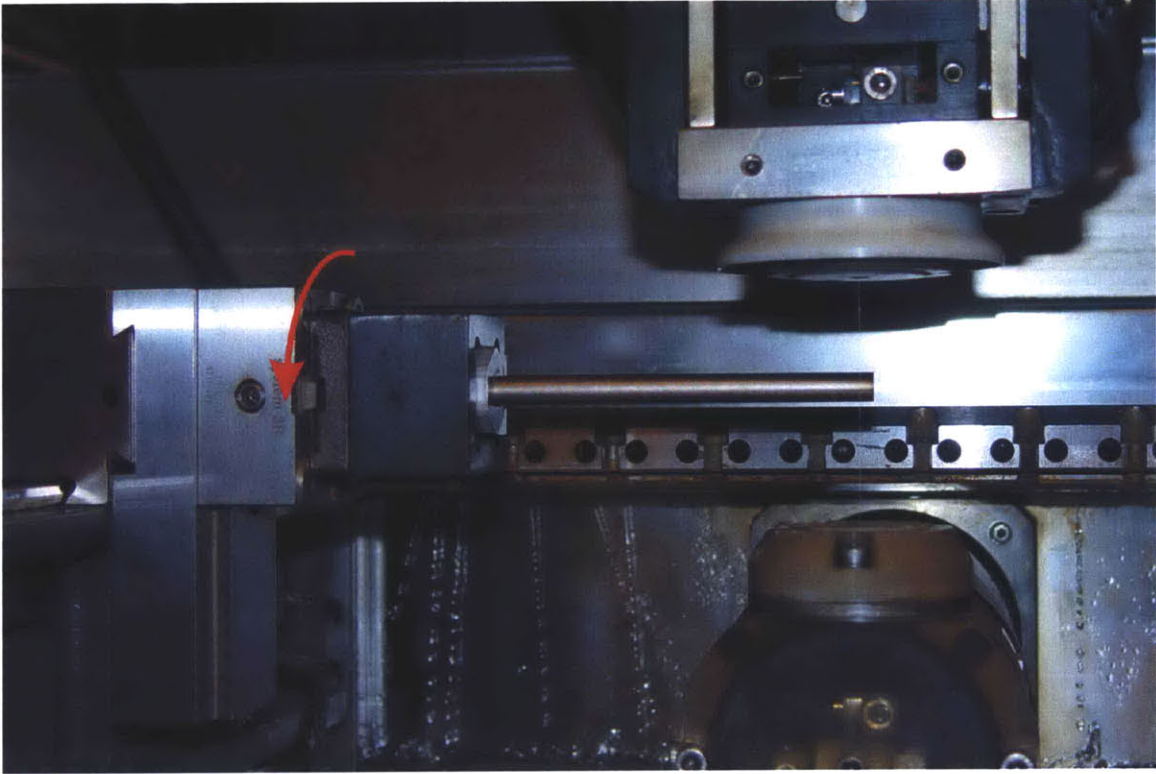


**Figure 4-10. Image of a workpiece clamped and suspended in the tank of the wire EDM machine. The rotation of the workpiece that is done after the first cut is complete is shown by the arrow.**

An edge-find command is executed on the wire EDM before each cut in order to ensure that the resulting machined array is at the desired location on the workpiece. In order to maintain accuracy, the workpiece is not normally removed from the System 3R fixture prior to the completion of the final cut. Also, it is desirable for the EDM cuts to be done in succession, with no repositioning of any of the clamps or fixtures in the EDM tank. It would, for example, be detrimental to the machining results to recalibrate the system, as is done during regular maintenance, between wire EDM cuts.

Additional smaller clamps or blocks with precision surfaces are used as adapters in conjunction with the System 3R equipment. An image of several clamps manufactured for use in the machining of microelectrode arrays using wire EDM is shown in Figure 4-11. Clamp A is used in order to prevent damage from occurring to the electrode array when it is removed from the workpiece by wire EDM as shown in Figure 4-12. Clamp B is used for mounting a rod into the EDM for machining. It was also used to create honeycomb-shaped arrays, though a more accurate fixture was later constructed as shown

in Figure 4-22. Clamp C is used to remove the electrodes from their base after they have been secured into an insulating substrate as shown in Figures 4-13 and 4-14. It is not removed from the System 3R fixture at any time, in order to preserve the alignments of its cuts. Clamp D is an earlier design of an adapter used to mount the workpiece into the System 3R fixture. All of the clamps were manufactured by wire EDM.

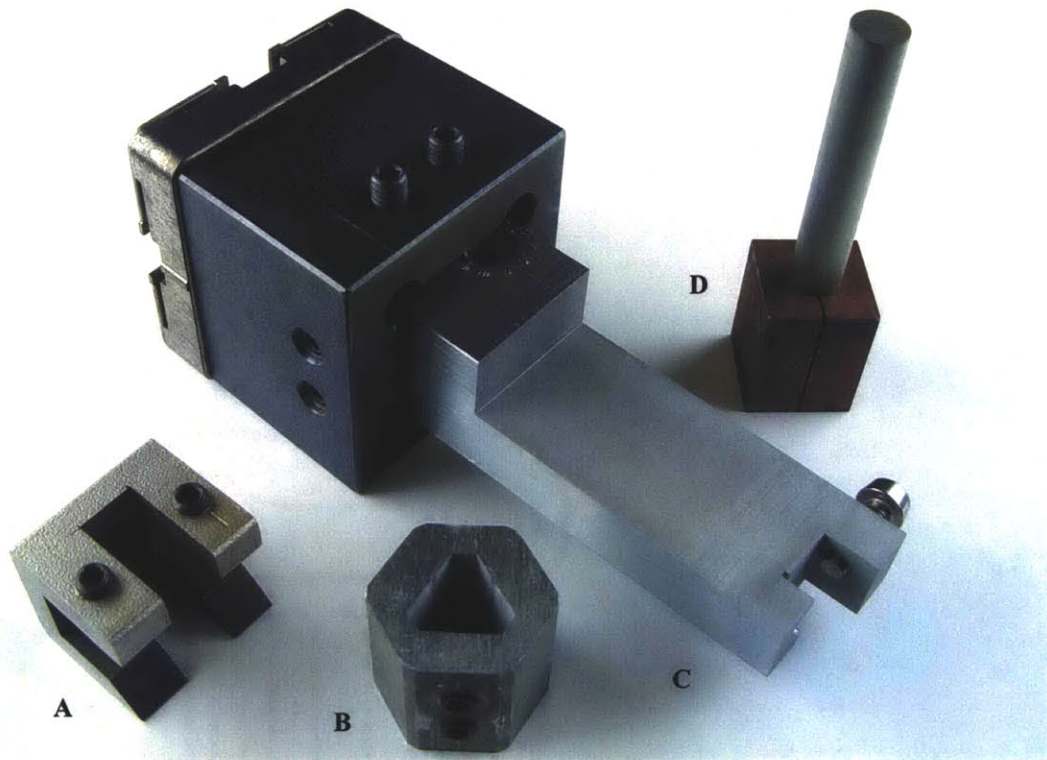


**Figure 4-11. Image of several clamps used in the fabrication of microelectrode arrays by wire EDM.**

Though the best accuracy will result when one reclamps a workpiece as little as possible, it is sometimes necessary, in order to perform other manufacturing steps, to separate the microelectrode array and its base from the stock. Because microelectrode arrays are delicate structures, they require special attention when they are handled. Figure 4-12 shows an image of a microelectrode array clamped so that it will not be damaged when it is separated from the rod. The clamp, also shown in Figure 4-11, prevents the array from falling to the bottom of the EDM tank and also decreases the likelihood of the EDM wire breaking. The separating EDM cut is made perpendicular to the microelectrodes.

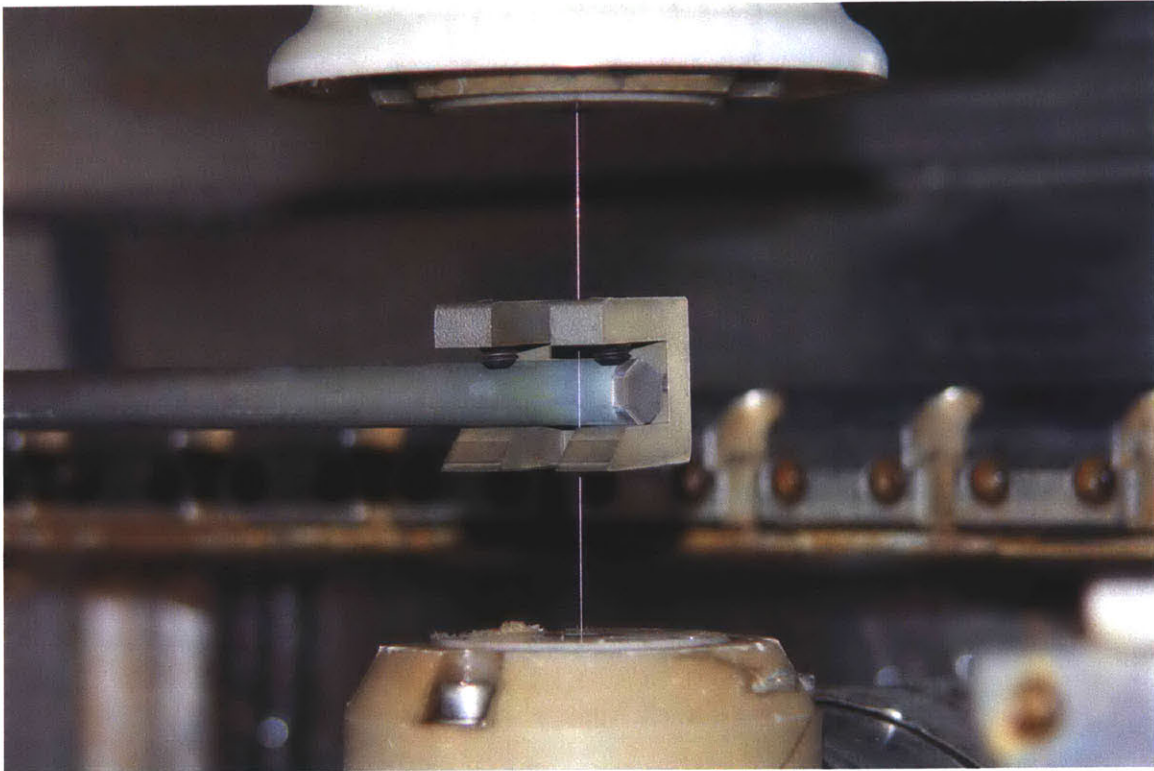


**Figure 4-12. Image of a microelectrode array clamped in order to prevent damage from occurring when it is separated from the rod. When the wire cuts through the rod, the clamp will hold the array in place.**

After the electrodes are secured into an insulating substrate, as described in Section 4.8.1, the assembly is removed by wire EDM. Alignment is important when the microelectrode array is separated from its base. The base is held as close to the initial machining angle as possible so that the back ends of the electrodes are cut as evenly as possible. Figure 4-13 shows an image of a microelectrode array being held in place as it is removed from its base. An image of this fixture is also shown in Figure 4-11. In this case, the array assembly weighs very little and has relatively large surface area. This causes the assembly to move slowly enough through the water in the EDM tank so that it can be carefully retrieved without any damage occurring.

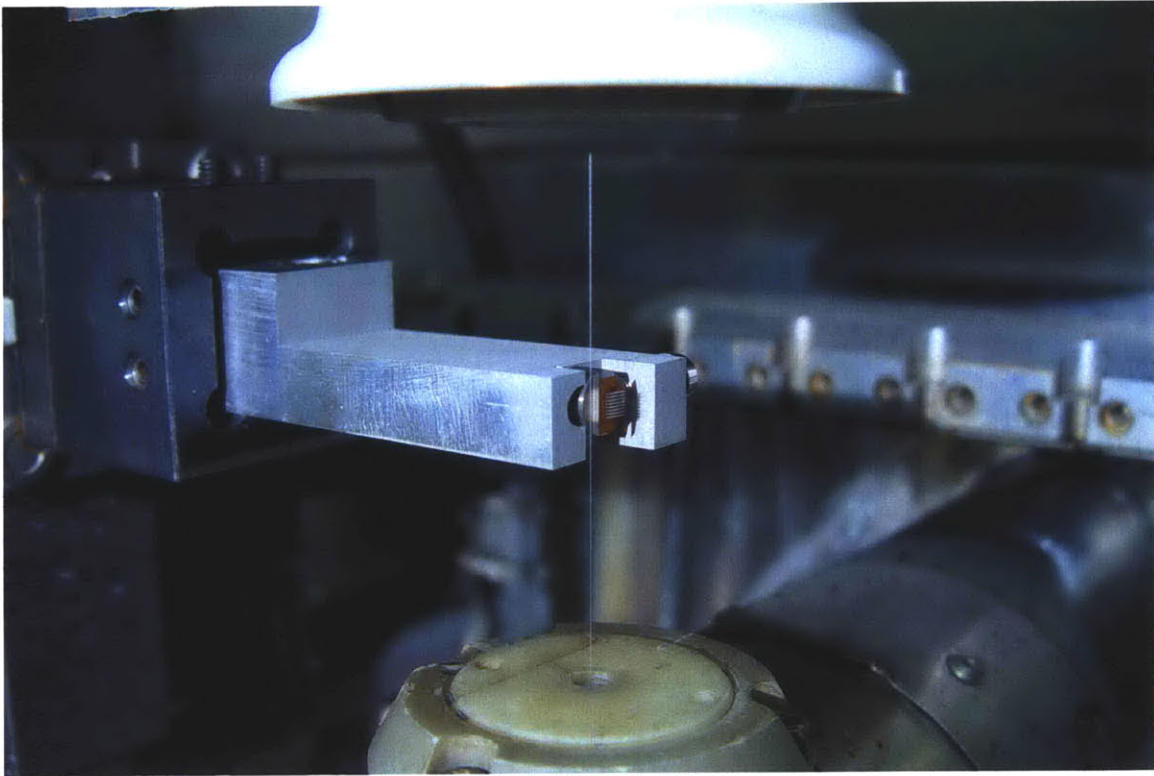


**Figure 4-13. Image of a microelectrode array held in place with a specially-designed fixture just before being removed from its base by wire EDM.**

The EDM wire passes between the polyimide substrate, which is epoxied in place, and the titanium alloy base section of the microelectrode array. A single, straight cut is performed through the base sections of the electrode in order to separate the assembly from its metal base. Figure 4-14 shows images of closer views of the array held in place by the fixture for this removal process.



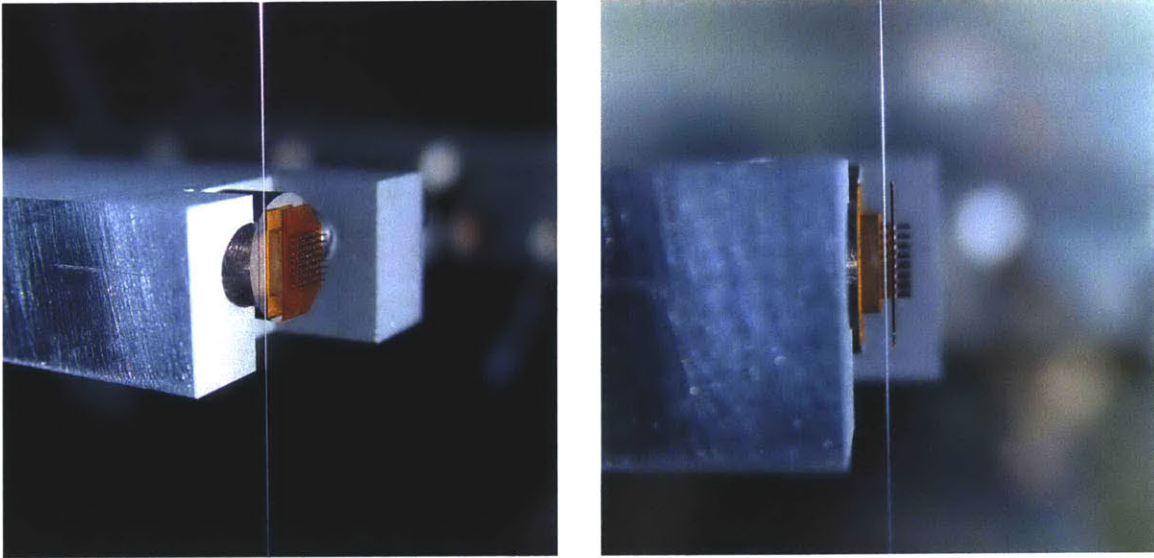


Figure 4-14. Magnified images of the microelectrode array, epoxied into the insulating substrate, just before being removed from its base by wire EDM.

#### 4.4.3 Machining Time Estimates

Because of the thicknesses of the electrodes in the arrays, the roughing cuts used in machining microelectrode arrays are performed at much lower powers than would normally be used. This is done primarily to reduce the amount of heat generated in doing the cut. If a full-power cut were used, one would often find that the tips of the electrodes have curved as a result of the heat generated. The power levels used are likely lower than they need to be and could be adjusted to increase the machining speed. Table 4-1 shows typical time durations for the two cuts that are performed in creating the TEAS arrays. The values are for cuts made in a 10 mm diameter titanium alloy (Ti90-Al6-V4) rod.

Table 4-1: Example wire EDM cutting durations for a titanium alloy microelectrode array cut from a 10 mm diameter rod.

First EDM Cut Through the Stock		Second EDM Cut After Part Rotation	
Type of Cut	Time (s)	Type of Cut	Time (s)
Roughing Cut	9475	Roughing Cut	1177
First Finishing Cut	301	First Finishing Cut	274
Second Finishing Cut	277	Second Finishing Cut	275
Total Machining Time	10,053	Total Machining Time	1726
<b>Total Machining Time for the Two EDM Cuts: 11,779 s</b>			

The total machining time for the example cuts shown in Table 4-1 was 11,779 s, or just over 3.25 hours. This excludes the time required to setup the cuts and to remove the microelectrode array from the stock upon completion of the cuts. The machining time could be reduced by using a piece of stock with a cross-section that is closer to the dimensions of the array. For example, a beam with a 5 mm by 5 mm cross-section would yield a faster overall machining time. Additionally, it would reduce the likelihood of the EDM wire breaking while performing the cuts. It has been observed that the likelihood of a wire break occurring is greatest when the EDM wire is traveling through a quickly-decreasing thickness of material, as is the case at the far side of a cut through a cylindrical rod.

#### **4.4.4 Electrode Materials**

Stainless steel, titanium (99.6+ %), titanium-aluminum-vanadium alloy (Ti90-Al6-V4), and tungsten carbide are the materials that were primarily used in developing the use of wire EDM as a method for the fabrication of microelectrode arrays. Arrays consisting of straight and uniform electrodes with suitable surface finishes were successfully machined using each of these materials. Titanium was chosen as the electrode material for the first prototype of the TEAS mechanical front end, and titanium alloy was used for the second prototype. These materials were chosen due to their strength, their resistance to corrosion, and their biocompatibility. For both of the TEAS prototypes, the electrodes were electroplated with platinum and then largely coated with parylene. The machined metal would not normally be in direct contact with the brain. Biocompatibility is an issue, however, because if, for whatever reason, the electroplating were to peel or crack off, or if an electrode were to break off during the surgery, one would want any exposed material to have as little detrimental effect on the animal as possible.

If stainless steel and tungsten carbide were shown to be nontoxic when left in the brain for long durations, these metals should be considered as alternatives to titanium because of their higher yield strengths. With the use of a stronger material, one could create arrays of microelectrodes with similar strengths, but with smaller electrode cross-sections. These arrays would occupy smaller volumes, which would likely decrease the

trauma caused to the animals upon insertion of the arrays. Alternatively, for a given degree of trauma caused in inserting an array of wider electrodes, one could insert an array with thinner electrodes built with a stronger material in a larger configuration, thus providing a greater number of recording sites. For acute experiments, titanium has little benefit over stainless steel or tungsten carbide, and in this case it makes sense to use one of the stronger metals.

An additional consideration is whether it is preferable to use a more or less brittle material in fabricating the microelectrodes. For example, electrodes manufactured from tungsten carbide, as well as from silicon, will break off if a lateral force is applied to them, whereas electrodes manufactured from titanium, titanium alloy, or stainless steel will bend under similar circumstances. Though tungsten carbide electrodes will accept more force than electrodes made of titanium or stainless steel before permanently deforming, the bending of an electrode is likely a more agreeable alternative than the fracturing of an electrode. This is likely the case both in handling the array, where the electrodes could potentially be bent back to their original positions, as well as in implanting the array, where the electrodes would remain attached to the device.

For clinical implants, where general costs are inherently much higher and the costs of the materials used in constructing the devices become less significant, one should consider machining the electrodes from a precious metal such as platinum, iridium, or a platinum-iridium alloy. As can be seen by comparing the elastic moduli and the strength values in Table 3-1, these materials can potentially outperform silicon, titanium, and even stainless steel. In addition to being a very biocompatible option, using one of these metals would eliminate any need for electroplating and would likely improve the signal integrity of the system by reducing the number of junctions present in the design.

#### **4.4.5 Chemical Etching**

After the microelectrode arrays are machined and are ready to be electroplated, they are placed in hydrochloric acid (HCl, 37 % approx.), heated close to its boiling point, in order to remove any oxide layer present, before being moved immediately into the electroplating solution. This procedure was followed in the fabrication of the two

TEAS prototypes. After following this procedure a few times, however, it became apparent that the aspect ratio of the electrodes in an array structure could be increased dramatically by leaving the array in the acid bath for longer durations of time. This acid etching process is demonstrated in Figure 4-15, where titanium microelectrodes, originally electrical discharge machined to widths of 80  $\mu\text{m}$ , were chemically etched in a heated hydrochloric acid bath for 10 minutes [10]. Electrode widths of about 40  $\mu\text{m}$  were obtained in this case, though this process can yield even finer microelectrodes. As can be seen in Figure 4-15, the finer detail such as the ledges on the electrodes remains uniform and intact during the etching process. Additionally, the electrode tips are sharpened during the process.

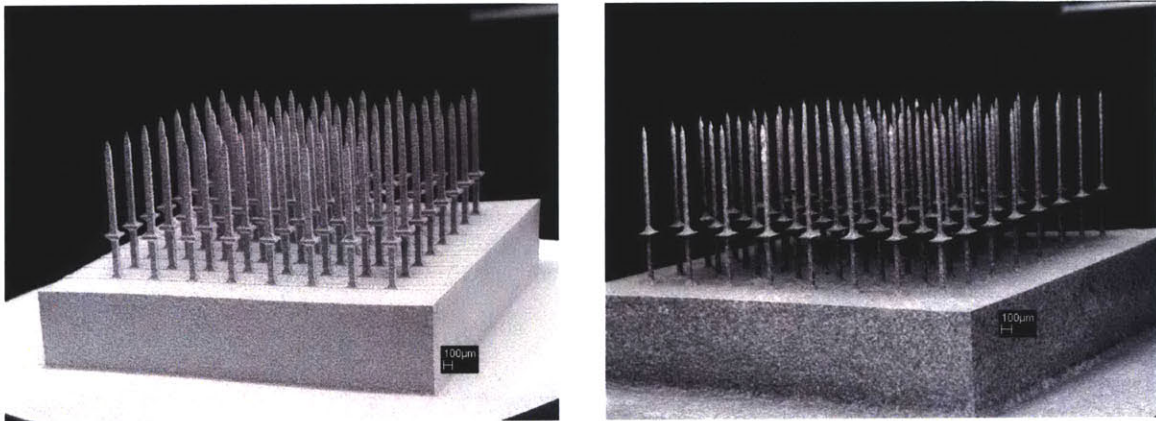


**Figure 4-15. SEM images of a titanium microelectrode array before (left) [8,11] and after (right) it has undergone the chemical etching process.**

Chemical etching was found to occur uniformly on all surfaces of a titanium (99.6+ %) array, at a rate of roughly 2  $\mu\text{m}/\text{min}$ , when the array is completely submerged in hydrochloric acid (HCl, 37 % approx.) that had been brought to a boil. Figure 4-16 shows an SEM image of a titanium microelectrode array with a human hair. The electrodes have been chemically etched to about half of their initial widths.

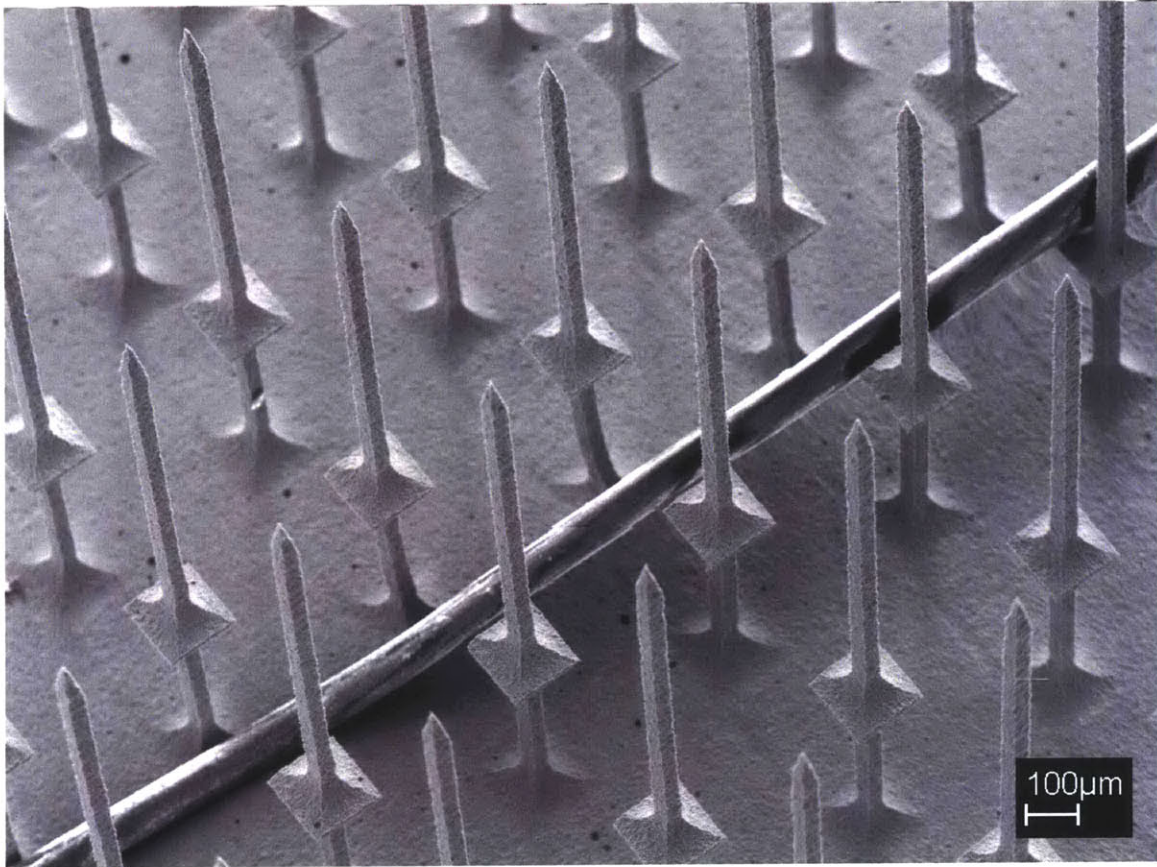


**Figure 4-16. SEM Image of a titanium microelectrode array with a human hair.**

In addition to providing a uniform process for increasing the aspect ratio of the array electrodes, this process eliminates the need to do the later passes in the wire EDM cuts. The later EDM passes are meant to further improve the surface finish obtained in the process, but when chemical etching is done, the final surface finish is due to the etching process and the degree of finish that was present before etching has little effect on the final result. This translates into a time saving in the wire EDM step. The number of passes used to produce the arrays was reduced from six to three without any noticeable difference in outcome when chemical etching was done. The number of passes could likely be reduced even further. Because the chemical etching process is uniform and tends to flatten surfaces while sharpening edges and features, it was found to be a good precursor to electroplating. Also, because the acid gold strike used in electroplating contains hydrochloric acid, one can move directly from the etching bath into this first electroplating step without any chance of oxidation occurring.

#### 4.4.6 Electroplating

Platinum has historically been considered the best interface material when recording bioelectrical activity. It was for this reason, as well as its biocompatibility, that platinum was chosen as the electroplating material for the TEAS microelectrode array prototypes. Gold was also often used for electroplating many of the experimental arrays that were constructed in the development of the fabrication processes.

Electroplating is a process that may be best left to industry experts, as obtaining a good result often seems to be as much art as science. Nonetheless, the microelectrode arrays were electroplated in the laboratory and satisfactory results were obtained. The first two TEAS prototypes were electroplated with platinum. The plating solution that was used was Platinum AP, ready to use solution, manufactured by Technic, Inc. [41]. Technic acid gold strike, ready to use solution, was used immediately before applying the platinum in order to improve adhesion. As discussed in detail in Section 4.4.5, a heated hydrochloric acid bath (HCl, 37 % approx.) was used immediately before placing the array in the acid gold strike electroplating solution in order to remove any oxide layer present. Figure 4-17 shows scanning electron microscope images demonstrating the result of electroplating the arrays.

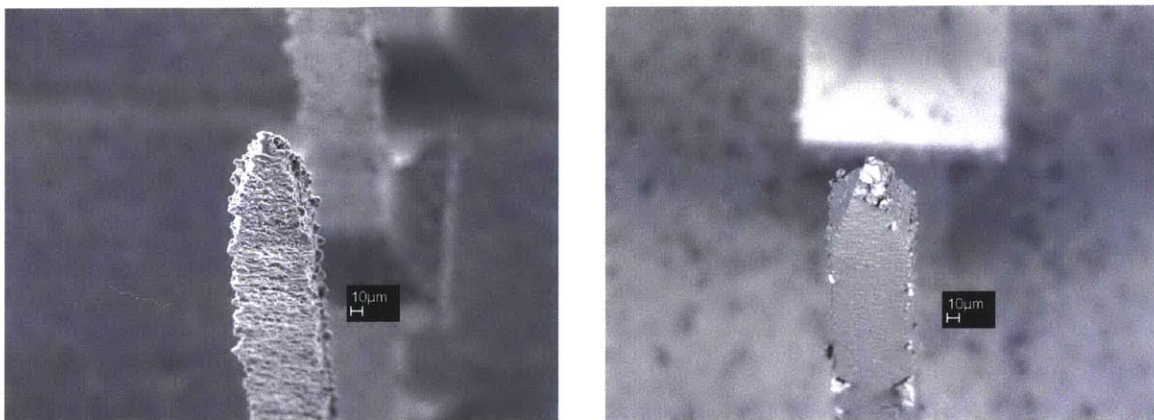


**Figure 4-17. SEM images of titanium alloy microelectrode arrays before (left) and after (right) they have been chemically etched and electroplated with gold.**

As can be seen in Figure 4-17, the electroplating process has the effect of smoothing the surface. Some of this effect may be attributed to the use of hydrochloric acid prior to the application of the acid gold strike. Only minimal chemical etching was

used in the case shown in Figure 4-17, however, and one can still see the finer surface finish that results from electroplating. The fine grain size of the electroplated gold is likely responsible for obtaining this finish. The blobs of gold apparent in Figure 4-17 (right) could likely be eliminated by altering one or more of the parameters involved, such as the voltage, the temperature, or the concentration of the electroplating solution.

#### 4.4.7 Other Fabricated Microelectrode Arrays

Though arrays of electrodes with final lengths of about 1 mm were constructed for the TEAS prototypes, the methods discussed above can be used to create structures with much larger aspect ratios and much higher electrode densities. Microelectrode arrays with electrode lengths of 5 mm have been machined successfully using these techniques. And, although obtaining even longer electrodes has not at this time been attempted, it is likely possible, especially when using a combination of wire EDM and chemical etching. Figure 4-18 shows a titanium alloy microelectrode array with electrodes exceeding 5 mm in length. The electrodes are 100  $\mu\text{m}$  in width.

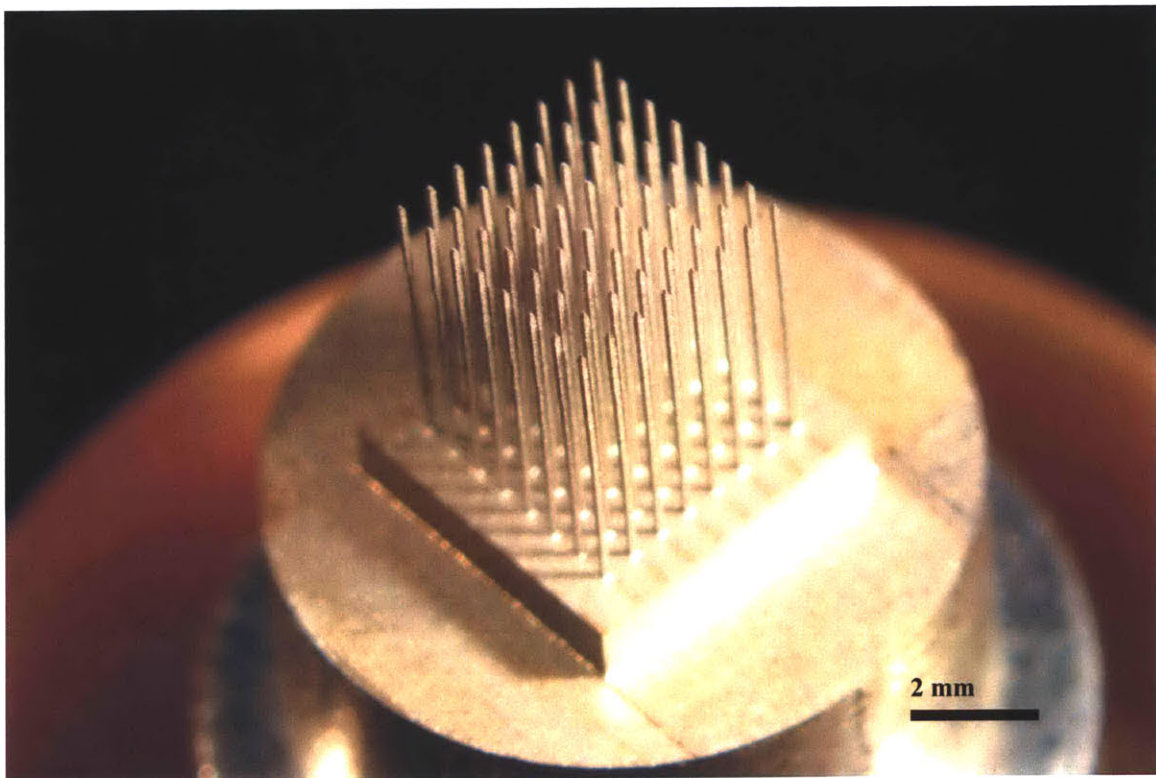
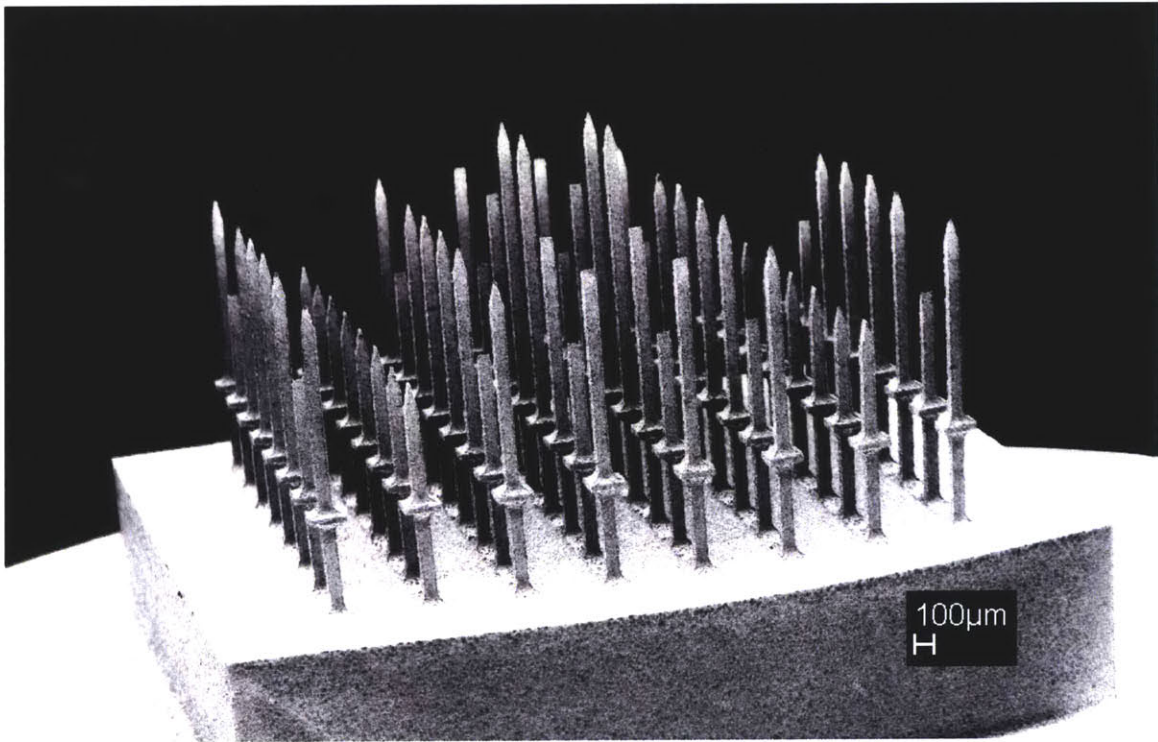


Figure 4-18. Image of a microelectrode array with electrode lengths exceeding 5 mm.

The aspect ratio of the array shown in Figure 4-18 is greater than 50:1. Using the chemical etching process highlighted in Section 4.4.5, one could etch this array in order to decrease the widths of the electrodes by half. This would give an aspect ratio of over 100:1.

The processes developed to produce the TEAS microelectrode arrays can be used to produce arrays with electrodes that have a range of lengths. The image shown in Figure 4-19, taken with a scanning electron microscope, shows an electrode array, machined from titanium alloy (Ti90-Al6-V4). Its has electrodes 0.65 mm, 1.15 mm, and 1.65 mm in length, from the top surfaces of the ledge features to the electrode tips. Using wire EDM, one is limited by line-of-sight cuts and therefore not all of the electrode tips will have the same shape. This could possibly be avoided by cutting the tips bluntly, that is, horizontally. One could then use an etching process to sharpen the tips as needed.



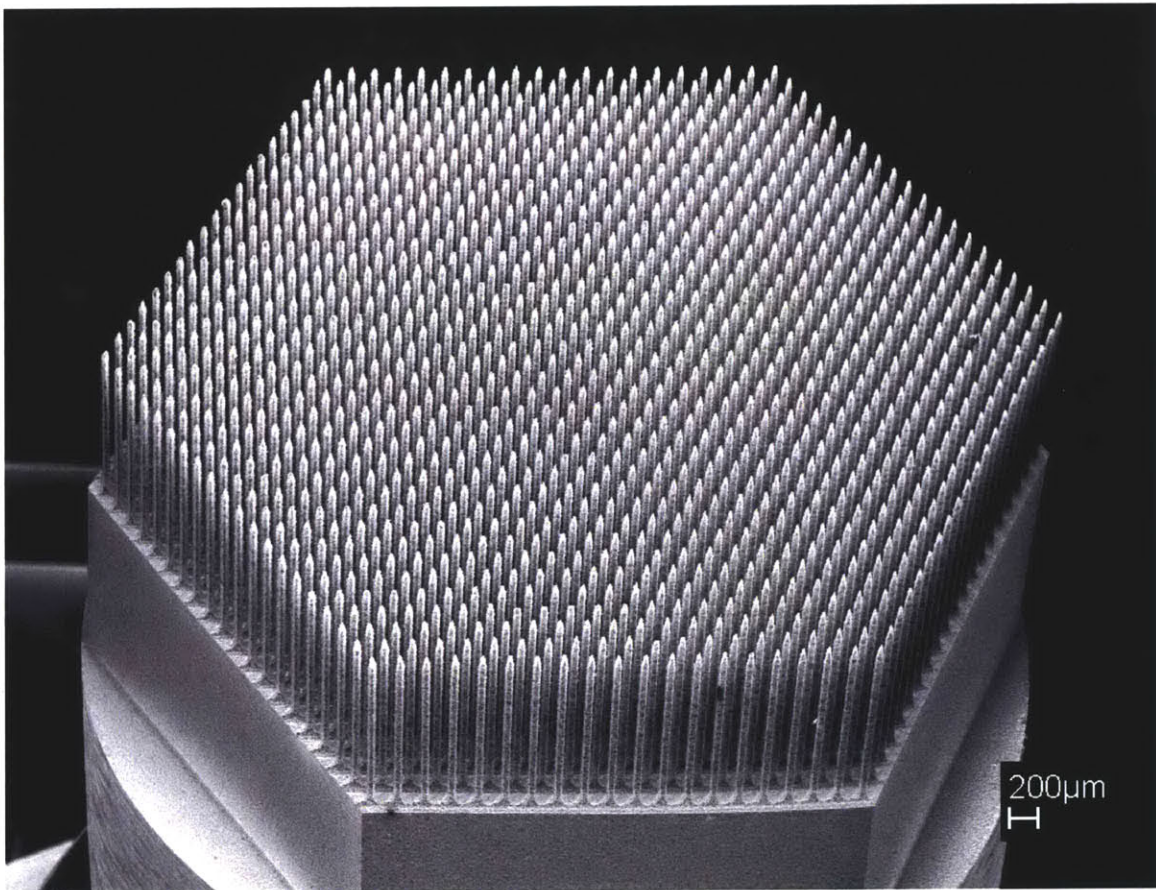
**Figure 4-19. SEM image of a microelectrode array that was machined to contain electrodes of varying lengths [10].**

Microelectrode arrays with inter-electrode spacings of 250 µm have also been machined using these methods. The spacing is limited only by the size of the wire used in the EDM process. The structures in this document were all machined using a 100 µm



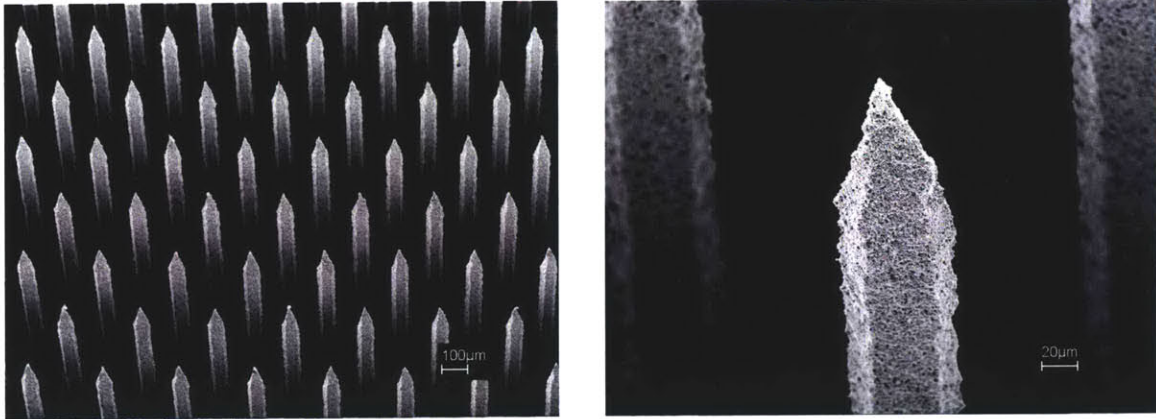
diameter EDM wire. With this wire, the minimum cut size is about 170  $\mu\text{m}$ . Even tighter inter-electrode spacings could be obtained using a 30  $\mu\text{m}$  diameter EDM wire, though the cutting speed would be greatly reduced and there would be further difficulties such as an increased likelihood of the EDM wire breaking while machining.

Honeycomb-shaped microelectrode arrays of hexagonal microelectrodes have also been created using these methods. Three EDM cuts are performed and the workpiece is rotated by 60 degrees after performing each cut. Figure 4-20 shows a SEM image of an 1141-electrode honeycomb-shaped array of hexagonal electrodes machined from titanium alloy (Ti90-Al6-V4). The electrodes in this array are all equidistant from their six nearest neighboring electrodes.



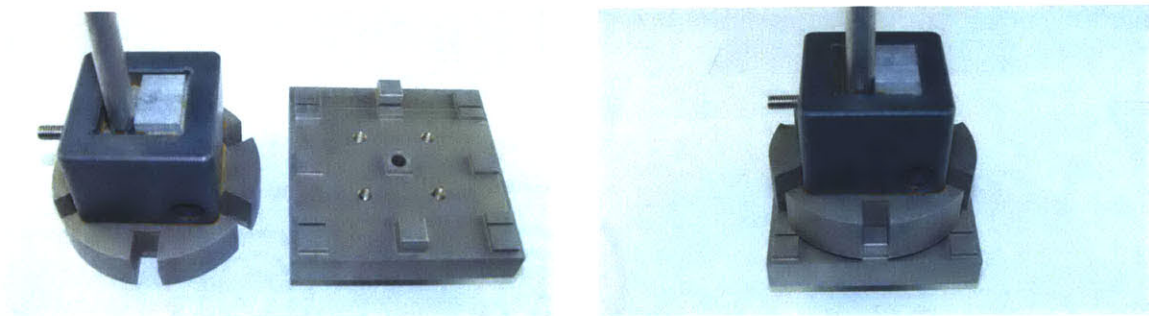
**Figure 4-20. SEM Image of an 1141-electrode titanium alloy array that was machined in a honeycomb pattern.**

Figure 4-21 shows magnified SEM images of an 1141-electrode titanium alloy microelectrode array after it has been chemically etched and electroplated with gold.



**Figure 4-21. SEM images of hexagonal microelectrodes after they have been electroplated with gold.**

In order to create honeycomb-shaped arrays such as the ones shown above, one must rotate the arrays by 60 degrees twice without introducing any misalignment by adding rotation about other axes. A special clamp was designed and manufactured in order to obtain these structures. The clamp was machined from stainless steel by wire EDM and is shown in Figure 4-22.



**Figure 4-22. Image of a fixture used when making honeycomb-patterned arrays. The fixture is capable of rotating the array 60 degrees with minimal misalignment and was manufactured from stainless steel by wire EDM.**

For this method of manufacturing microelectrode arrays to become viable for mass production, it is advantageous to be able to machine several microelectrode arrays in parallel. Figure 4-23 shows an image of forty-nine 100-electrode arrays that were machined from titanium-aluminum-vanadium alloy (Ti90-Al6-V4). In order to save time and wire in machining these arrays, preliminary cuts were done using 250 µm diameter EDM wire in order to achieve a pattern of forty-nine 5 mm by 5 mm elevated regions. These elevated regions were then machined into forty-nine 100-electrode arrays by performing two wire EDM cuts using the 100 µm diameter EDM wire.

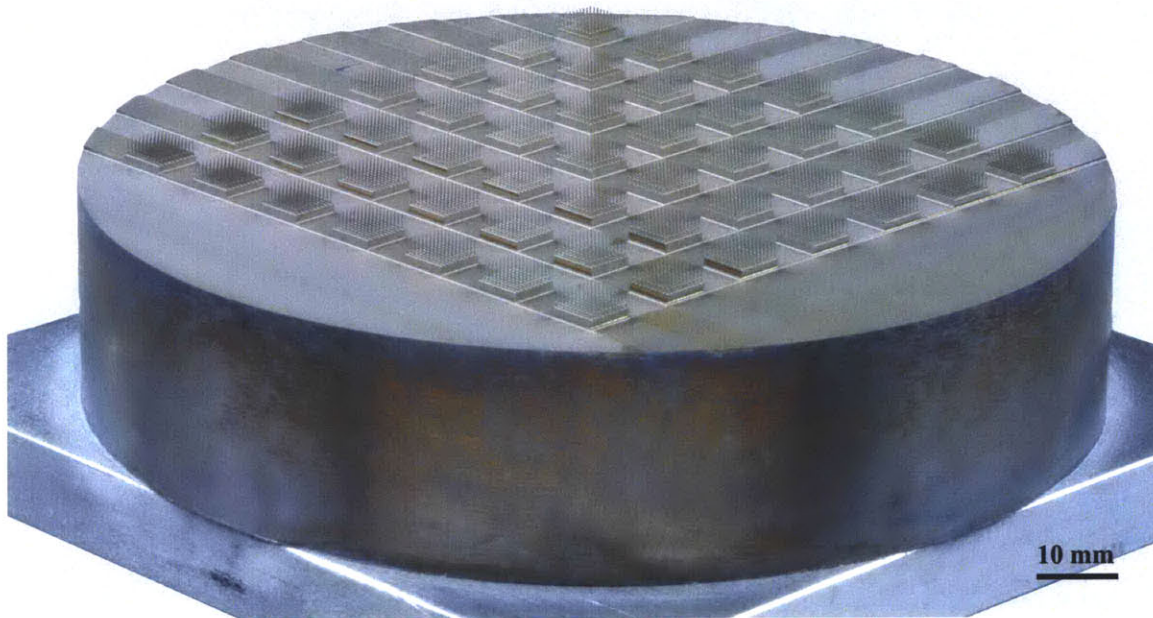


**Figure 4-23. Image of forty-nine 100-electrode arrays that were electrical discharge machined in parallel from a 100 mm diameter disk of titanium alloy.**

Figure 4-24 shows magnified images of the arrays that were machined in parallel. These arrays have inter-electrode spacings of  $500\ \mu\text{m}$ , and the electrodes have the same dimensions as those used for the TEAS arrays shown in Figure 4-8.

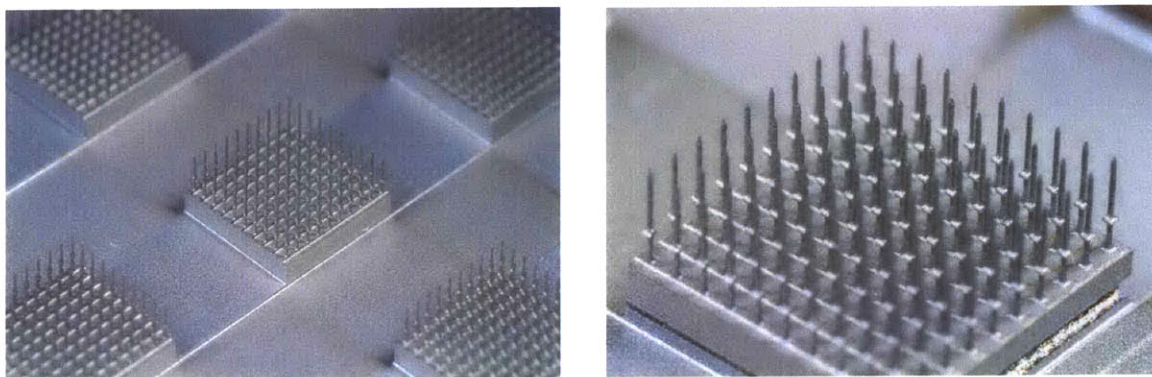


**Figure 4-24. Magnified images of the 100-electrode arrays that were machined in parallel. The elevated sections are 5 mm square and the arrays' inter-electrode spacing is  $500\ \mu\text{m}$ .**

The machining of the arrays in parallel not only reduces the number of manual steps involved, but it also leads to a substantial reduction in machining time. For

example, the forty-nine 100-electrode arrays machined from titanium alloy shown in Figures 4-23 and 4-24 took roughly 24 hours to machine, or about 0.5 hours per array. This time could be substantially reduced by using a more appropriately sized piece of stock with a square cross-section. In addition to reducing the amount of material that would need to be machined, the number of EDM wire breaks encountered while machining the arrays would be reduced. In comparison, as discussed in Section 4.4.3, the time required to machine a single 64-electrode titanium alloy array from a 10 mm diameter rod is typically over 3.25 hours. At 3.25 hours of machining per array, manufacturing forty-nine of them would require 159.25 hours, or almost a solid week of machining. As can be seen from this example, machining the arrays in a parallel batch process can dramatically reduce the manufacturing time required per array.

## **4.5 Insulating Substrate Fabrication**

The electrodes of the arrays must be electrically isolated from one another. If an array assembly is to be surgically implanted as a single entity, its electrodes must be held together in some way. Whatever method and materials are used to link the electrodes together must do so without compromising the isolation of the electrode recording channels. In addition to being instrumental when the array is assembled, the insulating substrate also has the importance of being the part of the assembly that rests on the surface of the brain after implantation.

### **4.5.1 Substrate Alternatives**

One process that was considered was melting a glass from powder form in order for it to flow and then solidify between the electrodes. The array would be positioned with the electrode tips pointing upward, and the glass would be made to flow between the electrodes in order to form a substrate. After the glass has hardened, the back of the array could be ground flat. This process was found to be problematic, however, because the high temperatures required to melt the glass were found to damage the arrays.

Injection molding is another process that was considered. An apparatus would need to be created in order to impede the injected material from flowing up the

electrodes. One possible option would be to manufacture a female mask for the array using sink electrical discharge machining, for example. A second option would be to use a temporary, hardening material such as a photoresist or a wax as a mask while the injecting is done, and then to dissolve or remove it afterward. Another potential problem that would have to be addressed if using traditional injection molding is that of the high temperatures involved and the deformations that would occur as the plastic cools. Another possible process involves the application of epoxy. Epoxy is an attractive material in that it can be used entirely at room temperature if need be, as it can be cured using a variety of methods. Epoxy could be used in a similar fashion to either of the above methods.

Two problems are central to all of the methods highlighted above. The first problem is that of fluids wicking up the electrodes. This problem becomes increasingly pronounced as the inter-electrode spacing of the microelectrode array is reduced. The second problem involves the gripping and handling of the microelectrode array while additional machining and assembly is done. Two ways of handling this are to temporarily reinforce the electrode array using a removable material, or to build some handling surfaces into the array itself. One could even leave on an additional temporary segment that would be removed in a final step. Jigs and clamps would nonetheless need to be manufactured in order to reliably accomplish the assembly tasks. Some form of electrical pads must be accessible for connection to the electrical front-end circuitry. A further consideration is that it is desirable for human intervention to be as far removed from the process as possible. The process would ideally be one that could be upgraded to semi-automatically create several arrays in parallel, or at least in quick succession.

#### **4.5.2 The TEAS Insulating Substrate**

For the TEAS mechanical front end, a polyimide substrate is used to electrically isolate the microelectrodes from one another and to provide a foundation for the array assembly. For the first two TEAS prototypes, Kapton 500HN, from DuPont [18], was used as the substrate material due to its biocompatibility and its machinability. The substrate is 127  $\mu\text{m}$  in thickness and was machined using an LPKF [42] ProtoMat 95s/II rapid prototyping system. Holes, arranged in a pattern that corresponds to the inter-

electrode spacing of the array, are first created using a 101.6  $\mu\text{m}$  endmill in the system's 60,000 RPM spindle. The substrate contour is then machined in a similar manner. Because the design and machining of the substrate is based on computer aided design (CAD) and computer numerical control (CNC), designs can be easily altered in order to meet the needs of a particular application. A design, either extracted from a solid model or created as a drawing, is imported into the LPKF system software as a DXF file. The dimensions of the substrates used in the TEAS prototypes are about 8.5 mm by 6 mm and their shape matches the contour of the tip of the connector cable. The substrate is made large enough as to allow the array to be handled with forceps, as shown in Figure 4-25.

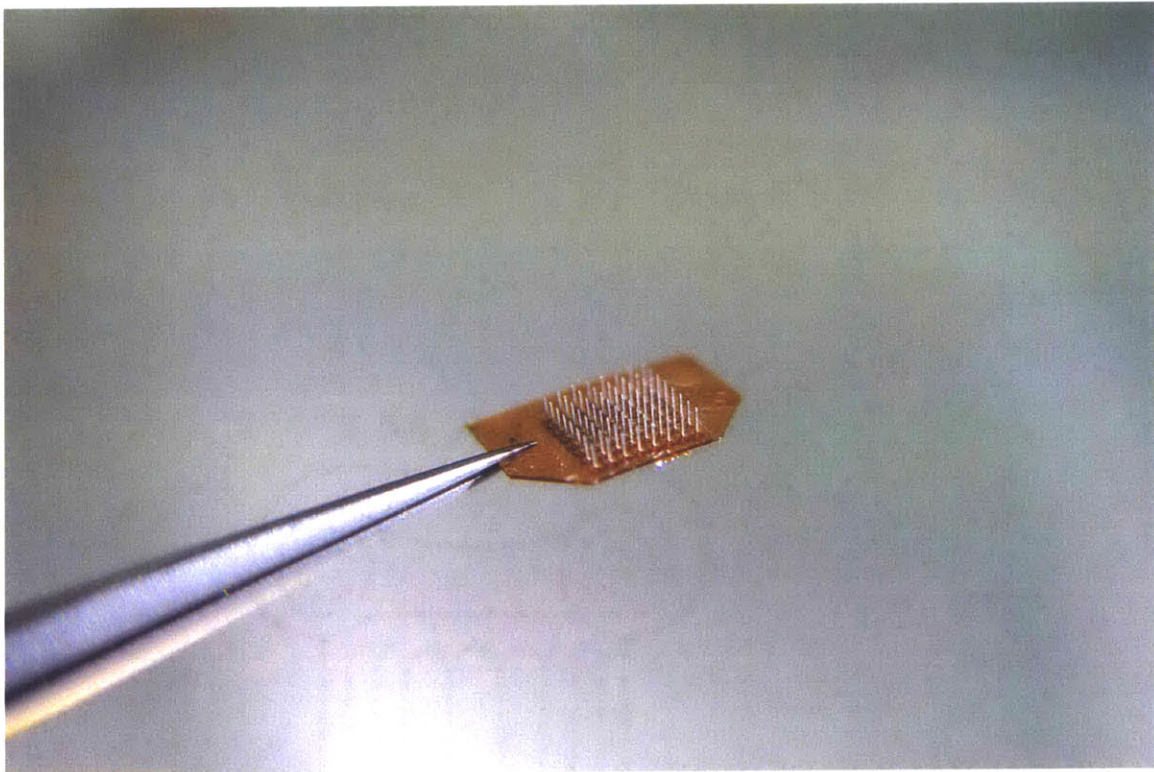


**Figure 4-25. Image of a microelectrode array epoxied into a polyimide substrate and held with forceps.**

The insulating substrate is epoxied in place as discussed in Section 4.8. Using a machined substrate reduces many of the problems associated with wicking that occur if a fluid is simply introduced at the base of the array. Additionally, the back ends of the electrodes remain accessible for later removal of the array structure by wire EDM, as

demonstrated in Section 4.4.2. The back ends of the electrodes are also subsequently available for connection to pads on the connector cable.

### **4.5.3 Other Manufacturing Methods**

Milling was used as a manufacturing method for the insulating substrate because it was found to give adequate results for what was needed for the first prototypes. For denser arrays, and arrays with thinner electrodes, other methods may be better suited. Machining using laser ablation could alternatively be used for creating the insulating substrate. Experiments were done using a Resonetics [43] Maestro 1000 excimer laser micromachining center, and satisfactory results were obtained. The edges of the cuts were cleaner than those obtained by milling, though the milling cuts could be cleaned up significantly using a razor blade under a microscope. It is desirable to avoid this cleanup step if possible, however, due to its manual nature.

A modification to the TEAS method of manufacturing microelectrode arrays involves the application of epoxy onto the back surface of the insulating substrate. The epoxy would be applied after the array assembly has been removed from the metal base by wire EDM, and the epoxy would cover part or all of the back ends of the electrodes. The back side of the array would then be ground flat so that a pattern of conductive regions would be obtained. A fixture would be required in order to grip and align the array while grinding. This process would fit well with automated mounting techniques such as flip chip [44] technology.

## **4.6 Electrical Insulation**

Obtaining desirable electrical impedance values at the electrode tips is critical to recording meaningful data. This normally means that recording sites must be isolated and correctly sized in order to achieve the desired electrical impedance values. Impedance is a function of the surface area at the interface between the electrode metal and the brain. Because the microelectrodes are made entirely of metal, an electrically insulating material is used to encapsulate the electrodes, with exception of the recording sites.

Some early experimentation was done applying polyimide to electrode arrays. Several methods were attempted in order to obtain uniform coatings. One method was to dip the electrodes in a liquid polyimide, such as a Parylin PI 2555 or PI 2556 polyimide, from DuPont [18]. A second method was to secure the array to a silicon wafer, add the liquid polyimide, and then to spin the wafer at 400 to 1000 RPM using a Solitec [45] model 5100 wafer spinner in an attempt to achieve a uniform thickness. A baking step is required following both of these application methods. It was determined, however, that parylene deposition was better-suited to meet the TEAS coating requirements. The process is not affected by surface tension and gravity as a liquid process is, and it can be done with no baking step. The coating is done at ambient temperature, is very conforming and uniform, and is pinhole free. Parylene deposition can also be a highly automated process and generally yields predictable and repeatable results.

Parylene is a generic name for a family of polymers normally applied as protective coatings and is recognized as a good solution for encapsulating surgically implanted devices. Of the parylene family, parylene C, or poly-monochloro-para-xylylene, is the most commonly used and was chosen as the insulating material due to its physical properties and its biocompatibility. Its application is normally pinhole free and offers the lowest permeability of moisture and gases of the parylenes. Glaxyl C, the parylene C used for the second TEAS prototype, available from Para Tech Coating, Inc. [46] has a tensile strength of 69 MPa, a yield strength of 55 MPa, and a dielectric constant of 3.10 at 1 kHz. It also has a USP Class VI biocompatibility rating.

#### **4.6.1 Parylene Deposition**

A schematic of the parylene deposition process is shown in Figure 4-26. The parylene C dimer, dichloro-para-cyclophane, is loaded into the vaporizing chamber. It is then brought under vacuum to an absolute pressure of about 130 Pa and is heated to a temperature of about 150 °C. The dimer is vaporized and passes into a pyrolysis zone, which is normally at about half the pressure in the vaporizer and at a temperature of about 680 °C. At this temperature, the dimer is converted into a monomer. The reactive monomer is then attracted to the cold trap, as shown in Figure 4-26, and enters the deposition chamber, which is at ambient temperature and an absolute pressure of about



13 Pa. The reactive monomer immediately condenses onto the surfaces and substrates that are present in the chamber. Because of the close proximity of the molecules, polymerization immediately takes place. A conforming coating of uniform thickness is deposited over all surfaces, including sharp edges, crevices, and pores. One has to be careful to mask any connectors or other surfaces that are not to be coated. A tape that is capable of holding a seal at an absolute pressure of 13 Pa is required. Also, because the process will coat all of the surfaces in the deposition chamber with parylene, one must pay particular attention to how the parts are mounted in the chamber. One of the key benefits of parylene deposition is that the coated objects remain at ambient temperature throughout the process. The process is complete when all of the dimer in the vaporizer has moved through the coating process. A vacuum gauge monitors the coating progress, and the procedure is completed when the vacuum level drops past a set value, signaling that the dimer supply has been exhausted. A wax-covered test strip is normally included in the deposition chamber for each deposition. The thickness of the parylene deposition is normally measured by peeling back the parylene that was deposited on the test strip, and then measuring it with a micrometer.

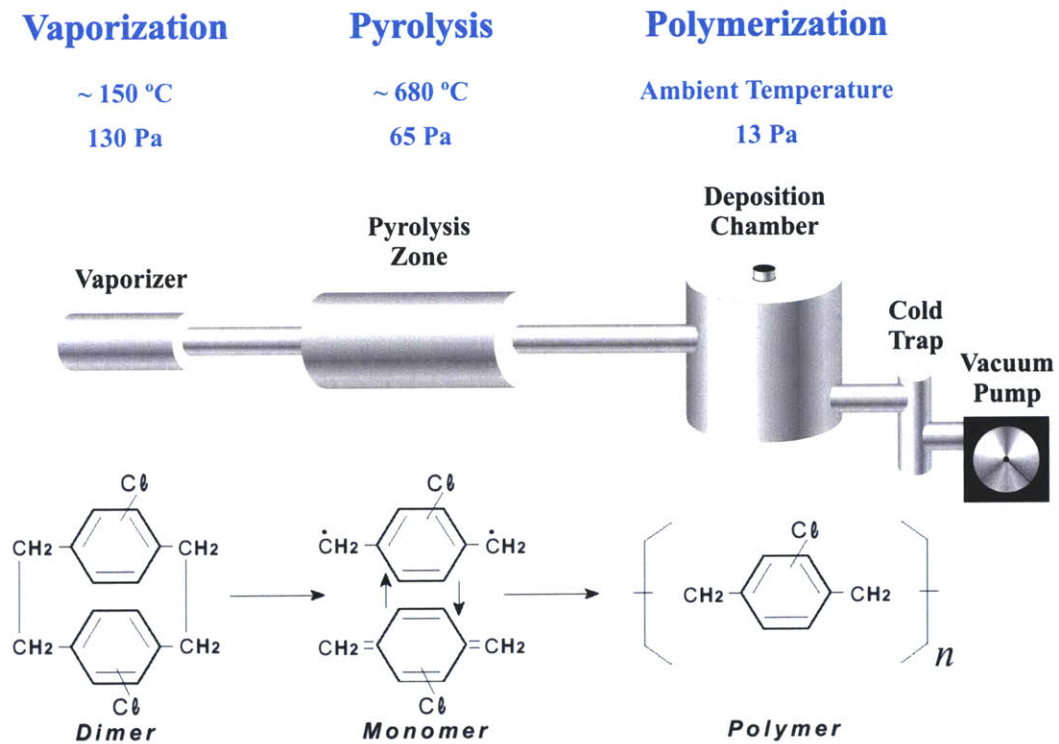
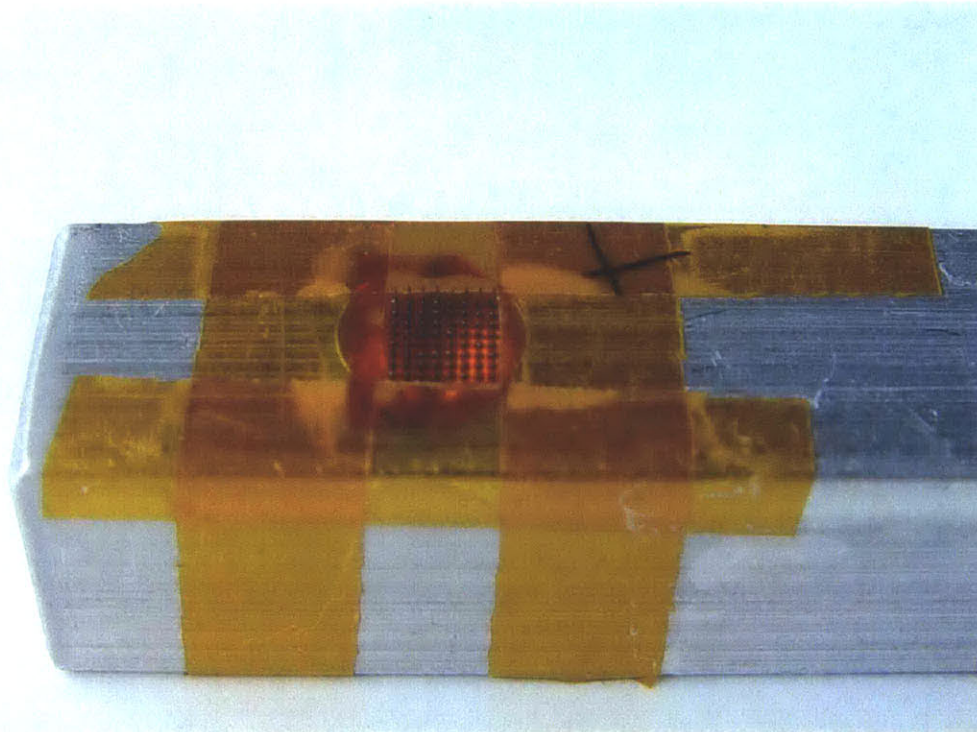


Figure 4-26. Schematic showing the parylene coating process.

For the first TEAS prototype, the entire mechanical structure was coated with a 15  $\mu\text{m}$  layer of parylene C. The connector end of the array assembly was masked with tape, and the structure was suspended by that end for the parylene deposition. By coating the entire structure, electrical insulation along the electrodes is provided, and a seamless biocompatible protection is obtained over the entire surface of the array assembly. This was seen as the ideal solution, but the process may be more difficult to implement in parallel, as it requires the entire mechanical front end to be constructed prior to the parylene deposition, as well as before the removal of the parylene from the electrode tips. It was determined that the 15  $\mu\text{m}$  layer of deposited parylene was too thick for the TEAS application and is discussed in more detail in Section 5.3.

For the second TEAS prototype, a much thinner 3  $\mu\text{m}$  layer of parylene C (Galxyl C, available from Para Tech Coating, Inc. [46]) was deposited using a Model 3000 Lab Top Coater, manufactured by Para Tech Coating Inc. For this second prototype, the deposition was made before the microelectrodes, held in the insulating substrate by epoxy, were soldered to the connector cable. The back ends of the microelectrodes were masked as shown in Figure 4-27. A hole was drilled into a piece of aluminum, and then the array was carefully mounted above the hole and fixed in place with tape. Four array assemblies were mounted this way and coated with parylene at the same time for redundancy. The arrays were not removed from the aluminum fixture until the insulation had been removed from the recording sites at the electrode tips.



**Figure 4-27. Image of the TEAS microelectrode array assembly fixed in place for the parylene deposition process.**

## **4.6.2 Insulation Removal**

As explained in Section 3.4.2, the initial target for the impedance values of the electrodes was  $50\text{ k}\Omega$  to  $100\text{ k}\Omega$  at  $1\text{ kHz}$ , when recorded using a platinum reference electrode in  $0.9\%$  saline. In order to achieve electrode impedance values in this range, one must be able to expose a controlled amount of surface area at the tip of each electrode. For the first TEAS prototypes, it was decided to fabricate the electrodes with varying amounts of exposed surface area in order to obtain a range of impedance values at the electrode tips. This also increases the likelihood of creating an electrode with a suitable impedance value, while at the same time it allows one to investigate which impedance values work best. Also, one can more easily calibrate the parameters in the insulation removal process if one has a resulting range of impedance values.

Whatever type of electrical insulation is used to coat the microelectrodes must either be masked from the electrode tips upon deposition, or be removed from the tips afterward. In order to obtain recording surfaces with impedance values in a specified

range, the masking or removal process must be accurate and repeatable. For the two prototypes of the TEAS mechanical front end, parylene was used to provide the electrical insulation. Although masking the electrode tips with photoresist or wax prior to the deposition was considered, a coat-then-remove process was used. Some experimentation was done using an oxygen plasma to etch parylene, and though etching did occur, it was eventually not chosen as the removal method due to the need to mask the rest of the array assembly. Because parylene is impervious to most chemicals and all but the strongest acids, laser ablation was chosen as the method for parylene removal.

### 4.6.3 Laser Ablation

For the TEAS prototypes, parylene was removed from the tips of the microelectrodes by laser ablation. Fluence ( $\text{J}/\text{m}^2$ ) is a measure of the energy density delivered to the material that is being ablated. In order ensure that parylene is ablated, it is desirable to be in a range from the upper plastics to just below the metal ablation range, for instance in the range from  $50 \text{ kJ}/\text{m}^2$  to  $100 \text{ kJ}/\text{m}^2$ .

**Table 4-2. Target Fluence Levels for General Classes of Materials [43].**

<b>Material</b>	<b>Target Fluence (<math>\text{kJ}/\text{m}^2</math>)</b>
Plastics	10 to 50
Glass	20 to 100
Ceramics	100 to 300
Metals	100 to 400

A range of exposed surface areas at the tips of the electrodes, from  $25 \mu\text{m}$  to  $90 \mu\text{m}$ , was attempted for the first prototype array assembly in order to experiment with different electrode impedance values. A PSX-100 excimer laser, manufactured by MPB Communications Inc. [47], was used for ablating the electrode tips of the first prototype. The laser typically operates at a wavelength of  $248 \text{ nm}$ , with a maximum pulse energy of  $5 \text{ mJ}$  and a maximum average power output of  $0.5 \text{ W}$ . Technical difficulties with the

laser arose when doing the ablating, and it was likely running at a low energy level. A range of impedance values were obtained, but the thicker-than-necessary layer of deposited parylene also likely contributed to a poor ablation result. See Section 5.1 for more details.

For the second TEAS prototype, four assemblies consisting of electrodes epoxied into the insulating substrate were each coated with a 3  $\mu\text{m}$  layer of parylene prior to the laser ablation step. A Resonetics [43] Maestro 1000 excimer laser, operating at a wavelength of 248 nm, was used to perform the laser ablation. The laser was operated at a pulse energy of 160 mJ, a pulse rate of 200 Hz, and a pulse width of 1  $\mu\text{s}$ . An iris was used to limit the size of the ablated region and therefore blocked some of the energy. The number of pulses executed per electrode was varied from 20 to 100 across the arrays by row. Figure 4-28 shows SEM images of the electrode assembly used for the second TEAS prototype after undergoing laser ablation. The array tips are bright in the SEM images due to the higher electron densities recorded by the detectors in the SEM. These bright areas can be interpreted as the effect of the laser ablation on the parylene coating.



**Figure 4-28. SEM images of a parylene-coated assembly, consisting of platinum-coated electrodes epoxied into a polyimide substrate, after the electrode tips have undergone laser ablation.**

A magnified SEM image showing a typical result of laser ablation is shown in Figure 4-29. The image is of the electrode viewed directly from above. One can see the pyramid structure of the tip of the electrode.

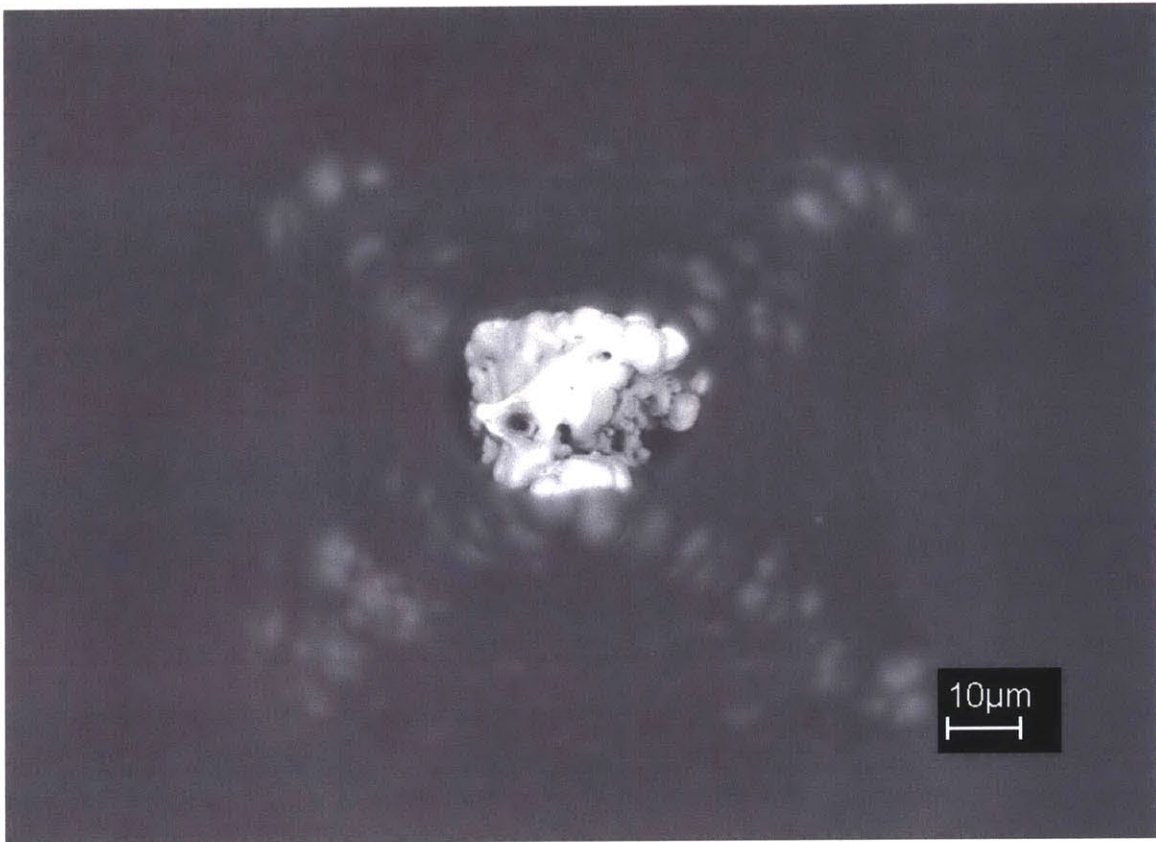


**Figure 4-29. SEM image of a parylene-coated electrode that has had its tip laser ablated.**

Performing laser ablation with the Resonetics system was found to be challenging, largely due to parallax errors encountered between the line-of-sight of the CCD camera vision system and the laser beam. Some trial and error and experimentation was required in order to strike the first electrode targets. Fortunately, the machine includes an XY stage with a repeatability of  $\pm 2 \mu\text{m}$ . Its use allowed one to move accurately from one electrode to the next in a semi-automatic fashion.

A second difficulty encountered while performing the laser ablation was the focusing of the laser beam. Focusing the beam is required in order to get a clean ablation pattern. Though the electrodes are of a constant length, focusing the beam at the tip of an electrode is difficult. Because the arrays were arranged two to a fixture, one array in each fixture was used for experimentation, calibration, and for focusing. This allowed the second array in each fixture to be machined with no need for experimentation. The electrical results from the laser ablation process can be found in Section 5.1.

In order to automate the laser ablation process as much as possible, focusing areas ideally should be machined into the array structures, level with the microelectrode tips but distanced from the electrodes laterally. After focusing the laser, then setting two or three reference points, a computer numerical control (CNC) system could be programmed to ablate all of the array tips in an automated process. Several arrays could be processed in parallel using this method.

## **4.7 Connector Cable Fabrication**

Common to all microelectrode array designs is the problem of how best to connect the array to the electronics. Whether the electronics are to be implanted into the body or whether a percutaneous connector is to be used, the electrical signals must be transferred reliably between the microelectrodes and the front-end electronics. Due to the constrained dimensions and the environment involved, there is no simple solution to this problem. The current state of the art, represented for example by the Bionic array [24], manufactured by Cyberkinetics Inc. [25], still typically uses individual, hand-soldered insulated wires for connection. While this has delivered satisfactory results, it is less than ideal and does not scale very well as the number of electrodes is increased. Ideally, the connector cable should be strong, biocompatible, and highly flexible. During surgery, the array must be able to be maneuvered and positioned, without the presence of any restoring forces. The materials used should not degrade over time, and must be strong so that the connector can be handled during the implantation of the device. The connection process should be as automated as possible, in order to insure quality control.

### **4.7.1 The TEAS Connector Cable**

In the TEAS design, the electronic modules, with the exception of some power circuitry, are secured to the skull beneath the skin of the animal. A connector cable is used to link the mechanical array structure to the front-end electronics. The components of the connector cable used for the TEAS prototypes are shown in Figure 4-30. They include a flexible printed circuit board (PCB) and an 80-pin surface-mount connector.



**Figure 4-30. Image of the components of the TEAS prototype connector cable. They include a flexible PCB and an 80-pin connector [8,11]. (Photo: Jan Malášek)**

The connector cables for the TEAS prototypes were manufactured using flexible PCB technology [11]. The cable consists of a thin copper layer surrounded by polyimide. Cadence Allegro Expert [48] was used to create the layout of the connector cable. The connector was designed to meet the specifications given by the neuroscience collaborators at Brown University. The cable built for the TEAS prototypes was 56.3 mm long, 8.52 mm wide at the tip, where the microelectrode array is secured, and 22.9 mm wide at the base, where the connector is attached to the electronic front-end. An 80-pin Molex [49] surface-mount connector was used to attach the front-end electronics to the connector cable. Sixty-four parallel 50.8  $\mu\text{m}$  wide copper traces, spaced 152.4  $\mu\text{m}$  apart, run the length of the connector cable. The cable is about 50  $\mu\text{m}$  thick. Gold-plated pads were included in the design for soldering the connector to the flexible PCB at the electronics end, and through holes were used for aligning and soldering the electrode array structure at the array end. The use of through holes at the array end of the connector



cable, surrounded by gold pads, was seen as a good solution for the prototypes as it allowed the microelectrode array to be connected in the laboratory without the need for specialized machinery.

Because the brain of the animal may move a distance of up to 2 mm with respect to the skull, it is important to provide some strain relief in the connector cable. Laser cuts, 50.8  $\mu\text{m}$  wide and about 30 mm in length, centered between adjacent pairs of traces, allow for independent movement of the traces. These cuts were made when the flexible PCB was manufactured, and they greatly increase the overall flexibility of the connector cable and help to decouple the microelectrode array from the base of the connector.

As with the previous two fabrication processes, the design of the flexible PCB was accomplished using a CAD process. The connector cable specifications can be altered with minimal difficulty.

#### **4.7.2 Other Connector Designs**

Other processes that were investigated in order to fabricate a suitable cable included the machining of traces using a rapid prototyping system, such as the LPKF [42] ProtoMat 95s/II, or possibly using EDM, and then coating the resulting structure with parylene. Parylene is a well-suited insulating material for the connector cable. It is strong, and less susceptible to degradation than polyimide. It is also deposited in a process that insures a conforming, pinhole-free coating. The use of copper as a construction material should be avoided if possible in a biological application, but it remains today the standard metal used in PCB manufacturing. Gold, platinum, and titanium are better-suited materials from a biocompatibility standpoint, and they should be used wherever possible.

### **4.8 Assembly and Encapsulation**

The assembly of the TEAS prototypes included several manual steps. These were not automated primarily in order to keep the processes in the laboratory and to allow the processes to be developed iteratively. Most of the assembly processes could be replaced by more automated procedures.

### 4.8.1 Securing the Insulating Substrate

The design of the microelectrode arrays used for the TEAS prototypes includes ledges built into each of the electrodes. These ledges are used as attachment points when securing the electrodes into the insulating substrate. The insulating polyimide substrate was coated with a thin layer of EPO-TEK 301 epoxy, a USP Class VI compliant epoxy manufactured by Epoxy Technology Inc. [50], and lowered over the electrodes. This was done under a microscope, with the aid of a specially-designed fixture as shown in Figure 4-31.

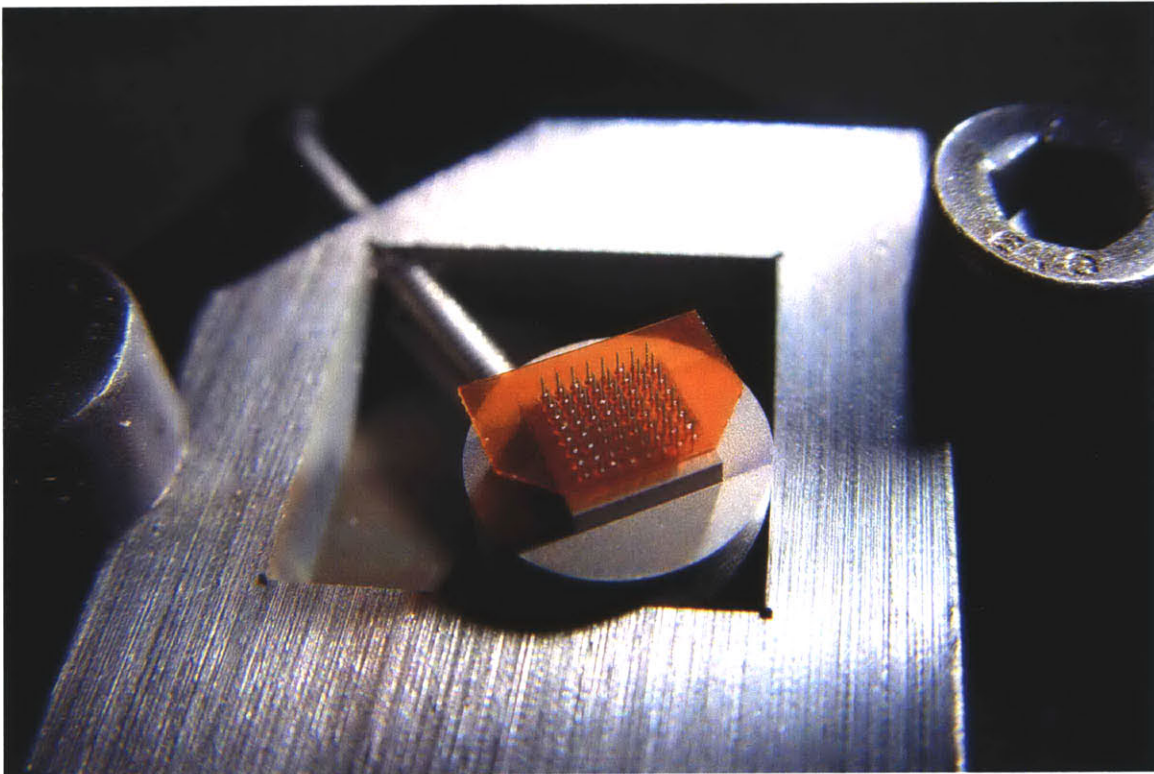


**Figure 4-31. Image of a TEAS microelectrode array held in a fixture while the insulating substrate is epoxied to the electrodes.**

The epoxy was applied evenly over the top of the insulating substrate, filling the holes, before it was lowered over the electrodes. The surface tension on the epoxy kept it in the holes and at the ledges. No epoxy was found either on the upper portions of the electrodes after the substrate was secured in place. Also, no interfering epoxy was encountered below the substrate when the electrode array assembly was freed from its metal base section by wire EDM, as shown in Figures 4-13 and 4-14. Some attempts

were made to apply epoxy at the base of the electrodes using a syringe after the substrate had been lowered into place over the electrodes, but this was deemed unnecessary and put the electrodes in danger of being bent.

#### 4.8.2 An Alternative Design

As the inter-electrode spacing of the microelectrode arrays becomes tighter, an alternative to the use of ledges may be needed. An image showing an alternative to the ledges used in the first TEAS prototypes is shown in Figures 4-32 and 4-33. The honeycomb-shaped, 1027-electrode tungsten carbide microelectrode array pictured here has an inter-electrode spacing of  $250\ \mu\text{m}$  between all nearest neighbors. A glass substrate with a matching hole pattern, has been lowered over the array. Shorter tungsten carbide stumps, machined concurrently with the electrodes, are used to support the substrate at the desired elevation while it is secured.

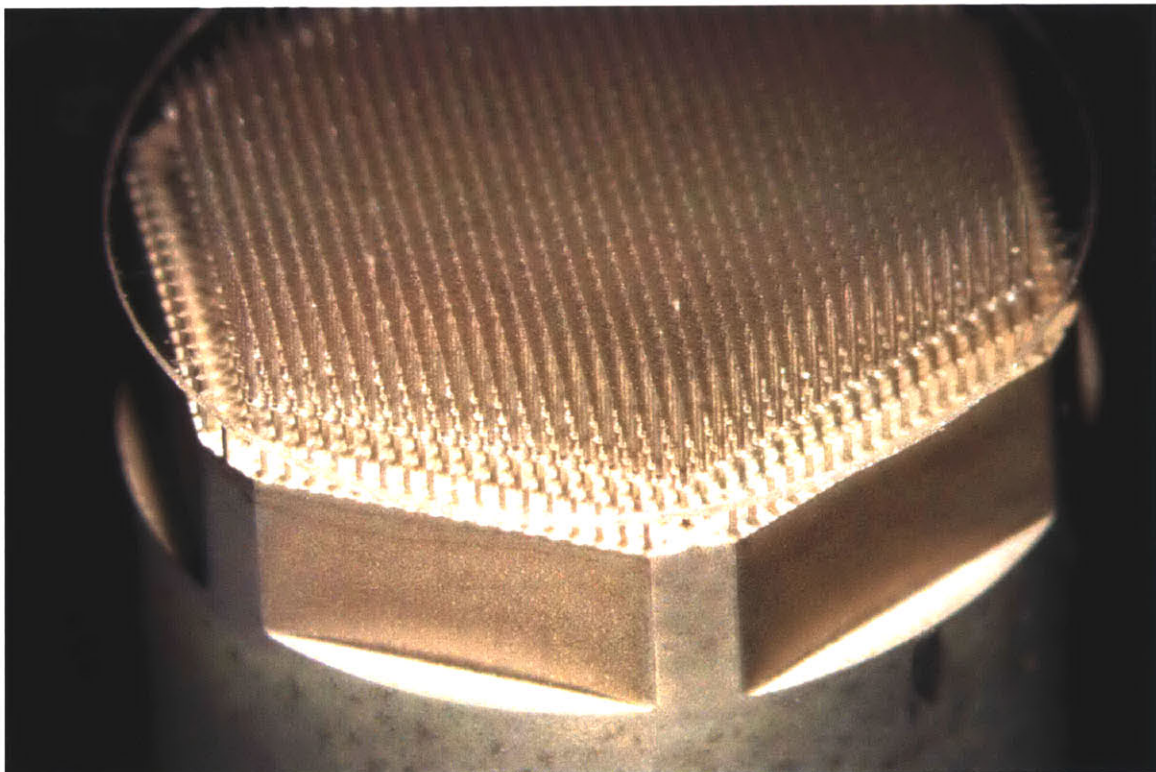


**Figure 4-32.** Image of a honeycomb-shaped tungsten carbide 1027-electrode array with a glass substrate mounted over the microelectrodes. The inter-electrode spacing is  $250\ \mu\text{m}$ .

Figure 4-33 shows a magnified view of the electrode supports holding the substrate at the desired elevation. After the substrate is secured, the assembly would be removed by EDM as in the TEAS case. The shorter supports would also be cut, but would simply fall clear as they would not be epoxied to the substrate.

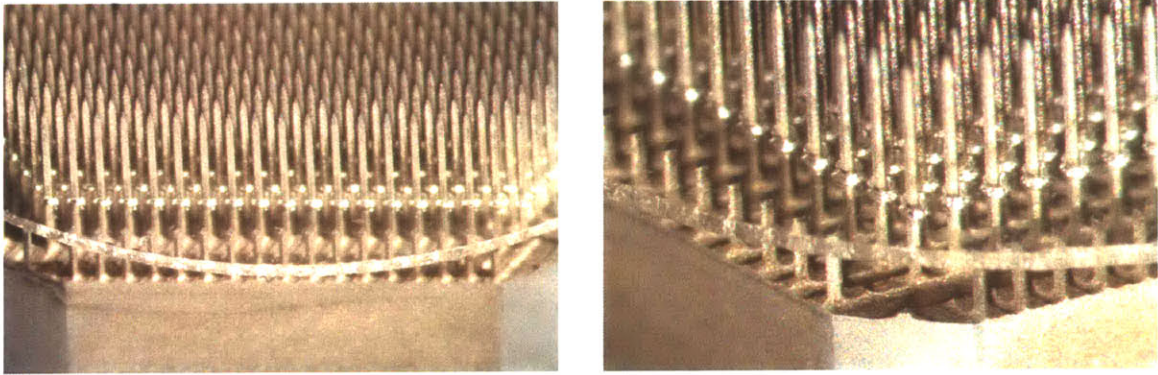


**Figure 4-33. Images showing the shorter supports used to position the substrate while it is secured.**

### **4.8.3 Electrical Connection**

Because the array assembly is delicate, a special fixture for soldering the electrodes to the connector cable was designed and machined by wire EDM. The TEAS microelectrode array assembly is shown held in the fixture in Figure 4-34.

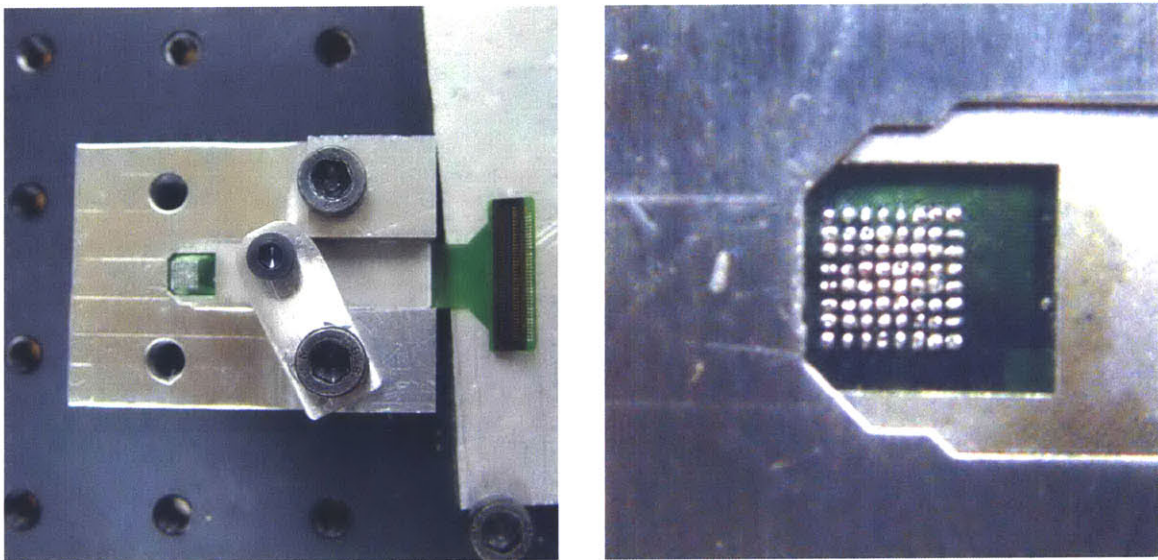


**Figure 4-34. Images of an array assembly held in a soldering fixture (left) and of the solder junctions that join the electrodes to the connector cable (right).**

The TEAS microelectrode array assembly, consisting of the microelectrodes epoxied into the insulating substrate as shown in Figure 4-25, is placed in the fixture shown in Figure 4-34, electrodes facing downward. A trench is included in the fixture along the length of array connector cable so that the substrate is supported with the electrodes hanging free from damage. The assembly is secured in several steps: First, the insulating substrate and electrodes are slid into position. The connector cable is then moved into place over the back ends of the electrodes, which are inserted through the holes in the cable. An aluminum insert is then placed over the entire assembly and secured by swinging the metal arm shown in Figure 4-34 (left) over the assembly and by tightening the smaller screw shown at the center of the image. The array is held firmly between the aluminum insert above and the fixture base below, with the electrodes suspended downward in the trench.

The electrodes are individually connected to the connector cable by soldering their back ends to the pads that surround the through holes in the connector cable. For the TEAS prototypes, the soldering was performed after the electrodes were electroplated with gold in order to increase solder adhesion. Solder does not adhere well to titanium and titanium alloy. The entire procedure was performed beneath a stereomicroscope. A close-up of the soldering result is shown in Figure 4-34 (right).

A more automated method for connecting the electrodes to the connector cable is needed. Two methods that could be used in the place of soldering are wire-bonding or flip chip technology [44]. Prior to the connection of the first TEAS prototype, some experimentation was done in an attempt to electroplate the connections with gold. All of the traces in the flexible PCB were attached to the electroplating equipment at the connector end, and it was hoped that the gold, deposited on the electrical pads at the electrode end, would eventually contact the back-ends of the electrodes until firm connections were formed. The results of the experimentation were inconclusive, and soldering was performed due to time constraints. In addition to further development of the electroplating method, other connection methods could include the use of a conducting epoxy or a silver paint. The evaporation of a metal such as gold, platinum, or titanium onto the structure using an E-beam evaporator, masked as needed, might provide yet another method of obtaining the necessary connections.

#### **4.8.4 Final Coatings**

For the TEAS prototypes, the solder joints were covered with a thin layer of Loctite 365 UV-curing adhesive [51] for protection purposes. In the case of the first prototype, Loctite 365 was also used to cover the Molex [49] connector and the PCB adapter [11], see Figure 5-4, which attached the Omnetics [52] connectors. The entire assembly, including the microelectrode array, the insulating substrate, and the soldered flexible PCB connector cable was then coated with parylene. This all-at-once conforming coating is seen as the best solution.

For the second TEAS prototype, several substrates of microelectrodes were parylene coated at once, as discussed in 4.6.1, and the soldering was performed afterward. In this case, Loctite 365 was used as the outer encapsulating material on the back of the array. It was also applied with a syringe between the insulating substrate and the flexible PCB connector cable. No additional coating was added to the flexible PCB cable for the second prototype. This use of less encapsulation was seen as acceptable for the second set of implantations due to their acute nature. It is recommended that parylene be used for the outer coating wherever possible.

# Chapter 5: Results

## 5.1 Electrode Characterization

There are several unknowns involved when implanting microelectrode arrays into the brain of an animal, foremost being the locations of the neurons in relation to the recording sites on the electrodes. Ideally, one would like to insert a high-impedance electrode, with a recording site that has a small surface area, immediately next to a neuron. The likelihood of this occurring for a given electrode is not great, however. By examining the contours of the brain, neuroscientists and surgeons can locate general regions within the brain. For the first TEAS prototype, the region of interest was the motor cortex, whose neurons are typically found at a distance of about 1 mm beneath the surface of the brain. These are macroscopic estimates, however. Without a means of fine-tuning the electrodes' individual positions by, say, adjusting their respective depths, one must resort to a more probability-based approach. Because ideal impedance values were not known, and because the manufacturing parameters required to accurately obtain specific electrode impedances were not yet determined, electrodes with a range of impedance values were created. With lower-impedance electrodes, one is more likely to record neural activity in general, but that activity has an increased chance of being buried by noise. With higher impedance electrodes, the potential for a clear recording is increased, but one is less likely to record signals because the recording sites must be physically closer to the neurons. When several electrodes are inserted together, however, the likelihood of one or more electrodes being placed within good recording range is increased.

For the TEAS prototype arrays, the goal was to create a range of impedance values from 50 k $\Omega$  to 100 k $\Omega$  at 1 kHz when measured by immersing the electrodes and a reference electrode in 0.9 % saline. This selected range of values was based on values similarly measured on a Bionic [24] microelectrode array system known to give satisfactory results. Once implanted, all of the electrodes were tested.

An effort was made to characterize the microelectrodes of the TEAS prototypes by measuring their impedance values in vitro. The measurements were done using an Agilent / Hewlett Packard 4194A Impedance/Gain-Phase Analyzer [53] by connecting to one array electrode at a time via a connector cable. The microelectrode array and a 30 mm square, platinum reference electrode were immersed in 0.9 % saline at room temperature in order to take the measurements.

In the fabrication of the first prototype of the TEAS microelectrode array assembly, significant technical difficulties were encountered during the laser ablation procedure, as briefly mentioned in Section 4.6.3. The 15  $\mu\text{m}$  thick parylene coating added to these difficulties, as more pulses were required in order to remove the necessary material. These conditions generally led to larger than desired impedance values. A range of values was measured, however, and it was hoped that some electrodes would be capable of recording neural activity. Although the state of the excimer laser used for ablating parylene from the electrode tips of the first prototype was such that the pulse energy was decreased significantly below the desired fluence level ( $\text{J}/\text{m}^2$ ), the thickness of the parylene that had to be removed certainly contributed to the poor result. In the cases where suitable impedance values were obtained, the parylene was sufficiently removed immediately at the electrode tips, but a surrounding shielding layer remained. Holes at the electrode tips were machined from above, through the parylene, leaving a less than desirable geometry. The low fluence values of the laser pulses likely also led to more melting and less vaporizing of the parylene at the electrode tips. These issues were largely solved for the development of the second TEAS prototype by the use of a much thinner layer of parylene insulation and the use of a much more powerful laser, as discussed in Section 4.6.3.

For the second prototype of the TEAS mechanical front end, a much thinner, 3  $\mu\text{m}$  thick layer of parylene was deposited on the microelectrodes. Using an excimer laser capable of generating much higher fluence levels, a more desirable range of impedance values was obtained. Figure 3-2 shows an example of an impedance measurement displayed by the impedance analyzer.



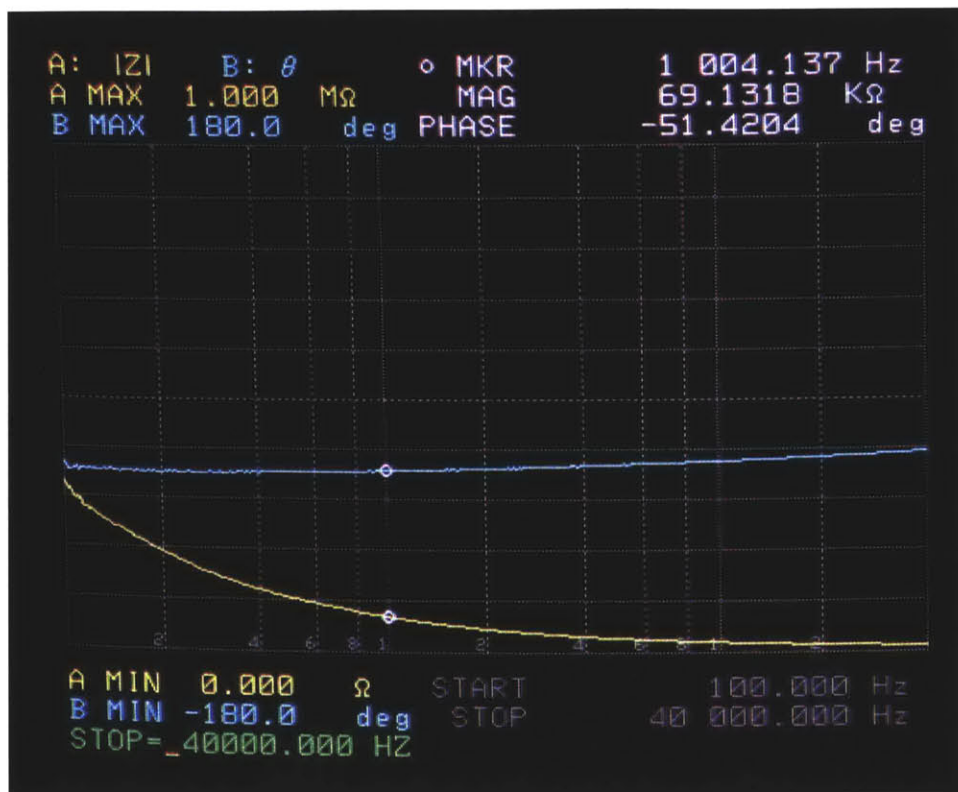


**Figure 5-1. Image of a typical plot from the impedance analyzer. The TEAS microelectrode array was immersed in 0.9 % saline and a platinum reference electrode was used. (Photo: Ariel Herrmann)**

Impedance curves were generated for all the electrodes of the second TEAS prototype array assembly. The impedance curves all exhibited shapes similar to that shown in Figure 5-1. One can see that the marker is set at 1004.137 Hz in the screenshot, which displays a value of 69.1318 kΩ at that frequency. The accuracy of the impedance measurements was approximately 0.16 kΩ at the mean measured value. The curves appeared to be generally shifted along the vertical axis depending on the electrode characteristics.

An attempt was made to produce a range of electrode impedance values by varying the number of laser pulses that were used to ablate each electrode. As mentioned in Section 4.6.3, a Resonetics [43] Maestro 1000 excimer laser, operating at a wavelength of 248 nm, was used to perform the laser ablation. The laser was operated at a pulse energy of 160 mJ, a pulse rate of 200 Hz, and a pulse width of 1 μs. An iris was installed and used at the end of the optical path length in order to reduce the spot size at the

ablation sites. For the platinum coated titanium alloy microelectrode array shown in Figures 4-28 and 4-29, which later formed the basis of the second TEAS prototype assembly, four different numbers of pulses were used. The pulses were performed in sets in order to allow for slight corrections in the positioning of the laser beam. Some feedback was possible due to the pulse sets being visible on a monitor, as relayed by a magnifying CCD camera. Typically, after the first set of pulses was completed for a given electrode, the delivery point of the pulses would be adjusted by 2 to 3  $\mu\text{m}$ . The electrodes were divided into four groups by pairs of rows. Three groups were ablated with 100, 75, and 50 pulses, in sets of 25 pulses, and the fourth group was ablated with 20 pulses in two sets of 10 pulses.

The impedance value at 1 kHz is commonly used for reference for neural electrodes, and it is this value that was used to characterize the measured impedances. Because the plots of impedance versus frequency are similar in shape, one can extrapolate a general curve from the 1 kHz value. The impedance values were found to generally range between 10  $\text{k}\Omega$  and 200  $\text{k}\Omega$ , with the exception of several values in the 4  $\text{M}\Omega$  to 5  $\text{M}\Omega$  range and a few even higher. Because the  $\text{M}\Omega$ -range values are so much greater than the remaining and expected values, they are likely due to poor solder connections. The average impedance, measured at 1004.137 Hz with the impedance analyzer as outlined above, was found to be 1.929  $\text{M}\Omega$  with a standard deviation of 3.229  $\text{M}\Omega$ . The distribution was substantially skewed by the  $\text{M}\Omega$ -range values. There were 21 impedance measurements above 1  $\text{M}\Omega$ : 6 in each of the 20, 50, and 100-pulse groups, and 3 in the 75-pulse group. The average of these values was 5.718  $\text{M}\Omega$ . The average impedance for the remaining 43 electrodes was much lower at 77.93  $\text{k}\Omega$  and had a standard deviation of 76.78  $\text{k}\Omega$ .

Figure 5-2 shows a graph of electrode impedance, measured at 1004.137 Hz as outlined above, for each of the groups of electrodes that received varied numbers of laser pulses. The 21 electrodes with impedance values measured to be above 1  $\text{M}\Omega$  at 1 kHz were excluded from the data for this graph.

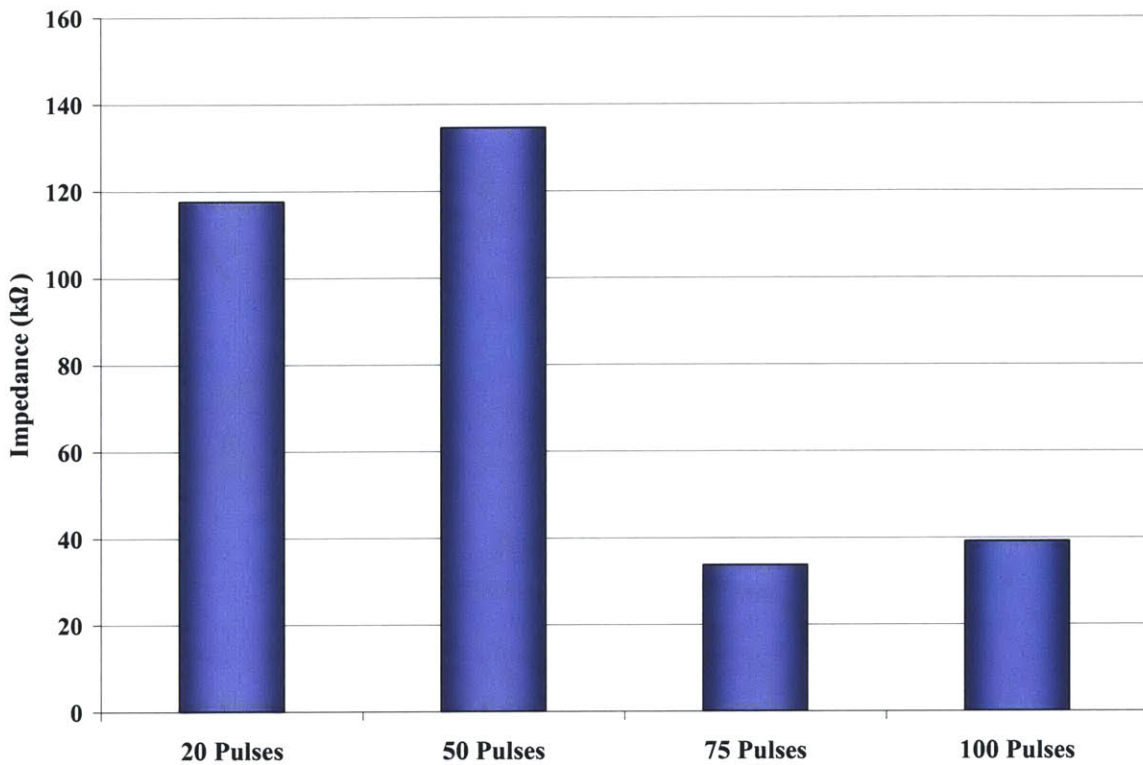


**Figure 5-2. Graph showing the effect on the measured electrode impedance values from changing the number of laser pulses used when ablating parylene from the electrode tips.**

The error involved in recording these values with the impedance analyzer was considerable. Values obtained from multiple trials for a single electrode were found to vary by as much as 25 %. Furthermore, variations in the ablation process could have contributed to the discrepancy in impedance values among electrodes within each group. The readjusting of the electrodes between sets of pulses may have led to differences in the exposed surface areas, and therefore in the impedance values. The surface finishes at the electrode tips may also have affected the obtained impedance values. Uneven distributions of electroplated material would have had unpredictable effects on the obtained electrode impedances. Although a trend can be seen in Figure 5-2, with higher numbers of pulses leading to lower impedance values, as one would perhaps expect, more data must be collected in order to obtain conclusive results.

Figure 5-3 shows a graph of the electrode impedances obtained after delivering varying numbers of pulses. The electrodes with impedances greater than 1 MΩ, believed to have poor connections, were given null values in the graph.

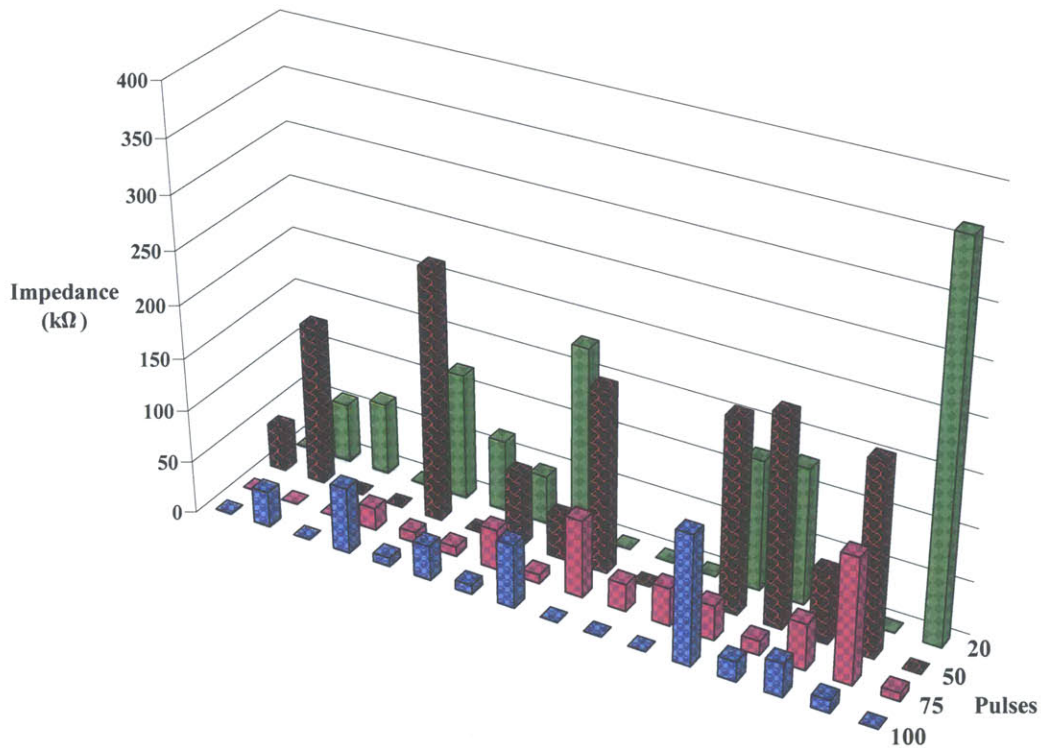


**Figure 5-3. Graph showing the effect of changing the number of laser pulses used on the resulting electrode impedances.**

Upon inspection of the graph shown in Figure 5-3, it is apparent that the measured impedance values varied a great deal. The standard deviations for the groups of well-connected electrodes that underwent laser ablation were found to generally decrease with an increased number of pulses. They were found to be 99.10 kΩ, 72.71 kΩ, 31.76 kΩ, and 35.36 kΩ for 20, 50, 75, and 100 pulses, respectively.

If the laser pulses had high enough fluence values ( $J/m^2$ ), it is possible that the parylene was completely ablated from the target area within a small number of pulses. Subsequent pulses would then have had little effect. This may have been the case when the number of pulses was increased from 75 to 100, though more data are needed. If the fluence values were high enough, the laser would begin to ablate the metal of the electrodes.

It is advantageous to have the fluence of the laser beam as uniformly distributed as possible. The beam must also be well-focused in order to produce an ablated area with a clearly defined border. It is important to consider that the effect of administering 25

additional laser pulses at the chosen parameters may have been secondary to other effects such as the imprecision of locating the laser relative to the small-scale geometry of the electrodes and the differences in the surface finish of the exposed electrode tips.

In order to obtain more control over the electrode impedance values resulting from the laser ablation process, further study and testing is needed. Additional laser parameters could be altered, and the use of masks in order to more accurately control the dimensions of the obtained ablated regions could be further explored. Also, improved electrical connections between the electrodes and the connector cable are required, whether by soldering or by another method. More investigation is needed into the effect of the underlying surface finish and the properties of the electroplated metal on the resulting impedance values. Although further experimentation and process refinements are required, laser ablation was shown capable of producing electrode impedances in the desired range. With computer numerical control (CNC) and controllable energy delivery, it also has the capabilities required to evolve into a semi- or fully-automated process.

## **5.2 Implantation of the Prototypes**

The first implantation of a TEAS mechanical front end prototype was done early in the development of the TEAS project. It was decided that a TEAS microelectrode array should be implanted and tested in an animal while the electronic modules were still being engineered. The microelectrode array was designed to be modular enough to be tested with an alternate data acquisition system. It was thought that the surgery would, at the very least, expose the members of the TEAS engineering team to the environment in which the implantation is done and in which the array must function. If needed, modifications could be made to the design of the microelectrode array assembly in order to improve its performance or to aid in future implantations.

### **5.2.1 Implantation into a Monkey**

The first TEAS microelectrode array prototype was implanted and tested in a wired configuration in a *Macaca mulatta* monkey. The animal was soon to be sacrificed

due to health problems, and it was decided that the TEAS team could have the opportunity to implant and test the prototype before the sacrifice. Chronic recording could be done and the microelectrode array could be tested in a configuration very similar to that planned for the TEAS system. Additionally, non-miniaturized prototypes of the analog electronic front end and the digital section could be tested by connecting to the array percutaneously.

For this first implantation, the electrode signal paths were connected to an external data acquisition system using percutaneous connectors manufactured by Omnetics Connector Corporation [52]. Cables connected to a multichannel acquisition processor (MAP), manufactured by Plexon Inc. [54], were mated with the Omnetics connectors when chronic neural activity recordings were taken. A printed circuit board (PCB) adapter was manufactured using an LPKF [42] ProtoMat 95s/II rapid prototyping system [11]. The adapter was used to attach the Omnetics connectors to the Molex [49] connector on the flexible PCB connector cable that forms part of the prototype TEAS array assembly. The Omnetics connectors and PCB adapter are shown in Figure 5-4.

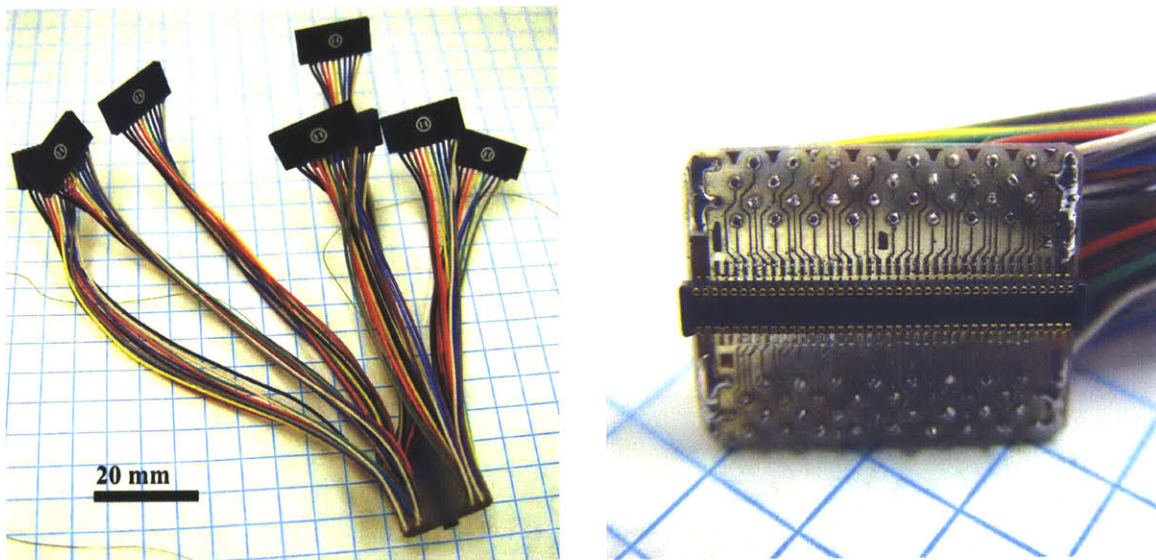


**Figure 5-4.** Images of the percutaneous connectors (left) and the printed circuit board adapter made to connect the TEAS mechanical front end to the data acquisition system. (Photos: Robert Dyer)

The Molex surface-mount connector, which mates with the female part on the TEAS assembly, can be seen in the center of the PCB adapter as shown in Figure 5-4 (right).

The animal used for the first implantation of the TEAS prototype had undergone previous implantations into the brain region. Following the normal preparation of the animal prior to surgery, additional time was required to remove a prior implant, as well as coats of acrylic and other materials that had been used to secure the device. The presence of a prior implant in the animal limited the options open to the surgeons for implanting and securing the TEAS prototype. For example, much of the skin on the crown of the animal's head was no longer available for covering the site of the implantation. The percutaneous connectors had to be surrounded by additional materials.

After the previous implant was removed and the animal's skull was cleared of all preexisting adhesives, the skull at the region of interest was removed and a flap was cut in the dura mater covering the brain. An image of the animal's skull and an exposed region of its brain is shown in Figure 5-5. Note that the screw observed in Figure 5-5 remained from the previous implantation.

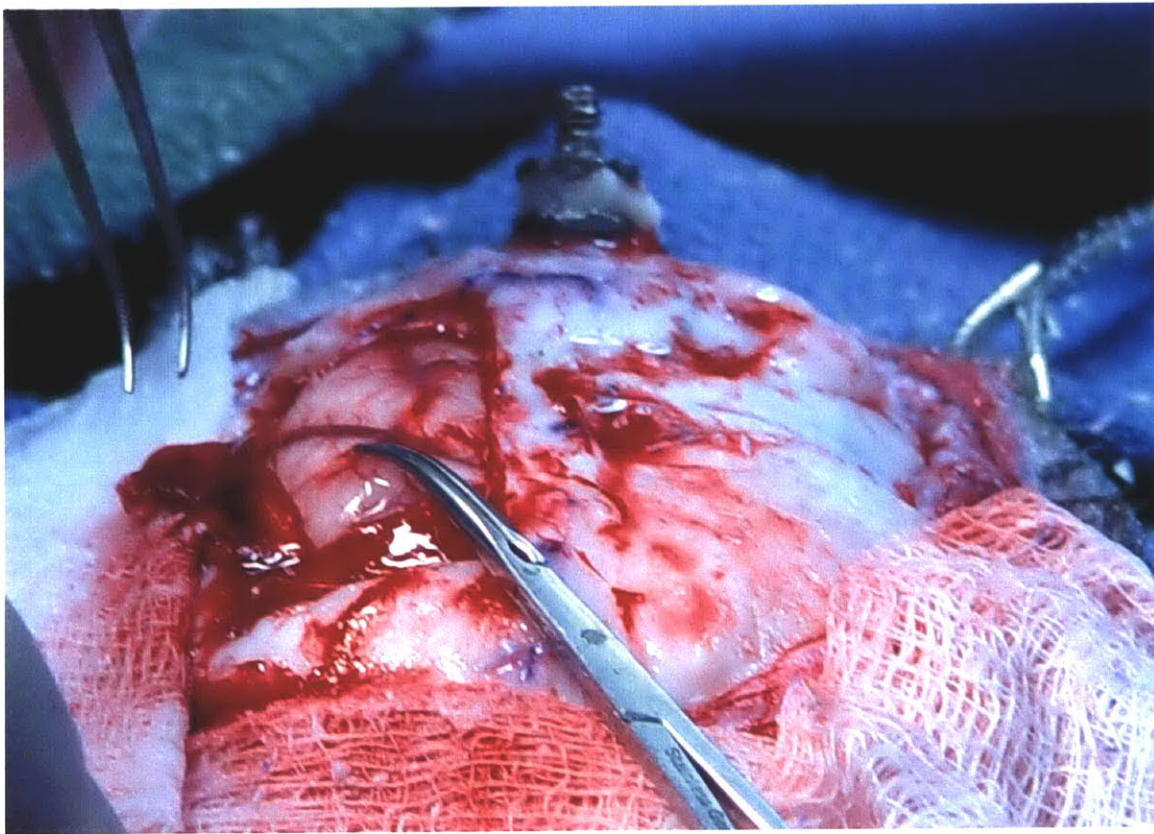


**Figure 5-5. Image of the monkey's skull and an exposed portion of its brain prior to the implantation.**

Following the uncovering of the brain at the region of interest, the array microelectrodes were positioned over the target location of the animal's motor cortex, with the base section of the assembly extending over the animal's skull. The base of the TEAS prototype was then secured to the skull using an acrylic adhesive and two bone screws as anchors, as shown in Figure 5-6.

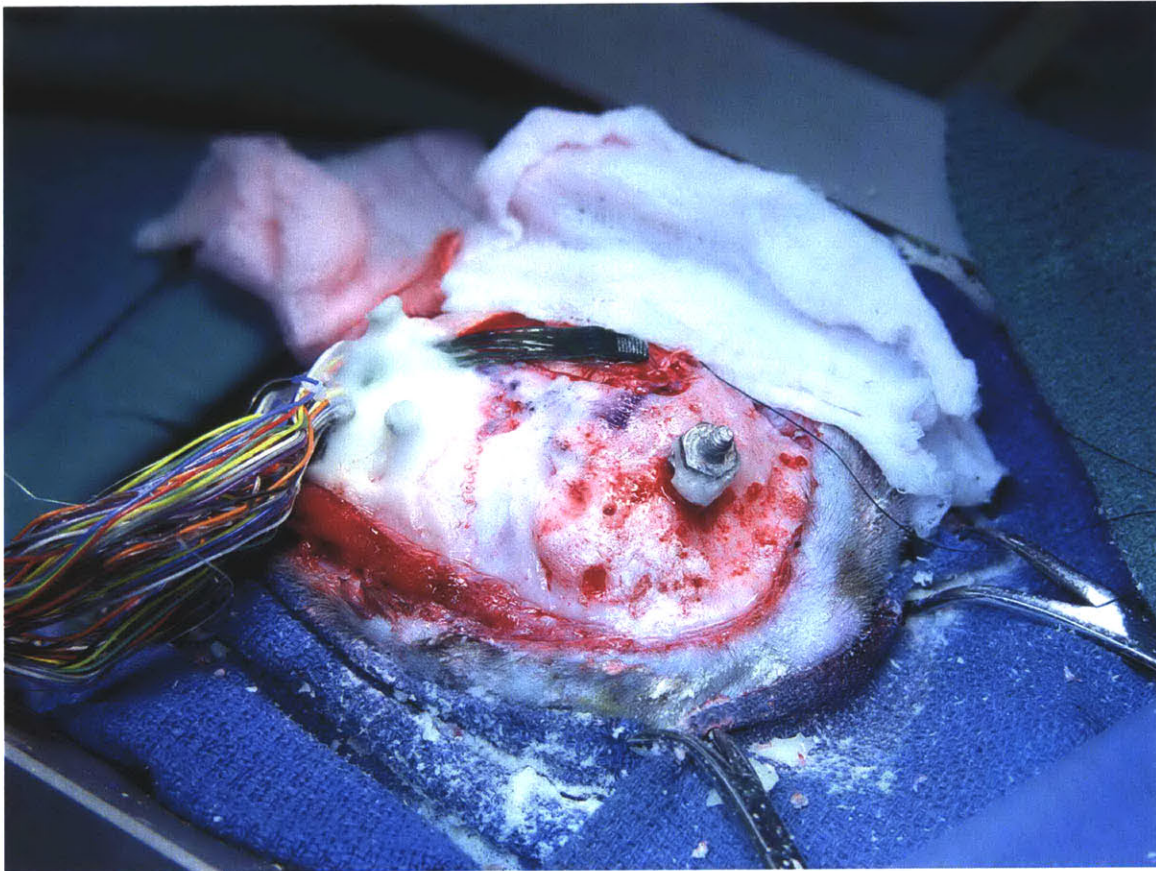


**Figure 5-6. Image of the TEAS microelectrode array assembly cemented into place prior to insertion.**

A Bionic [24] pneumatic inserter, manufactured by Cyberkinetics, Inc. [25], was used to implant the microelectrode array into the brain. An image of the inserter positioned above the array moments before insertion is shown in Figure 5-7. The inserter was fastened to the operating table and delivered a timed and controlled impulse to the back of the array.



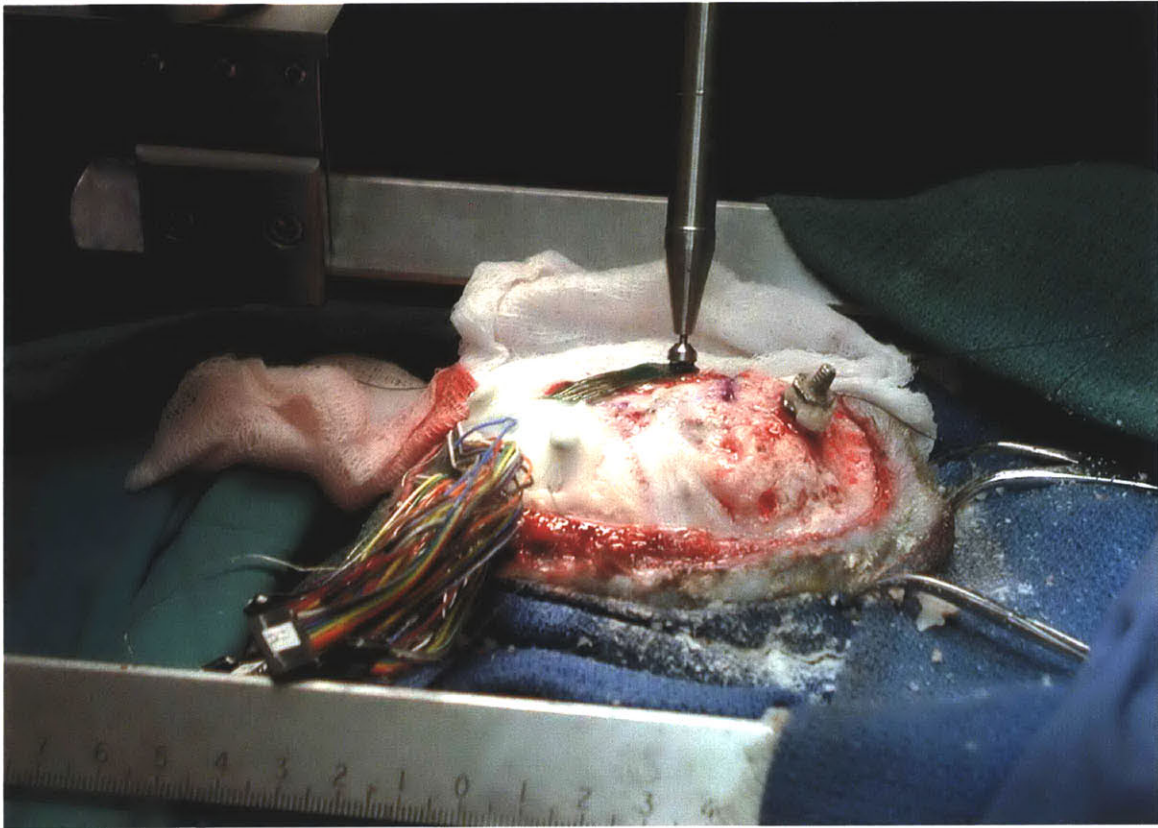


**Figure 5-7. Image of the microelectrode array moments before insertion with a pneumatic insertion tool [11]. (Photo: Jan Maláček)**

After the array was inserted, the flap of dura mater was sutured back into place, covering the exposed region of the brain. The site was covered with a layer of GORE-TEX [55] in order to protect the brain by providing a smooth, flexible barrier under which it could move. The GORE-TEX layer was then covered with a layer of acrylic adhesive. Once this first layer of acrylic had hardened, the Omnetics [52] connectors were moved into place and secured over the skull of the animal. Figure 5-8 shows the acrylic being applied over the Omnetics connector cables. The encapsulating acrylic layer provided a hard, protective shell over the site of the implant.

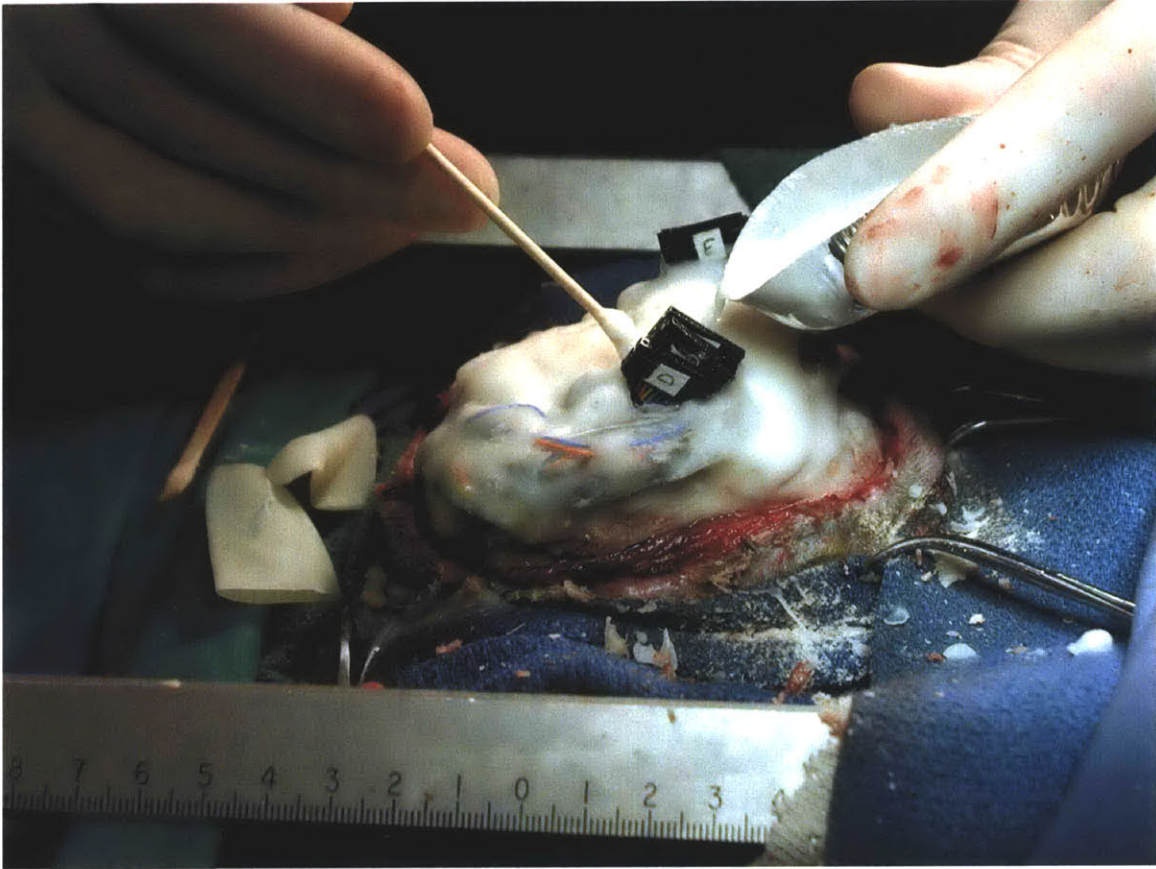


**Figure 5-8.** Image of the final acrylic encapsulating layer being applied [11]. (Photo: Jan Malášek)

The mechanical results and the electrical recordings obtained from this first implanted prototype are discussed in Sections 5.3 and 5.4, respectively.

### **5.2.2 Implantation into Mice**

The second prototype of the TEAS mechanical front end was implanted into two mice in acute experiments. These experiments were performed in order to verify the second TEAS prototype's ability to record neurological data, thus validating the parameters and methods used in producing the recording sites at the tips of the microelectrodes. Although the device was designed to be implanted into a monkey, it was decided that the use of mice would be more appropriate for these experiments. The array was oversized for a mouse's brain, but the dimensions were such that it fit on a single side of the animal's cortex. It was decided that the array would be inserted slowly using a micromanipulator, rather than using a pneumatic tool to generate an impulse, as

was done with the first TEAS prototype assembly. This allowed the electrodes to be inserted to less than their full depth, which was necessary due to the size of the animal's cortex. Also, this allowed for the hunting of neural activity at several electrode depths in the animal's brain as the array was inserted.

As was done for the first implanted TEAS prototype, a PCB adapter was connected to the array assembly and soldered to cables supplied by the neuroscientists in order to interface with their data acquisition system. Individual ground and reference wires were also attached to the cables in order to create the necessary return path. A Cerebus data acquisition system, manufactured by Cyberkinetics, Inc. [25], was used to perform the recording. Once attached to the connector cables, the array assembly was mounted onto a micromanipulator, as shown in Figure 5-9.

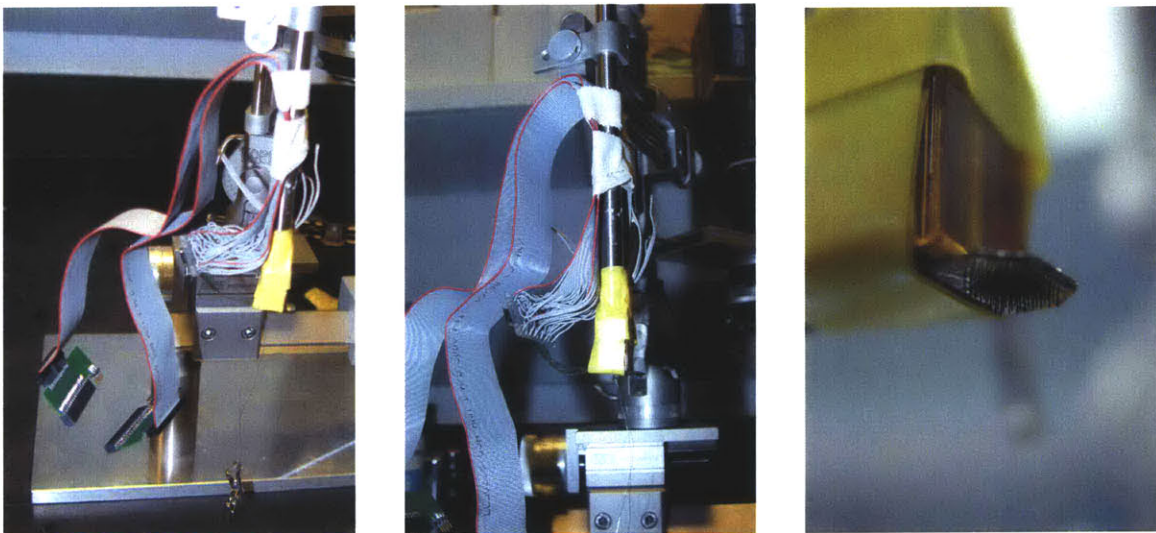


**Figure 5-9. Images of the microelectrode array assembly mounted onto a micromanipulator for implantation.**

After the mouse had been anesthetized, secured, and prepared for the surgery, a craniotomy was performed on the animal. The microelectrode array was then positioned over the left side of the animal's brain, as shown in Figure 5-10. The micromanipulator allowed the microelectrode array to be carefully positioned over the brain prior to insertion.

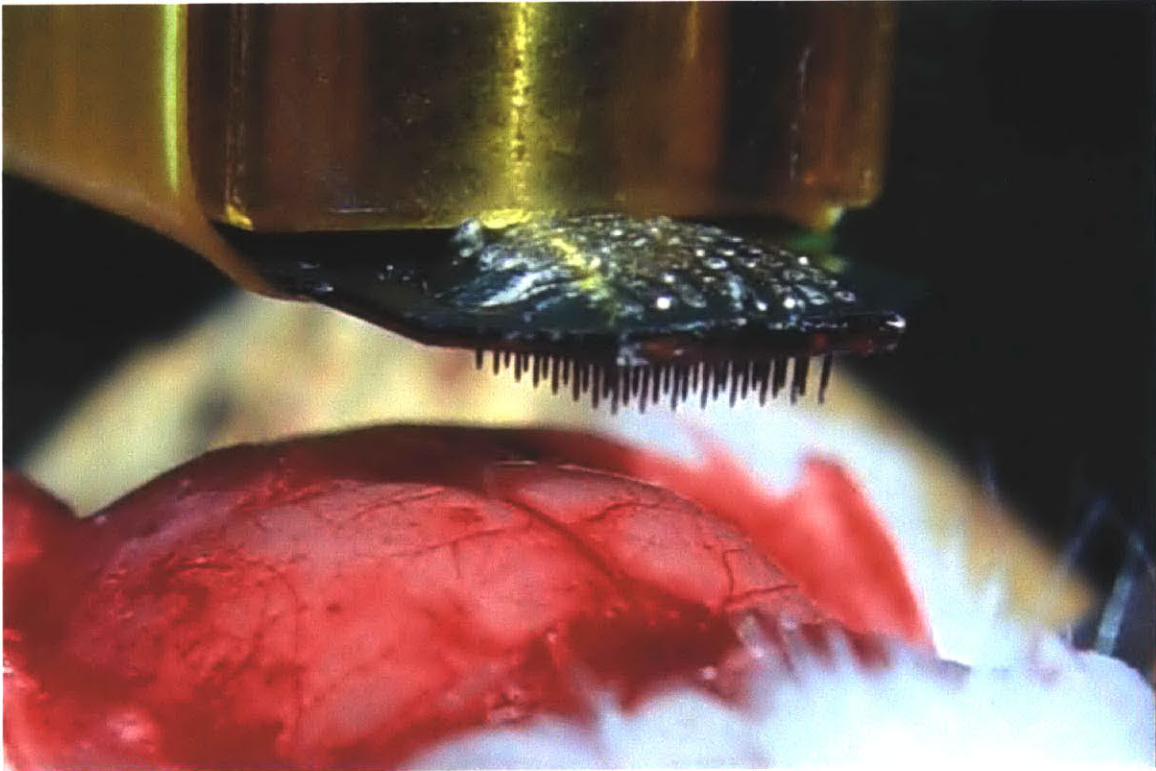


**Figure 5-10. Image of a microelectrode array above the mouse brain before implantation.**

The microelectrodes were lowered directly downward until they slowly penetrated into the brain. Some dimpling occurred upon insertion of the electrodes. Because the dura mater on a mouse's brain is so thin, it was decided that rather than attempt to remove it prior to the insertion of the prototype, the array would be made to penetrate through the dura mater.

The 128-channel Cerebus [25] data acquisition system was specially designed for intracortical recording of extracellular action potentials. Waveforms were presented from designated channels after the measured signals crossed selected thresholds. Several filters allowed the data to be searched quickly for neural spikes. Recordings were made at several electrode depths. The array was later removed, and the procedure was repeated after reinsertion of the array into the right side of the animal's brain.

After some analysis, an implantation was performed on a second mouse using the same prototype and following a similar procedure. The neurological recordings that were obtained from these experiments are discussed in Section 5.4.

### 5.3 Mechanical Results

The microelectrode arrays of the two implanted TEAS prototypes proved to be more than strong enough for the implantation procedures. Upon removal and inspection, the microelectrodes were all found to be intact, and their overall structure was unchanged. No bending of the electrodes or other deformation was observed. The parylene coating also exhibited no signs of wear, weakening, or peeling as a result of the implantation. Additionally, no signs of infection or other biological problems were observed upon removal of the arrays or after a biopsy implied from the site of the first implanted prototype.

The 15  $\mu\text{m}$  layer of deposited parylene used to insulate the first TEAS prototype was determined to be much thicker than required. This contributed to two key concerns with the first TEAS prototype: the poor laser ablation results that were encountered when fabricating the prototype, as discussed in Section 5.1, and the higher than desired stiffness of the flexible PCB connector cable. From the implantation procedure of the first TEAS prototype assembly, it was apparent that the flexibility and plasticity of the connector cable should remain an important consideration in the design of microelectrode array assemblies. Even with the laser cuts included in the design to increase flexibility, restoring forces on the cable observed during the surgery were somewhat problematic. The connector cable was manually bent into position during the surgery so that the array would rest on the brain prior to the insertion of the microelectrodes. The stiffness of the connector cable limited the options for where the microelectrode array and the base of the connector cable could be positioned. Figure 5-11 shows the surgeons attempting to permanently deform the flexible PCB to the contour of the brain.

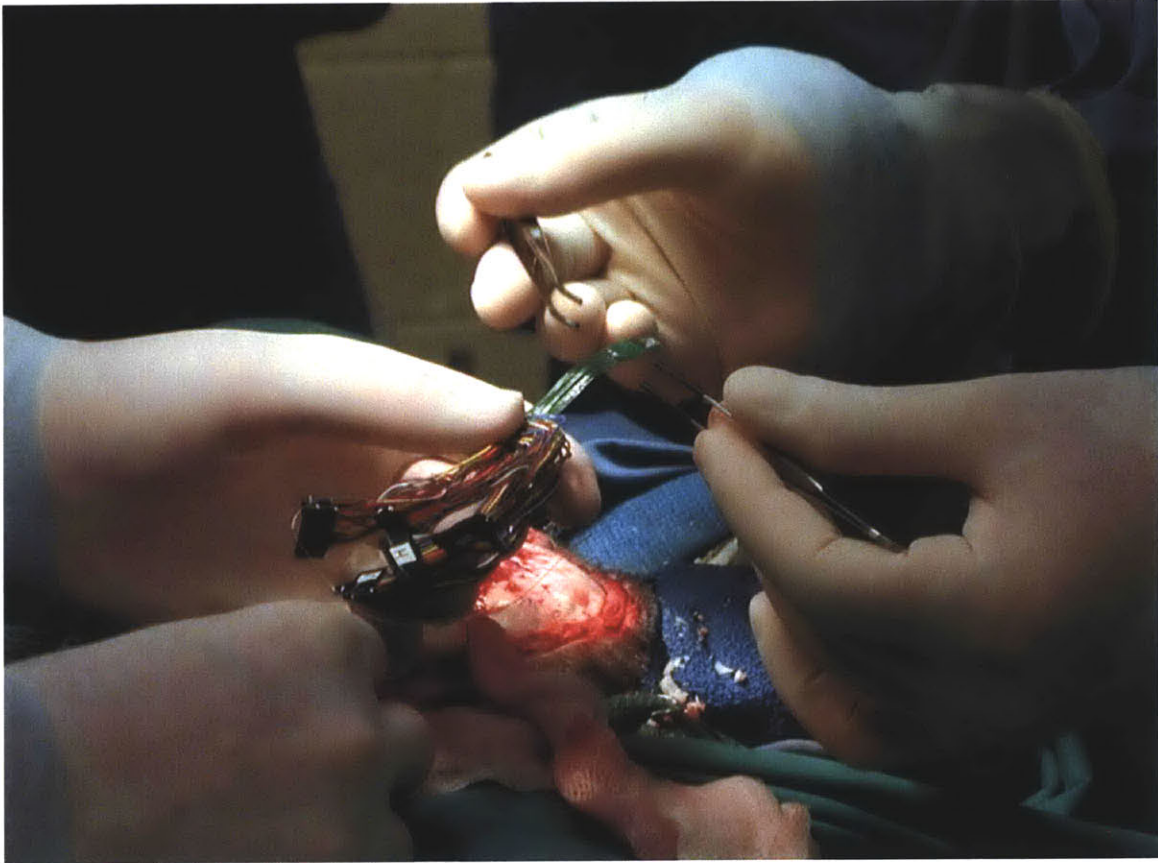


**Figure 5-11. Image of the surgeons attempting to deform the connector cable to the shape of the brain [11]. (Photo: Jan Malášek)**

Ideally, the microelectrode array should be completely mechanically decoupled from the electronics module. One should be able to position these two modules independently from one another. This requirement leads to the need for a substrate to be present on the microelectrode array, so that it can be maneuvered with forceps. The flexibility of the PCB connector cable could be increased by widening the laser cuts, or by dissolving some of the polyimide from the cable. Nevertheless, alternative connector cable designs should also be considered. The use of flexible PCB technology is convenient because the technology is well-developed. It is not ideal, however. The use of copper in the design should be completely eliminated if possible, and parylene would be a better choice as an encapsulant over polyimide. In either case, the use of parylene as an encapsulating material is still advisable when the device is to be implanted for an extended period of time.

Although the mechanical and electrical components of the TEAS design were created to be modular, the surgical environment is such that the components should be connected prior to the implantation procedure. When the modules are connected beforehand, it can be done using a microscope and precision equipment if needed. Also, an encapsulating layer can be applied over the connection point. Likewise, if a percutaneous connector is used, it should be connected to the microelectrode array assembly prior to implantation.

For the acute experiments, the microelectrode array was more complex than it needed to be. In this case the experiments were undertaken in order to validate the design and the manufacturing methods used in developing the array. If a similar array assembly were developed specifically for acute recording, however, it would be best to keep it as simple as possible, preferably allowing it to connect directly with the data acquisition system that was being used for recording. This would eliminate the need to fabricate specialized adapters. By decreasing the number of electrical connections, one could also potentially increase the quality of the recordings.

## **5.4 Neural Recording Results**

The first prototype of the TEAS mechanical front end was implanted in a *Macaca mulatta* monkey for 31 days. During that period of time, chronic recordings were made by connecting the percutaneous connector, attached to the microelectrode array, to a multichannel acquisition processor (MAP), manufactured by Plexon Inc. [54]. Unfortunately, no obvious neural spike patterns were observed during these recordings. This was likely largely due to overly high electrode impedance values, as discussed in Section 5.1.

The second prototype of the TEAS mechanical front end was implanted in two mice in acute experiments lasting several hours. Neural recordings were made using a Cerebus data acquisition system, manufactured by Cyberkinetics, Inc. [25]. The system was new, and a significant amount of time during the first procedure was spent becoming accustomed to the intricacies of its software. The software is capable of filtering, sorting,

and recording neural spikes on all of its 128 channels in real time. By setting the thresholds and waveform filters, one can selectively display the data of interest.

Characteristic neural spike patterns were observed during the second procedure. Example neural spike waveforms are shown in Figure 5-12. The markers represent the data points that were sampled and recorded at 32 kHz. The curves are the result of low-pass filtering and interpolating the data.

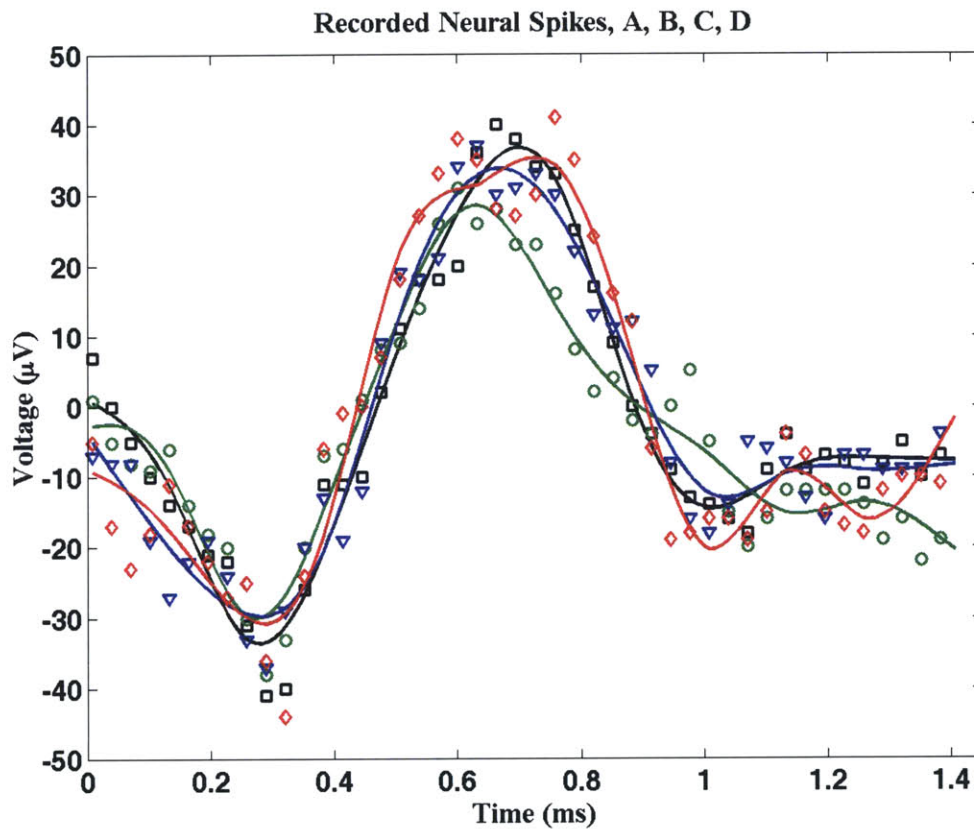


**Figure 5-12.** Plots of four neural spikes recorded from the cortex of a mouse.

Figure 5-12 shows four waveforms that exhibit the characteristic shape of extracellular-recorded action potentials. They were all recorded using the same microelectrode. Figure 5-13 shows individual plots of the four neural spikes with error bars representative of the noise observed while recording. The data displayed in Figures 5-12 and 5-13 were low-pass filtered at 7.5 kHz and high-pass filtered at 750 Hz while recording.



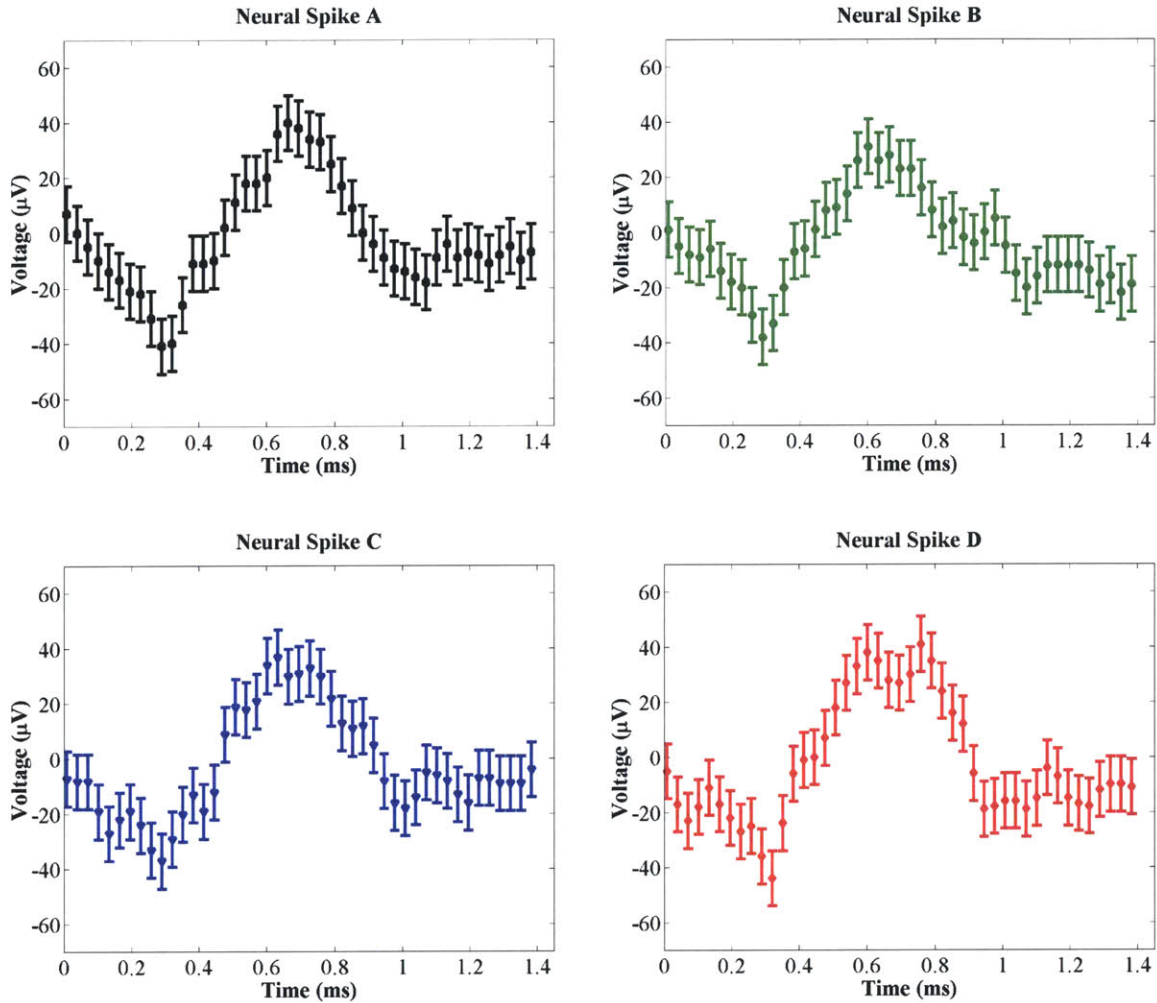


**Figure 5-13.** Plots of four neural spikes that were recorded from the brain of a mouse using the TEAS microelectrode array assembly.

It is well-established theory that most, if not all, of the information transmitted between neurons is encoded in the timing between the spikes, rather than in their shapes. In fact, if an action potential occurs, it normally generates the same waveform each time. Because a single electrode normally records from one, or possibly two, neurons, the shapes of the observed waveforms will be identical. This is one of the cues one looks for when searching for neural activity. Another cue is the occurrence of erratic, or non-repeating, spiking patterns. Neural spikes normally last 1 ms to 2 ms in the motor cortex, and fire at rates between 10 Hz and 300 Hz, with faster firing rates corresponding to faster muscle movement [15]. This kind of pattern was observed using the second TEAS prototype in a mouse.

## Chapter 6: Conclusion

A summary of the development of brain microelectrode array systems, specifically for use in the TEAS project, has been provided. New methods of developing microelectrode array assemblies have been presented. Central to these methods is the use of wire electrical discharge machining (wire EDM) in creating the microelectrode array structures. This process has yielded impressive results in terms of feature size and aspect ratios. It also allows for the use of nearly any conductive material, including strong, biocompatible materials such as titanium, titanium alloy, and stainless steel. Because it is a computer numerically controlled (CNC) process, and utilizes computer aided design (CAD), it also produces very repeatable and predictable results. Designs can be modified to suit particular applications. When coupled with a chemical etching technique, microelectrodes with lengths greater than 5 mm, widths less than 40  $\mu\text{m}$ , and inter-electrode spacings of 250  $\mu\text{m}$  have been fabricated successfully. This method has been shown to scale well, with arrays having been produced in parallel at a dramatic time saving. Because the microelectrodes are machined from a solid piece of stock, the relative dimensions of points on the array are accurately known, and reference points, for use in other steps of the assembly process, can be machined into the base of the array structure.

Other innovations have been presented and evaluated, such as the use of the insulating substrate to hold the microelectrodes in place during assembly and the development of a flexible printed circuit board (PCB) connector cable, with laser cuts to add mechanical flexibility. The use of parylene as an encapsulant has been explored, as well as the use of laser ablation as a method for obtaining accurate recording sites with the correct dimensions. The use of CAD, CNC, and the potential for parallel assembly and fabrication were important considerations in all of the process involved in the manufacturing of the TEAS arrays.

Two prototypes of the TEAS mechanical front end were assembled and implanted successfully in one monkey and two mice. Mechanically, the arrays performed well in all cases. The machined electrodes proved strong enough for insertion both by

pneumatically-generated impulse and by micromanipulator. No biocompatibility problems were encountered with the electrodes or the materials used for encapsulation. Electrically, after further refinement of the parylene removal process, neurological recording was achieved, and the manufacturing processes were validated. Neural spikes were observed and recorded using a device fabricated by these methods.

The TEAS project represents a significant step in the growing field of brain-machine interface devices. And, appropriately, the mechanical front end was developed using new, novel techniques that have proven viable in early experiments. Though more work is required in order to fine tune the manufacturing processes, they have in their early stages proven capable of creating strong, precise, microelectrode array assemblies, comparable with the current state of the art. As the densities and resolutions required for microelectrode applications increase in the future, and the need for the use of stronger electrode materials grows, the capabilities presented here will likely prove valuable to the development of brain-machine interfaces.

## Chapter 7: Future Work

While the individual elements of the TEAS mechanical front end were all designed using a CAD approach and fabricated using CNC machines, the assembly process currently requires some manual steps. Future work is required in order to remove as much of the human element from the assembly process as possible. The use of parallel processes must be further utilized and methods for smoothly progressing through the manufacturing steps need to be developed. For example, the use of reference points to align and automate the laser ablation process could be implemented.

Although laser ablation has been shown to be promising in the removal of parylene from the electrode tips, other methods are worth exploring. One possible method is the use of a non-line-of-sight oxygen plasma etching technique. Alternative methods for creating the flexible connector cable could be devised in an effort to increase its flexibility and biocompatibility. New methods of connecting it to the microelectrode array could also be explored.

Testing could be done in order to quantify the forces acting on the arrays as they are inserted. The effects of shape, geometry, inter-electrode spacing and choice of materials on the insertion forces could be determined in order to more appropriately choose the dimensions and shape of the microelectrodes.

Though the methods presented here have certain advantages over the methods currently used to produce similar structures, they are by no means an end-all solution. Further exploration of fabrication processes will always be possible. In an effort to further miniaturize the structures, additional work could be done investigating new building methods. For example, the use of microinjection molding, possibly using an epoxy, could be explored.

In the pursuit of a wireless neural prosthesis, further effort in the development of the TEAS or a similar system is required. Though TEAS used a commercial off the shelf (COTS) approach in the interests of minimizing complexity and reducing development time, miniaturization by integrating the electrical components and mounting them in die

form is likely required in order to create a viable BMI for clinical use. The development of a single-chip analog front end is a logical starting point for this effort.

Brain-machine interfaces for clinical use will inevitably emerge in the years to come, and the first models will likely involve the use of microelectrode array assemblies much like the prototypes developed for the TEAS. Prostheses that provide both output and input signals may one day be a reality, allowing the user to sense position and even to regain some sense of touch. Only the future will tell.

## References

1. Chapin, J. K. and Moxon, K. A. (ed.), *Neural Prostheses for Restoration of Sensory and Motor Function*. Boca Raton: CRC Press, 2001.
2. Donoghue, J., Connecting cortex to machines: recent advances in brain interfaces. *Nature Neuroscience Supplement*, 2002, 5, 1085-1088.
3. Nicolelis, M., Actions from thoughts. *Nature*, 2001, 409, 403-407.
4. Serruya, M., Hatsopoulos, N., Paninski, L., Fellows, M. and Donoghue, J., Instant neural control of a movement signal. *Nature*, 2002, 416, 141-142.
5. Kandel, E., Schwartz, J. and Jessell, T., *Principles of Neural Science, 4th ed.* New York: McGraw-Hill, 2000.
6. Martel, S., Hatsopoulos, N., Hunter, I., Donoghue, J., Burgert, J., Malášek, J., Wiseman, C. and Dyer, R., Development of a wireless brain implant: the Telemetric Electrode Array System (TEAS) project. *Proceedings of the 23rd Annual International Conference of the IEEE-EMBS*, Oct. 25-28, 2001, 3594-3597.
7. Burgert, J., Malášek, J., Martel, S., Wiseman, C., Fofonoff, T., Dyer, R., Hunter, I., Hatsopoulos, N. and Donoghue, J., Embedded electronics for a 64-channel wireless brain implant. *Proceedings of SPIE: Microrobotics and Microassembly*, Oct. 28-Nov. 2, 2001, 4568, 124-134.
8. Burgert, J., *Telemetric Brain Electrode Array: Wireless and Analog Subsystems*. Thesis, M. Eng. EECS, Massachusetts Institute of Technology, May, 2002.
9. Fofonoff, T., Wiseman, C., Dyer, R., Malášek, J., Burgert, J., Martel, S., Hunter, I., Hatsopoulos, N. and Donoghue, J., Mechanical assembly of a microelectrode array for use in a wireless intracortical recording device. *Proceedings of the 2nd Annual International IEEE-EMBS Special Topic Conference on Microtechnologies in Medicine and Biology*, May 2-4, 2002, 269-272.

10. Fofonoff, T., Martel, S., Wiseman, C., Dyer, R., Hunter, I., Hatsopoulos, N. and Donoghue, J., A highly flexible manufacturing technique for microelectrode array fabrication. *Proceedings of the 2nd Joint IEEE-EMBS and BMES Conference*, Oct. 23-26, 2002, 2107-2108.
11. Malášek, J., *Electronics for a Telemetric Brain Electrode Array System*. Thesis, M. Eng. EECS, Massachusetts Institute of Technology, May, 2002.
12. Maynard, E., Hatsopoulos, N., Ojakangas, C., Acuna, B., Sanes, J., Normann, R. and Donoghue, J., Neuronal interactions improve cortical population coding of movement direction. *Journal of Neuroscience*, 1999, 19, 8083-8093.
13. Carey, J. (ed.), *Brain Facts*. Washington, DC: The Society for Neuroscience, 2002.
14. Robinson, D., The electrical properties of metal microelectrodes. *Proceedings of the IEEE*, 1968, 56, 1065-1071.
15. Bear, M., Connors, B. and Paradiso, M., *Neuroscience: Exploring the Brain*. Baltimore: Williams & Williams, 1996.
16. Geddes, L. A. and Baker, L. E., *Principles of Applied Biomedical Instrumentation*. New York: John Wiley & Sons, 1975.
17. Nicolelis, M. A. L. (ed.), *Methods for Neural Ensemble Recording*. Boca Raton: CRC Press, 1999.
18. E.I. du Pont de Nemours and Company (DuPont), Wilmington, Delaware, USA, <http://www.dupont.com>.
19. Geddes, L. A., *Electrodes and the Measurements of Bioelectric Events*. New York: Wiley-Interscience, 1972.
20. Campbell, P., Jones, K., Huber, R., Horch, K. and Normann, R., A silicon-based, three-dimensional neural interface: manufacturing processes for an intracortical electrode array. *IEEE Transactions on Biomedical Engineering*, 1991, 38, 758-768.

21. Jones, K., Campbell, P. and Normann, R., A glass/silicon composite intracortical electrode array. *Annals of Biomedical Engineering*, 1992, 20, 423-437.
22. Bai, Q., Wise, K. and Anderson, D., A high-yield microassembly structure for three-dimensional microelectrode arrays. *IEEE Transactions on Biomedical Engineering*, 2000, 47, 281-289.
23. Hoogerwerf, A. and Wise, K., A three-dimensional microelectrode array for chronic neural recording. *IEEE Transactions on Biomedical Engineering*, 1994, 41, 1136-1146.
24. Bionic Technologies, LLC, Salt Lake City, Utah, USA, <http://www.bionictech.com>.
25. Cyberkinetics Inc., Providence, Rhode Island, USA, <http://www.cyberkineticsinc.com>.
26. *Metals Handbook, Vol.2 - Properties and Selection: Nonferrous Alloys and Special-Purpose Materials, 10th ed.* ASM International, 1990.
27. Sandvik AB, Sandviken, Sweden, <http://www.sandvik.com>.
28. Nayer, A., *The Metals Databook*. New York: McGraw-Hill, 1997.
29. Ross, R., *Metallic Materials Specification Handbook, 4th ed.* London: Chapman & Hall, 1992.
30. Gere, J., *Mechanics of Materials, 5th ed.* Pacific Grove: Brooks/Cole, 2001.
31. Young, W. and Budynas, R., *Roark's Formulas for Stress and Strain, 7th ed.* New York: McGraw-Hill, 2002.
32. *Basic Course, Robofil 1020 Machines, 4 990 130/E/08.92 ed.* Geneva: Charmilles Technologies, 2003.
33. Oberg, E., Jones, F., Horton, H. and Ryffel, H., *Machinery's Handbook, 26th ed.* New York: Industrial Press, 2000.



34. Charmilles Technologies SA, Geneva, Switzerland, <http://www.charmilles.com>.
35. Parametric Technology Corporation (PTC), Needham, Massachusetts, USA, <http://www.ptc.com>.
36. SolidWorks Corporation, Concord, Massachusetts, USA, <http://www.solidworks.com>.
37. Autodesk, Inc., San Rafael, California, USA, <http://www.autodesk.com>.
38. DP Technology Corp., Camarillo, California, USA, <http://www.dpotechnology.com>.
39. Engineering Geometry Systems (EGS), Salt Lake City, Utah, USA, <http://www.featurecam.com>.
40. System 3R International AB, Vällingby, Sweden, <http://www.system3r.com>.
41. Technic, Inc., Cranston, Rhode Island, USA, <http://www.technic.com>.
42. LPKF Laser & Electronics AG, Garbsen, Germany, <http://www.lpkf.de>.
43. Resonetics, Inc., Nashua, New Hampshire, USA, <http://www.resonetics.com>.
44. Lau, J. H. (ed.), *Flip Chip Technologies*. New York: McGraw-Hill, 1996.
45. Solitec Wafer Processing, Inc., San Jose, California, USA, <http://www.solitec-wp.com>.
46. Para Tech Coating, Inc., Aliso Viejo, California, USA, <http://www.parylene.com>.
47. MPB Communications Inc., Montréal, Québec, Canada, <http://www.mpbc.ca>.
48. Cadence Design Systems, Inc., San Jose, California, USA, <http://www.cadence.com>.
49. Molex Inc., Lisle, Illinois, USA, <http://www.molex.com>.
50. Epoxy Technology Inc., Billerica, Massachusetts, USA, <http://www.epotek.com>.

51. Henkel Loctite Corp., Rocky Hill, Connecticut, USA, <http://www.loctite.com>.
52. Omnetics Connector Corporation, Minneapolis, Minnesota, USA, <http://www.omnetics.com>.
53. Agilent Technologies, Inc., Palo Alto, California, USA, <http://www.agilent.com>.
54. Plexon Inc., Dallas, Texas, USA, <http://www.plexoninc.com>.
55. W. L. Gore & Associates, Inc., Newark, Delaware, USA, <http://www.gore.com>.